Polyamides x.34: A New Class of Polymers between Polyethylene and Polyamides

Dissertation

Zur Erlangung des Grades
eines Doktors der Naturwissenschaften

vorgelegt von
Moritz Ludwig Peter Ehrenstein
aus Ludwigshafen am Rhein

genehmigt von der
Mathematisch-Naturwissenschaftlichen Fakultät
der Technischen Universität Clausthal
Tag der mündlichen Prüfung:
12. Juli 2002

Vorsitzender der Prüfungskommission:	Prof. Dr. J. Fertig
Hauptberichterstatterin:	Prof. Dr. G. Schmidt
Berichterstatter:	Prof. Dr. H. Höcker
Berichterstatter:	Prof. Dr. G. Ziegmann

Meinen Eltern in Dankbarkeit gewidmet.

Table of Contents

List of Abbreviations, Constants, and Symbols

AABB	Polyamides made from Dicarboxylic Acids and Diamines
AB	Polyamides made from ω-Amino Acids
A	Moiety *A*
Bu	Butyl Group
c	Concentration
$(CH_2)_f$	*f* Number of Methylene Groups
conc.	Concentrated
Δ	Heat
D	Electron-Donating Substituent
DMF	*n*,*n*-Dimethylformamide
DMSO	Dimethylsulfoxide
DMTA	Dynamic-mechanical Thermal Analysis
DSC	Differential Scanning Calorimetry
ED	Electron Diffraction
eq	Equivalent
ESA	Ethanesulfonic Acid
GPC	Gel Permeation Chromatography
HDPE	High Density Polyethylene
i	Number of CH_2-Groups in Macromonomer used in Chapter 6
j	Number of CH_2-Groups in Macromonomer used in Chapter 6
λ	Draw Ratio
L_{cru}	Length of Chemical Repeat Unit
LDPE	Low Density Polyethylene
LSP	Lamella Stacking Periodicity
η_{inh}	Inherent Viscosity
MALDI	Matrix-Assisted Laser Desorption/Ionization
M	Monomer
Me	Methylene Group
$\overline{M}_w$	Weight-Average Molecular Weight
MS	Mass Spectroscopy
MSA	Methanesulfonic Acid
n	Degree of Polymerization
$\overline{n}$	Number-Average Degree of Polymerization
NMP	1-Methyl-2-pyrrolidinone
Nu	Nucleophile
p	Extent of Reaction
PA	Polyamide
PA-6	Polycaprolactam*
PA-7	Polyheptaneamide
PA-12	Polydodecaneamide

* The nomenclature which is used for the polyamides is similar to one used by M. I. Kohan in the Nylon Plastic Handbook; Carl Hanser Verlag: Munich, 1995.

PA-22	Polydocosaneamide
PA-x.y	AABB Polyamide
PA-5.7	Poly(pentamethylene heptanoamide)
PA-6.6	Poly(hexamethylene adipamide)
PA-6.12	Poly(hexamethylene dodecanoamide)
PA-6.18	Poly(hexamethylene octadecanoamide)
PA-12.12	Poly(dodecamethylene dodecanoamide)
PA-6.24	Poly(hexamethylene tetracosanoamide)
PA-2.34	Poly(dimethylene tetratriacontanoamide)
PA-4.34	Poly(tetramethylene tetratriacontanoamide)
PA-6.34	Poly(hexamethylene tetratriacontanoamide)
PA-8.34	Poly(octamethylene tetratriacontanoamide)
PA-10.34	Poly(decamethylene tetratriacontanoamide)
PA-12.34	Poly(dodecamethylene tetratriacontanoamide)
i-PP	Isotactic Polypropylene
PE	Polyethylene
PD	Polydispersity
Ph	Phenyl Ring
r	Reactant Ratio
R	Organic Residue
rI	Relative Intensity (^{1}H-NMR)
RT	Room Temperature
sI	Signal Intensity (^{1}H-NMR)
TEM	Transmission Electron Microscopy
Temp.	Temperature
T_d	Dissolution Temperature
T_g	Glass Transition Temperature
TGA	Thermogravimetric Analysis
THF	Tetrahydrofurane
T_m	Melting Temperature
TMS	Tetramethylsilane
TOF	Time-Of-Flight
W	Electron-Withdrawing Substituent
wt %	Weight Percent
X	Halogen
x	Number of Carbon Atoms in Diamine
y	Number of Carbon Atoms in Dicarboxylic Acid

Abstract

The aliphatic polyamides rank among the most important groups of engineering thermoplastics. They owe this status to excellent thermal and mechanical properties combined with ease of processing. Although this class of polymers has existed for a long time, no members of it have ever contained well-defined, aliphatic monomer segments with more than 22 methylene groups. The goal of this work was to prepare such polyamides, which could bring together characteristic properties of polyamide and polyethylene in one polymer.

The study focused on AABB polyamides because positive thermal properties, such as high melting temperature were deemed desirable – even though this necessarily meant a reduction in the number of amide groups. Accordingly, this required concentrating on methods for synthesizing well-defined, aliphatic diacids, i.e., unbranched and monodisperse. These conditions were necessary for optimum crystallization of the new polymers. The three-stage diacid synthesis of Hünig *et al.* proved to be highly practicable in this regard. It yielded highly pure 1,34-tetratriacontanedioic acid, which was then used together with the corresponding aliphatic diamines to produce the new x.34 polyamides (x = 2, 4, 6, 8, 10, 12) by melt condensation. Additionally, commercial 1,24-tetracosanedioic acid and hexamethylene diamine were used to synthesize PA-6.24 by melt polymerization.

However, PA-6.24 proved to have no unusual properties to distinguish it from classic polyamides. By contrast, the new PA-x.34 compounds exhibited interesting amphiphilic character and retained the good thermal properties for which polyamides are known, as exemplified by their melting temperatures in the range 166 to 190 °C. One amphiphilic property of the PA-x.34 compounds is a special solubilizing ability: they are not dissolved at temperatures of less than 50 °C by concentrated sulfuric acid, which breaks hydrogen bonds, whereas classic polyamides and PA-6.24 are. Instead, polyamides x.34 form a gel in concentrated sulfuric acid from which fibers can be spun at temperatures above 65 °C. On the other hand, 1,2,3,4-tetrahydronaphthalene, which is a solvent for polyethylene, was found to dissolve these novel polyamides at temperatures above 150 °C. At temperatures below 138 °C, a mixture of 27.5 wt % PA-6.34 in 1,2,3,4-

tetrahydronaphthalene is a gel, and can be spun into fibers again at 150 °C. Further evidence of their amphiphilic nature is the ability of PA-6.34 to markedly reduce the domain size in a 1:1 mixture of polyethylene and PA-6.

To better understand the PA-x.34 compounds, their crystal morphology and structure was studied by means of both transmission electron diffraction and X-ray diffraction. Their crystal structure was found to be very similar to that of classic polyamides. The polyamide chains crystallize in stacked layers, with the individual chains inside the layers linked by hydrogen bonds.

The maximum draw ratio (λ) of untreated polyamides is about $\lambda = 5$. This is not high enough for perfect orientation and so high-strength fibers cannot be obtained. The reason of this limitation is that the strong hydrogen bonds greatly restrict their movement in the crystalline phases. A study was made of the formation of a gel by PA-6.34 in concentrated sulfuric acid with the aim of finding a method that, once the hydrogen bonds are broken, would allow high-strength polyamide fibers to be made by plastic deformation. Maximum draw ratios of up to $\lambda = 20$ at 75 °C were obtained. However, the mechanical properties were not better than those of untreated PA-6.34 drawn at 150 °C ($\lambda = 5.3$). One possible reason is the bifunctionality of the sulfuric acid, which could conceivably build up a new network of hydrogen bonds that prevents the polymer chains from attaining the desired orientation. Another reason might be α_c-relaxation at 88 °C in the crystalline phase of polyethylene. There is very little scope for drawing polyethylene by plastic deformation below this temperature. Since the melting temperature of the PA-6.34/sulfuric acid gel is lower than this relaxation temperature, high draw ratios for this gel are not possible. High draw ratios would require a PA-x.60, for example, whose gel with sulfuric acid would have a melting temperature higher than 88 °C on account of the more extended aliphatic segments.

An attempt was made to produce such diacids with a chain length in excess of 60 methylene units by means of the polyhomologation method developed by Shea *et al*. It transpired that this method is theoretically capable of yielding very extended aliphatic diacids. However, it needs to be optimized. In addition to the limited solubility of the resultant intermediates the main problems were the appearance of methyl branching and the relative large polydispersity of the produced macromonomers.

Zusammenfassung

Die aliphatischen Polyamide bilden eine der wichtigsten Gruppen unter den technischen Thermoplasten. Sie haben ihre heutige Bedeutung aufgrund ihrer ausgezeichneten thermischen und mechanischen Eigenschaften erlangt, die mit einer unkomplizierten Verarbeitbarkeit gepaart sind. Trotz ihrer langen Existenz gibt es bislang keine Vertreter dieser Polymerklasse, die wohldefinierte, aliphatische Monomersegmente mit mehr als 22 Methylengruppen enthalten. Ziel dieser Arbeit war es, derartige Polyamide herzustellen, um möglicherweise die charakteristischen Eigenschaften von Polyamid und Polyethylen in einem Polymer zu vereinen.

Um die positiven thermischen Eigenschaften wie z.B. die hohe Schmelztemperatur trotz der zwangsläufigen Verringerung der Amidgruppen weiterhin beizubehalten, wurde nur die Klasse der AABB-Polyamide untersucht. Es wurden dementsprechend zunächst lediglich Synthesen wohldefinierter, aliphatischer Disäuren betrachtet, d.h. mit jeweils gleicher Kettenlänge und ohne Verzweigungen. Diese Bedingungen sind erforderlich, um eine optimale Kristallisation der neuen Polymere zu ermöglichen. Die dreistufige Disäuresynthese nach Hünig *et al*. hat sich als sehr praktikable Methode erwiesen. Auf diesem Weg wurde die 1,34-Tetratriacontandisäure in hoher Reinheit hergestellt. Aus dieser Säure wurden dann mit den entsprechenden aliphatischen Diaminen die neue Polyamide x.34 (x = 2, 4, 6, 8, 10, 12) durch Schmelzpolykondensation hergestellt. Zudem wurde in gleicher Weise auch das Polyamid 6.24 aus der käuflichen 1,24-Tetracosandisäure und Hexamethylendiamin synthetisiert.

Die Eigenschaften von Polyamid 6.24 sind vergleichbar mit denen von klassischen Polyamiden. Die Gruppe der Polyamide x.34 allerdings weist, neben den für Polyamide bekannten guten thermischen Eigenschaften, eine interessante amphiphile Natur auf. Die Schmelztemperaturen beispielsweise liegen je nach verwendetem Diamin im Bereich von 166 bis 190 ˚C. Zu den amphiphilen Eigenschaften der Polyamide x.34 zählt das besondere Lösungsverhalten: Für diese Polymere ist die wasserstoffbrückenspaltende konzentrierte Schwefelsäure bei Temperaturen unter 50 ˚C kein Lösungsmittel, im Gegensatz zu den klassischen Polyamiden und PA-6.24. In konzentrierter Schwefelsäure bilden die Polyamide x.34 Gele, aus denen sich oberhalb von 65 ˚C Fasern spinnen

lassen. Auf der anderen Seite ist 1,2,3,4-Tetrahydronaphthalin, ein Lösungsmittel für Polyethylen, in der Lage, die neuartigen Polyamide oberhalb von 150 ˚C zu lösen. Eine Mischung aus 37,5 Gew.-% PA-6.34 in 1,2,3,4-Tetrahydronaphthalin bildet unterhalb von 138 ˚C ein Gel, aus dem dann wiederum bei 150 ˚C Fasern gesponnen werden können. Ein weiterer Beleg für den amphiphilen Charakter der neuen Polyamide ist die Fähigkeit von PA-6.34, die Domänengrösse in einem 1:1-Gemisch aus Polyethylen und PA-6 deutlich zu verkleinern.

Um ein besseres Verständnis für die Polyamide x.34 zu erlangen, wurde ihre Kristallmorphologie und -struktur sowohl mit Hilfe der Transmissionselektronen-mikroskopie als auch der Röntgenbeugung untersucht. Dabei konnte gezeigt werden, dass ihre kristallinen Segmente ganz ähnlich aufgebaut sind wie die von klassischen Polyamiden. Die Polyamidketten kristallisieren in übereinandergelagerten Schichten, wobei die einzelnen Ketten innerhalb der Schichten durch Wasserstoffbrückenbindung verknüpft sind.

Die maximale Verstreckrate (λ) nicht vorbehandelter Polyamide liegt im Bereich von $\lambda = 5$. Dies reicht nicht aus, um hoch-orientierte und somit hochfeste Fasern herzustellen. Der Grund für die Limitierung der Verstreckrate ist die stark eingeschränkte Beweglichkeit in den kristallinen Phasen der Polyamide aufgrund der starken Wasserstoffbrückenbindungen. Die Fähigkeit von PA-6.34, in konzentrierter Schwefelsäure ein Gel zu bilden, wurde untersucht, um einen Gelverarbeitungsprozess zu finden, mit dem sich nach Lösen der Wasserstoffbrückenbindungen hochfeste Polyamidfasern durch plastische Verformung herstellen lassen. Es konnten maximale Verstreckraten von bis zu $\lambda = 20$ bei 75 ˚C erreicht werden. Allerdings konnte keine Verbesserung der mechanischen Eigenschaften im Vergleich zu unbehandeltem PA-6.34, welches bei 150 ˚C verstreckt wurde ($\lambda = 5.3$), festgestellt werden. Ein möglicher Grund ist die Bifunktionalität der Schwefelsäure, die es ihr ermöglicht, ein Netzwerk aus Wasserstoffbrückenbindungen aufzubauen, das die gewünschte Orientierung der Polymerketten verhindert. Ein anderer Grund für das oben erwähnte Verhalten könnte die sog. α_c-Relaxation bei 88˚C in der kristallinen Phase von Polyethylen sein. Unterhalb dieser Temperatur ist das Verstrecken von Polyethylen durch plastische Verformung stark limitiert. Da nun aber die Schmelztemperatur des PA-6.34/Schwefelsäure-Gels unterhalb dieser Relaxationstemperatur liegt, sind grosse Verstreckraten für dieses Gel nicht möglich. Um dies zu erreichen, müsste z.B. ein PA-x.60 synthetisiert werden, dessen

Schwefelsäuregel dann eine Schmelztemperatur oberhalb 88 ˚C aufweisen könnte aufgrund der längeren aliphatischen Segmente.

Bei dem Versuch, Disäuren mit einer Kettenlänge von über 60 Methyleneinheiten, wie oben vorgeschlagen, herzustellen, wurde die von Shea *et al.* entwickelte Polyhomologisierungsmethode angewendet. Es konnte in dieser Arbeit gezeigt werden, dass es im Prinzip möglich ist, auf diesem Weg sehr lange aliphatische Disäuren herzustellen. Allerdings muss diese Methode noch optimiert werden. Als Hauptprobleme für diesen Ansatz stellte sich, neben der limitierten Löslichkeit der erhaltenen Zwischenstufen, das Auftreten von Methylverzweigungen und die relativ grosse Polydispersität der erhaltenen Makromonomere heraus.

1. Introduction[1]

1.1 General Introduction

1.1.1 Structure and Properties of Polyamides

"Polyamides" (PA) is a collective term for a family of polymers which contain amide moieties (**1**) in their backbone (see Figure 1.1)[1,2].

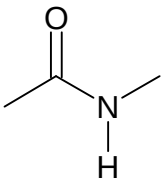

1

Figure 1.1: Chemical structure of the amide moiety.

Polyamides may be generally divided into three different classes: the synthetic i) aliphatic polyamides or nylons[2], and ii) aromatic polyamides (also known as aramides), and the iii) biological polyamides more commonly referred to as polypeptides, e.g. enzymes, α-keratine, silk-fibroin and collagen [3-5]. One interesting aspect of synthetic polyamides is that they feature the three essential interactions also encountered in all living organisms, namely covalent bonds, hydrogen bonds and van der Waals interactions. Due to this characteristic, understanding of structure-property relations of polyamides is useful not only with respect to their value as engineering polymers, but also to generate insight into aspects of the behavior and properties of their natural counterparts.

In all polyamides hydrogen bonds (H-bonds) are of distinct importance. These strong interactions, which may occur between the amide groups, are the origin of some remarkable advantages that polyamides display in comparison to more hydrophobic semi-crystalline polymers such as polyolefins and polyesters. A comparison of certain properties of linear aliphatic polyamides with those of, for example, high-density

---

[1] This thesis was conducted at the Institute of Polymers in the group of Prof. P. Smith at the Materials Department of the Eidgenössische Technische Hochschule (ETH) Zürich.

[2] As it is a common practice, nylon is here used as a synonym for AABB polyamides as well as AB polyamides; the latter are also referred to as *n*-nylons.

polyethylenes (HDPE) of comparable molecular weights shows that the presence of hydrogen bonds leads to substantial by better mechanical properties, such as relatively high wear- and abrasion-resistance combined with high toughness and stiffness, of the polyamides [6,7]. In addition, polyamides also offer substantially higher glass transition (T_g) and melting temperatures (T_m) than high-density polyethylene (see Table 1.1). Not surprisingly, the melting temperatures of polyamides decrease with a decreasing amount of amide groups in the polymer backbone; the melting temperature of PA-12, for example, is located in the same region as isotactic polypropylene (*i*-PP) (see Table 1.1).

Table 1.1: Selected thermal and mechanical properties of different polyamides in comparison to frequently employed polyolefins (commercial grades) [1,8]. Note that these values may vary, depending on the molecular weight, water content and solid-state structure of the polymers.

Polymer	**T_g (˚C)**	**T_m (˚C)**	**Tensile Modulus (MPa)**	**Tensile Strength (MPa)**
PA-4.6	78	295	3000	99
PA-6.6	66 - 80	257	3200	83
PA-6.12	50 - 60	219	2100	61
PA-6	59 - 75	220	3000	81
PA-12	54 - 62	178	1500	55
i-PP	- 15	167	690-960	40-60
HDPE	-130 - -110	132	550-1250	34-69

A variety of other characteristics, such as their dyeability, are contributed to the outstanding commercial success of polyamides over the last sixty years [9]. Among the major drawbacks of polyamides are their proneness to water, which they take up in measurable quantities and which affects their properties, and the fact that very high molecular weight versions are not readily produced and not stable at elevated temperatures [1].

Aliphatic polyamides, which are the subject of this thesis, generally are divided into two groups, i.e. AABB polyamides, in this thesis polyamide x.y, and AB

polyamides, also known as *n*-nylon or polyamide y, depending on the monomers used and their resulting molecular structure (see Scheme 1.1).

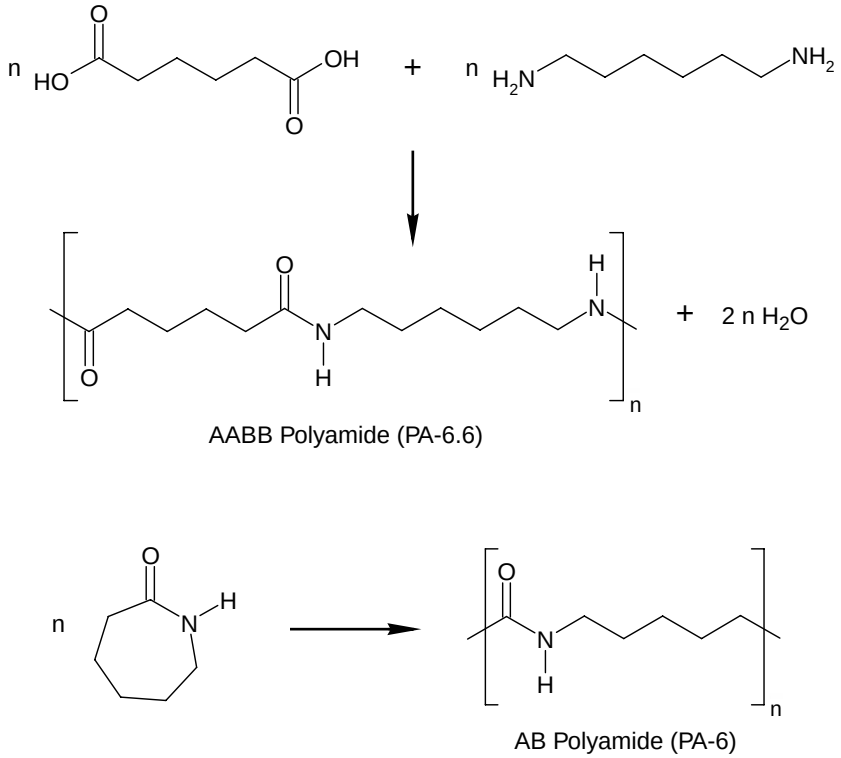

Scheme 1.1: Examples of AABB polyamide and AB polyamide: PA-6.6 and PA-6.

The AABB polyamides were discovered in 1934 by Wallace H. Carothers at E.T. du Pont de Nemours and Co., Inc. [10,11]. Poly(hexamethylene adipamide) or PA-6.6 was the first commercialized synthetic polyamide, and sold under the trade name Nylon. The most important representative of the *n*-nylons is polycaprolactam (PA-6), which was first synthesized by P. Schlack at I.G. Farbenindustrie in 1938 [12]. A wide spectrum of other AB and AABB polyamides was developed and investigated since then, but today, PA-6.6 and PA-6 together still capture more than 90% of the market of all polyamides (12.0 billion $ /year) [13-15].

Evidently, despite or perhaps in view of the overwhelming commercial success of the latter two polyamides, relatively little effort has been made to explore and exploit nylons that comprise extended aliphatic segments. The most notable exception is nylon 12, which is synthesized starting from 12-dodecanelactam. Its (comparatively modest) commercial success is based on the relatively low water absorption and the retention of elasticity and ductility at temperatures as low as - 50 °C by contrast to objects made from PA-6 which already become brittle at - 30 ˚C [2].

1.1.2 Potential Properties of Polyamides with Extended Aliphatic Segments

The incorporation of very extended aliphatic segments into polyamides may potentially lead to a class of amphiphilic[3] polyamides ("polysoaps"), which, in certain aspects, could bridge the existing gap between polyamides and polyolefins. One advantage of these polyamides will be a significant low water absorption, due to the smaller amount of amide groups, which will have a positive effect on the dimensional stability and reduction of the influence of humidity on their mechanical properties (Young's modulus of, for example, PA-6.6 is known to decrease from about 3.2 GPa for a dried sample to 1.6 GPa at 50 % relative humidity [1]). Consequently, the design and manufacturing of precision structural parts when made out of such polyamides with extended aliphatic segment is expected to be facilitated. Their anticipated amphiphilic character may also enable a variety of other applications. For example, these novel polyamides might be used as a hydrophobic coating material for hydrophilic surfaces (cf. Figure 1.2).

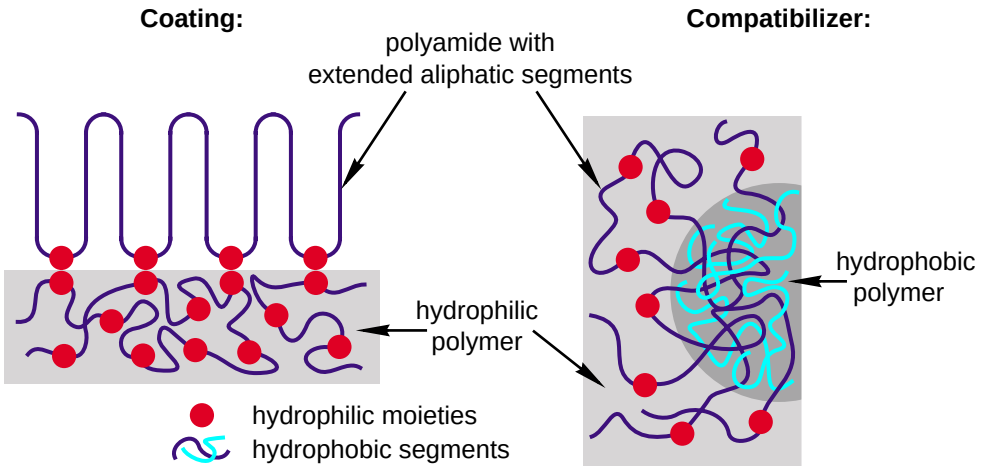

Figure 1.2: Scheme of an envisioned hydrophobic coating onto a hydrophilic polymer and the use as compatibilizer of polyamides with extended aliphatic segments.

In addition, the amphiphilic polyamides may be useful as polymeric "compatibilizer" for blends of, for example, conventional polyamides and polyolefins. Of interest in this context is the possibility to reduce the price of relatively "expensive" polyamides by blending the latter with less expensive polyolefins (price ratio PA-6.6/

[3] Amphiphilic polymer is referred to polymers which containing hydrophobic and hydrophilic groups in thier polymer chain.

HDPE 2.75 [14]), or to facilitate the recycling of polyolefin-polyamide fiber-mixtures, such as those that can be found in carpets, into useful new products (see Figure 1.2).

Another potential application of polyamides with extended aliphatic segments could be in the area of high-strength fibers. In order to produce high-strength polymer fibers, their constituent macromolecules need to be highly extended and well oriented [16]. This can be achieved, for example, by tensile deformation of flexible chain polymers to high draw ratios (typically > 20). For polyethylene there are several known processes which can be used to obtain the necessary high draw ratios [17-21]. In the case of polyamides this situation is different. The strong hydrogen bonds that are present in the crystalline phase prevent macromolecular motion and thus limit the drawability of these polymers significantly; typically only relatively low draw ratios (~4-5) are achieved (see Figure 1.3, approach 1) [22]. Alternative strategies for the processing of polyamides into highly oriented structures are shown schematically in Figure 1.3. Approaches 2 and 3 in Figure 1.3 towards highly oriented polyamides have been advanced and discussed in reference 22. Approach 2 is aimed at uncoiling the polyamide macromolecules and inhibiting interchain hydrogen bonds by complexing the amide groups with bulky sulfonic acids. It was indeed possible to achieve a chain extension for a polyamide 4.6-camphorsulfonic acid system of approximately 30 %. However, this extension was not enough in order to obtain highly oriented polyamide chains and, therefore, no high-strength polyamide 4.6 fibers can be produced by this approach. The third approach is based on a temporary breaking of the hydrogen bonds with sulfuric acid in order to reduce the size of the polyamide crystals to such an extent that it is possible to pull polymer chains through these crystals. Nylon 6.6 fibers could be highly oriented by this route, but, unfortunately, their mechanical properties are not improved, when compared to conventionally processed samples. One described reason could be that these chains are, in fact, highly oriented but not fully extended, and that the system adapts a shish-kebab-type structure [22]. The last approach relies on the a possibility to establish a deformation process in which all H-bonds between the polyamide chains are temporarily broken (i.e. though protonation with sulfuric acid), but a solid network exists that is comprised of ordered regions of aliphatic segments (cf. Figure 1.3, approach 4). Such material might display deformation properties similar to polyethylene [23,24]. This network could be formed by the extended aliphatic segments of the new polyamides when clearing the H-bonds with strong acids. In order to form this crystal lattice, these

segments have to be well-defined. The length should be exactly the identical and they should be unbranched. These requirements are derived from the consideration to meet the prerequisites for optimal crystallization.

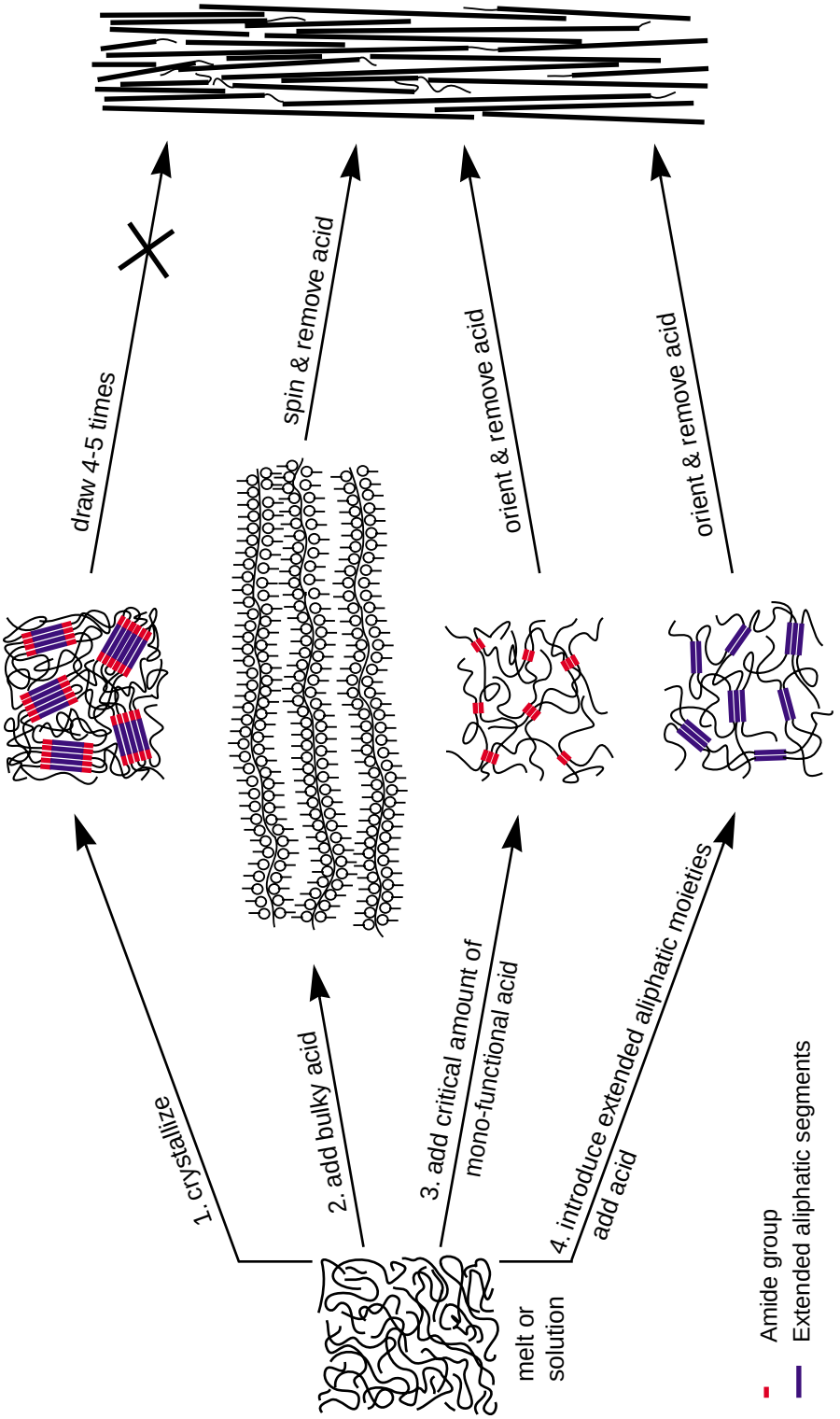

Figure 1.3 Different approaches to generate oriented structures of polyamides [22].

The melting temperature of polyamides is influenced by the “concentration” of amide groups (i.e. the ratio of amide to methylene units in the repeat unit) and the odd/even effect. The odd/even effect leads in the case of AABB polyamides to a significant lower melting temperature if one or both of the monomers contain an odd number of carbon atoms (e.g. PA-5.7, 228 ˚C; PA-6.6, 256 ˚C). AB polyamides show a higher melting temperature if the number of methylene groups is even (e.g. PA-7, 233 ˚C; PA-6, 223˚C). The reduction of the concentration of amide groups leads to a decrease of the melting temperature in both series of polyamides [25]. AABB polyamides usually exhibit higher melting temperatures than AB polyamides with a similar amide group concentration [1,26]. Thermodynamic considerations have been invoked to explain this difference in melting temperatures of these two aliphatic polyamide classes, and it has been attributed to the smaller change of the entropy of for example PA-6.6 (T_m= 255-257 ˚C) upon melting compared to the PA-6 (T_m= 220 ˚C) [26-30]. Thus, in order to keep the melting temperatures as high as possible the present work has been restricted to the investigation of AABB polyamides with an even number of methylene units.

A literature review yielded some reports that describe AABB nylons comprising extended (>dodecane) aliphatic segments [9,31-34]. The most important group of these polyamides contains carboxylic diacids, which are derived from unsaturated fatty acids such as oleic, elaidic, and linoleic acid [33]. Due to the nature of their synthesis, these diacids are usually branched and rather ill-defined. Nevertheless, polyamides based on these monomers occupy a relevant market niche in the area of adhesives, inks and coatings. Also, copolymers of these extended aliphatic diacids with caprolactam, hexatriacontanediamine and nonadioic acid have been described, presumably for use as high-impact-strength polyamides [32]. For zinc-chloride-resistant materials, another class of polyamide copolymers was synthesized [31], which contain only a fraction of extended aliphatic dicarboxylic acids or extended aliphatic diamines. Attempts to prepare homopolymers of the above-referred monomers were reported to have failed [31]. Careful studies of medium extended aliphatic segment polyamides (up to PA-6.18) were carried out by Jones *et al.* [34]. Unfortunately, no synthetic details and molecular characterization data were presented on these materials, which were referred to as research samples of I.C.I. [34]. The investigated highest homologue of the AB polyamides is nylon-22, which was reported to exhibit a melting temperature (T_m) of

around 145 °C, which is very close to the T_m of polyethylene and, thus, lacks the excellent thermal properties of the common lower nylons [35].

1.2 Extended Aliphatic Monomers

1.2.1 Uniform AA-Monomers

Unfortunately, only a few methods have been developed for the preparation of extended aliphatic carboxylic diacids [36-46]. Even fewer reports are available on the synthesis of the corresponding diamines, if desired, they could be derived from the corresponding diacids, for example by the *Schmidt-Reaction* or *via* an amide, followed by a reduction with lithium aluminium hydride [47-49].

One common method that may be employed to synthesize the desired well-defined extended aliphatic diacids is by oxidative ring-opening, which has been used in industry for many years, for example, in the synthesis of adipic acid from benzene. In the latter process, benzene is hydrogenated and subsequently oxidated in two different steps (see Scheme 1.2) [50].

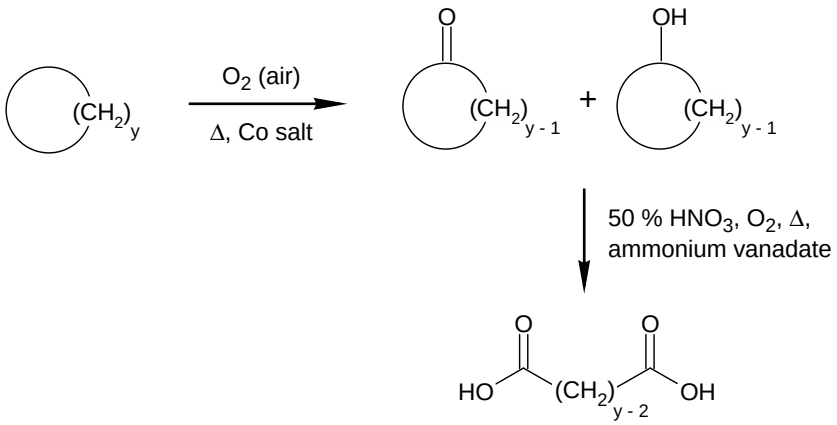

Scheme 1.2: Synthesis of a dicarboxylic acid via oxidative ring-opening.

This synthetic route can, in principle, also be employed for the synthesis of more extended carboxylic diacids, if cycloalkanes other than cyclohexane would be used. This method is, in fact, already used to synthesize 1,12-dodecanedioic acid from

cyclododecane, which can be produced *via* the Reed route from 1,3-butadiene (see Scheme 1.3) [51]. The successful synthesis of the dicarboxylic acid led to commercial success of PA-6.12 and PA-12.12 [1]. However, the fundamental problem of this elegant approach for the present work is the requirement of large aliphatic cycloalkanes the formation of which is a synthetic challenge.

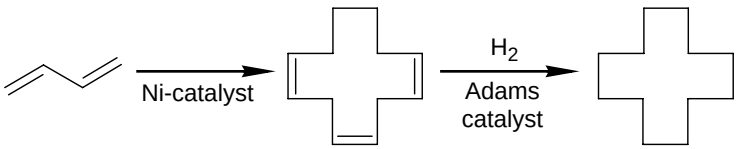

Scheme 1.3: Synthesis of cyclododecane.

Another potentially interesting approach is the electrochemical dimerization of alkyl dicarboxylate salts; this route is also known as the Kolbe electrolysis (cf. Scheme 1.4) [36,37]. In this process, at the anode a carboxyl radical is formed, and after decarboxylation the resulting alkyl radicals dimerize, resulting in a dialkyl dicarboxylate. Many different aliphatic diacids have been synthesized using this methodology. Already in 1925, David A. Fairweather was able to synthesize *n*-tetratriacontane dicarboxylic diacid, which, in fact, is the most extended aliphatic diacid synthesized, *via* this route. Unfortunately, the yield of the process (typically 13 %) is quite low [38].

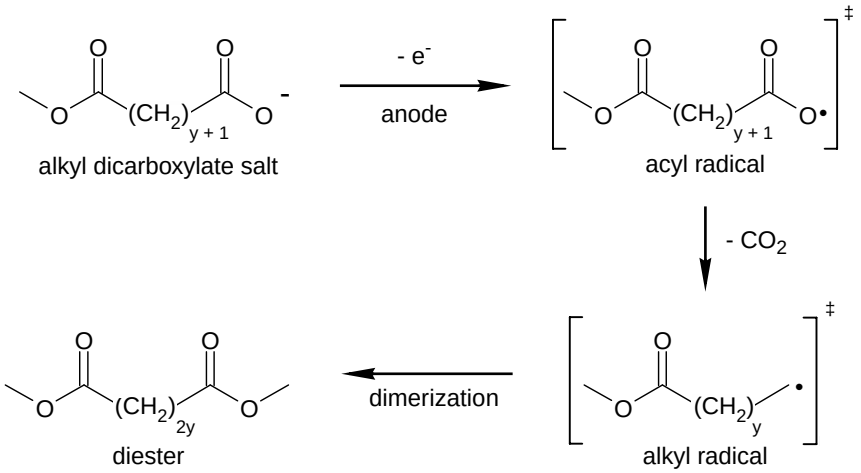

Scheme 1.4: Electrochemical synthesis of dicarboxylic diester.

Whiting *et al*. developed an interesting procedure to synthesize very long chain alkanes and functionalized derivatives like dicarboxylic acids [40,41]. This method is

based on a sequence of four reactions. The key step is a Wittig reaction between an ω-halo alkanal and phosphonium ylide (see Scheme 1.5). Each repetition of the reaction sequence leads to a chain doubled product of the starting ω-halo alkanal ethylene acetal. They were able to synthesize extended straight-chain alkanes of very specific length up to $C_{390}H_{782}$ and also a dicarboxylic acid containing 190 methylene groups. Unfortunately, they did not report any overall yield of the synthesis of the latter. An important advantage of this method is the possibility to convert relatively large amounts of materials, e.g. 3 kg. But, there are certain difficulties in this procedure such as, for example, side reactions, purification, and the partially long reaction time (up to 20 days for one step) [41].

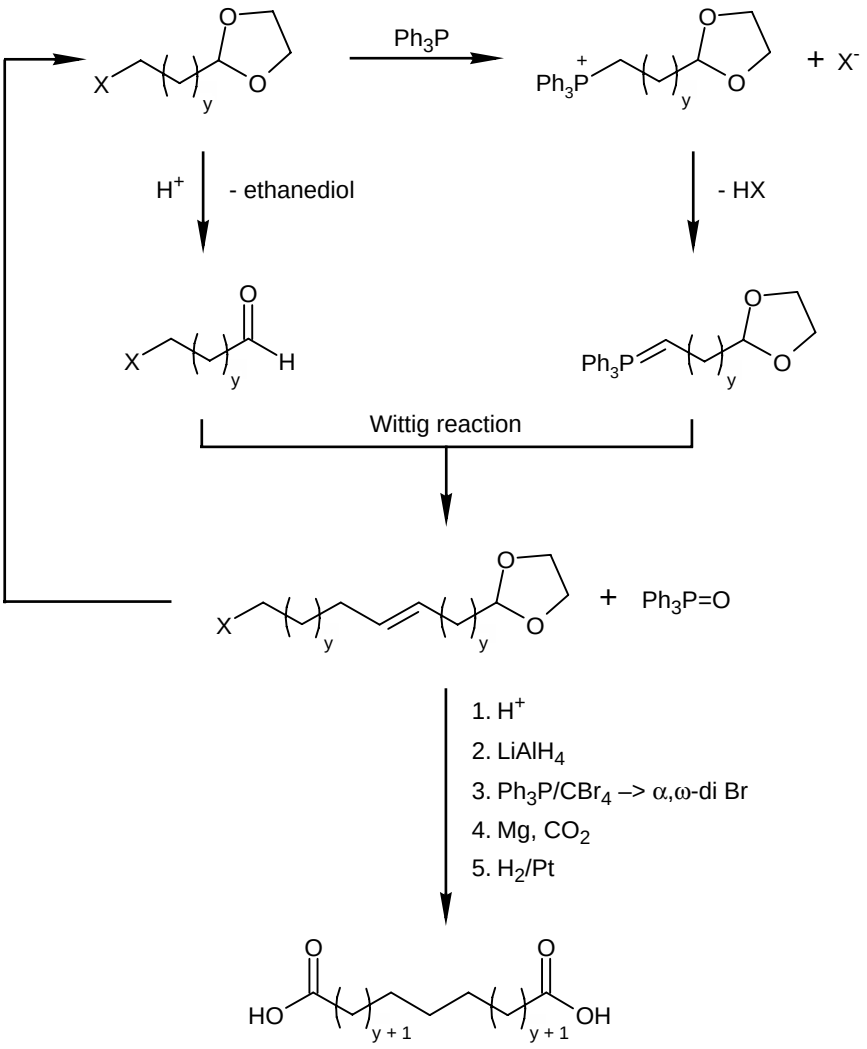

Scheme 1.5: Synthesis of extended aliphatic dicarboxylic acid via Wittig reaction. The first reaction sequence starts with y = 10.

Other ways to synthesize dicarboxylic acids are e.g. oxidation of natural alkenes [39], microbial conversion of alkanes [42,43], and the oxidative condensation of ω-alkine acids [44]. The most efficient and elegant method for synthesizing the desired well-defined dicarboxylic acids is the enamine-coupling route, originally proposed by Hünig *et al.* [46]. Because of its yield and good feasibility this synthetic path way was chosen for the present thesis; a detailed discussion of the latter can be found in Chapter 2.

1.2.2 Polydisperse AA-Monomers

Another approach for the synthesis of extended aliphatic dicarboxylic acids is *via* polymerization reactions which lead to less well-defined macromonomers. There are some reasons why polymers made with these macromonomers might be of interest. For example, as a compatibilizer for polyamides and polyolefins, the former do not need to be perfectly well-defined. In this case, it is more important to have very extended aliphatic segments, which are long enough in order to form loops in the corresponding polymer phase (see Figure 1.2) than to have a well-defined length of the segments. Critical here is that these extended aliphatic segments will “dissolve” in the polyolefin phase and, ideally, form entanglements with them, which should increase the strength of the interface between the incompatible polymer phases (see Figure 1.2). In addition, these segments should also be able to form a network which shows the same deformation behavior like polyethylene as it is already described above (cf. Figure 1.3). Hence, in this work systems with much more extended aliphatic segments than the ones described in the previous Section 1.2.1 were explored. A most promising method to synthesize such telechelic[4] oligomers is polyhomologation, developed by Shea *et al.* [52,53]. Efforts to adopt this synthetic framework for the synthesis of dicarboxylic acids with extended aliphatic segments are summarized in Chapter 6.

[4] Telechelic is referred to oligomers/polymers possessing two indentical reactive groups at both chain end of linear macromolecule.

1.3 Polyamide Synthesis

1.3.1 Formation of Amide Bond

In general, AABB polyamides are synthesized from bifunctional monomers by polycondensation, a term introduced by Carothers for this kind of reaction in analogy to the classical organic reaction in 1929 [54]. The amino group is one necessary functionality and the other may be a carboxylic acid derivative or a cyano compound. The reaction of these groups leads to the amide bond and a small molecule, e.g. water. There are at least four kinds of reactions, which are useful to form amide groups [15]. The most well-known reaction is the conversion of the carboxylic acid with an amine as depicted in Scheme 1.6 (reaction 1.1), which is conventionally carried out in the melt. In other reactions, different activated carbonyl compounds are used in conjunction with a diamine, such as esters (reaction 1.2), or acid chlorides (reaction 1.3). The latter reaction, conducted in solution, is called the *Schotten-Baumann* method, and a base is used to neutralize the hydrochloric acid formed. In addition a cyano group can react with the amine and in the presence of water to yield the amide bond (reaction 1.4) [15].

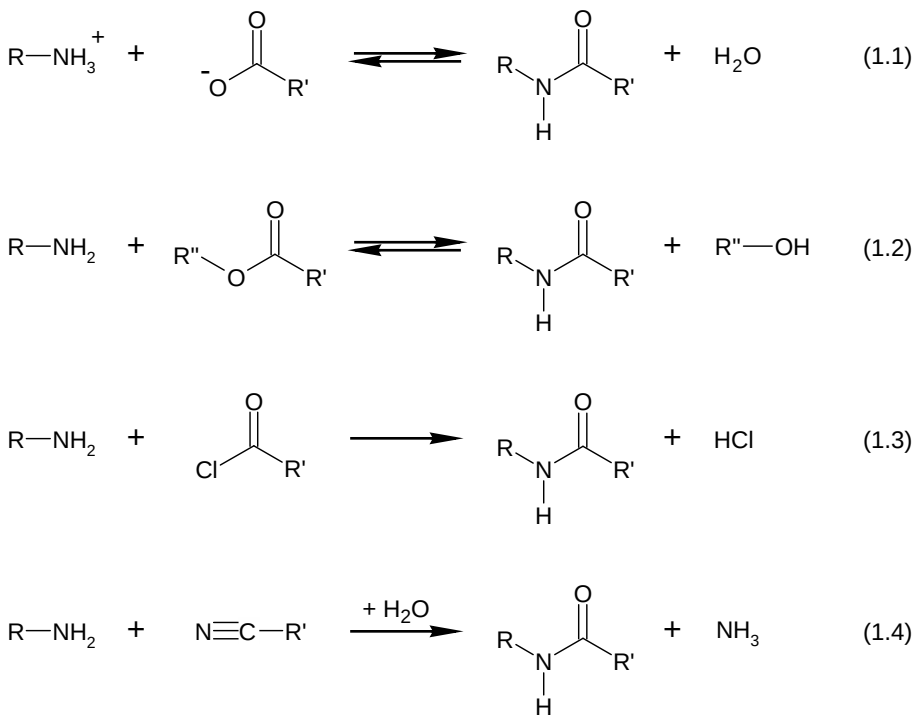

Scheme 1.6: Formation reactions of the amide bond starting from an amine.

Another way to form the amide bond is the reaction of a carboxylic acid with an isocyanate (Scheme 1.7). This reaction plays a secondary role in the polyurethane foaming process, because the development of carbon dioxide leads to blistering and subsequently to a foam [15].

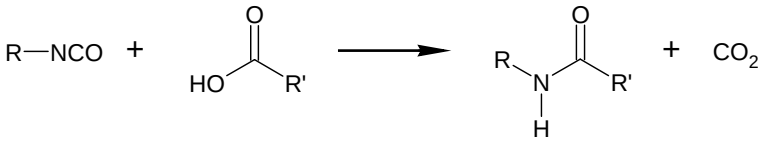

Scheme 1.7: Formation of an amide group starting from an isocyanate.

Finally, the anionic ring-opening polymerization of ε-caprolactam should be mentioned, which leads to AB polyamides. However, this reaction is not applicable for the synthesis of AABB polyamides. Of course, there are more amide forming reactions than mentioned here, but they appear to be less relevant in polymer synthesis.

1.3.2 Influences on the Molecular Weight of AABB Polyamides

The AABB polyamides, strictly speaking, cannot be considered as copolymers because none of the monomers is capable to form a polymer on its own. Careful control of the stoichiometry is of utmost importance in order to achieve a high average molecular weight of the polyamide. In addition, it is necessary to attain very high conversion to achieve high molecular weight material. These requirements are readily understood in terms of the Carothers Equation (EQ 1) [55,56] which relates the number-average degree of polymerization $\bar{n}$ of a polymer prepared by step growth polymerization to the reactant ratio *r* and the extent of reaction *p*.

$$\bar{n} = \frac{1 + r}{1 + r - 2rp} \qquad \text{(EQ 1)}$$

*Table 1.2: Variation of number-average degree of polymerization ($\bar{n}$) with reactant ratio (r) and extent of reaction (p). Key: * As $p \rightarrow 1$, $\bar{n} \rightarrow (1 + r)(1 - r)^{-1}$ [56].*

	$\bar{n}$ at				
r	***p* = 0.90**	***p* = 0.95**	***p* = 0.99**	***p* = 0.999**	***p* = 1.000***
1.000	10.0	20.0	100.0	1000.0	∞
0.999	10.0	19.8	95.3	666.8	1999.0
0.990	9.6	18.3	66.8	166.1	199.0
0.950	8.1	13.4	28.3	37.6	39.0
0.900	6.8	10.0	16.1	18.7	19.0

Table 1.2 gives values of $\bar{n}$ calculated by using Equation 1.1 and reveals the significant reduction in $\bar{n}$ when *p* is not one and/or *r* is less than unity. In order to achieve an equimolar stoichiometry, a so-called AH-salt is first produced by neutralizing a solution of the dicarboxylic acid with the diamine [15]. The term AH-salt is historical and derived from the salt formed from **a**dipic acid and **h**examethylene diamine and will be used in this thesis as a synonym of these kinds of salts. In the case of adipic acid and hexamethylene diamine, a methanol insoluble AH-salt with a perfect 1 : 1 stoichiometry is obtained.

1.3.3 Methods to Conduct the AABB Polycondensation

There are two possibilities to perform the AABB polycondensation. One is the thermal polycondensation which is carried out at elevated temperatures above T_m of the AH-salt without organic solvents and without any catalyst as a melt-polycondensation. The alternative synthesis is a solution-polycondensation, which is performed at lower temperatures with the aid of an organic solvent and using catalysts or acid acceptors. The solution-polycondensation is usually applied for polymers which do not melt prior to

decomposition such as aromatic polyamides. In this thesis a melt-polycondensation is used [1,15].

1.4 Objectives and Scope of Thesis

The objective of this thesis is to synthesize and examine properties of polyamides with extended aliphatic segments, a largely unexplored family of polymers. As pointed out above, these polymers are expected to exhibit a number of interesting characteristics that may be of potential use in areas as diverse as compatibilization of polyblends and high strength fibers.

In Chapter 2, the synthesis and characterization of the extended aliphatic 1,34-tetratriacontanedioic acid and the corresponding polyamide 6.34 (PA-6.34) is described. The different properties of this PA-6.34 are investigated and compared with the properties polyamide 6.24 (PA-6.24), which was also prepared. Special emphasis will be devoted to compatibilizing properties of PA-6.34. The additional representatives of novel series of polyamides x.34 (PA-2.34, PA-4.34, PA-8.34, PA-10.34, and PA-12.34) are discussed in Chapter 3, starting from their melt-polycondensation and followed by the investigation of their thermal, mechanical properties, and phase behavior. The morphology and crystal structure of these novel polyamides x.34 will be discussed in Chapter 4. The prepared crystals were investigated by means of transmission electron microscopy (TEM) as well as X-ray diffraction. In Chapter 5, the possibility to produce high-strength fibers of PA-6.34 is discussed with the focus on the gel processing of PA-6.34 in conc. sulfuric acid. The efforts to synthesize very large aliphatic dicarboxylic acids by using a polyhomologation reaction will be discussed in Chapter 6. In Chapter 7, the conclusions and outlook will finish this thesis.

1.5 References

[1] Kohan, M. I. *Nylon Plastics Handbook*; Carl Hanser Verlag: Munich, 1995.

[2] Vieweg, R.; Müller, A. *Kunststoffhandbuch: Polyamide*; Carl Hanser Verlag: München, 1966.

[3] Corey, R. B.; Pauling, L. *Proc. Roy. Soc. (Lond.) B* **1953**, *141*, 10.

[4] Flory, P. J. *Statistical Mechanics of Chain Molecules*; Wiley-Intersience: New York, 1969.

[5] Elias, H.-G. *Makromoleküle*, Wiley-VCH Verlag: Weinheim 1999; Vol. 1.

[6] Holzmüller, W. *Physik der Kunststoffe*, Akademie Verlag: Berlin, 1961.

[7] Margolis, A. F. *SPE Journal*, **1971**, *27*, 44.

[8] Vasile, C. *Handbook of Polyolefines*, Marcel Dekker: New York, 2000.

[9] Welgos, R. J. *Encyclopedia of Polymer Science and Engineering*; 2nd ed.; John Wiley: New York, 1988; Vol. 11.

[10] Carothers, W. H.: U.S. Patent 2,130,948 (1938).

[11] Carothers, W. H.; Graves, G. D.: U.S. Patent 2,163,584 (1939).

[12] Reimschuessel, H. K. *J. Polym. Sci.: Macromolecular Reviews* **1977**, *12*, 65.

[13] *Applid Market Information Group*: www.amiplastics.com, 2002

[14] *Plastics News:* www.plasticsnews.com, 2001.

[15] Bottenbruch, L.; Binsack, R. *Technische Thermoplaste*; Carl Hanser Verlag: München, 1998; Vol. 3/4.

[16] Carothers, W. H.; Hill, J. W. *J. Am. Chem. Soc.* **1932**, *54*, 1579.

[17] Southern, J. H.; Porter, R. S. *J. Appl. Polymer Sci.* **1970**, *14*, 2305

[18] Capaccio, G.; Ward, I. M. *Polymer* **1974**, *15*, 233.

[19] Gibson, A. G.; Ward, I. M.; Cole, B. N.; Parsons, B. *J. Mater. Sci.* **1974**, *9*, 1193.

[20] Clark, E. S.; Scott, L. S. *Polymer Eng. Sci.* **1974**, *14*, 682.

[21] Zwijnenburg, A.; Pennings, A. J. *Colloid & Polymer Sci.* **1976**, *254*, 868.

[22] Weenink, W. D. *Nylon-Sulfonic Acid Systems*; Diss. ETH No. 13037, Zürich, 1999.

[23] Smith, P.; Lemstra, P. J. *J. Mater. Sci.* **1980**, *15*, 505.

[24] Smith, P.; Lemstra, P. J.; Booij, H. C. *J. Polym. Sci. Polym. Phys. Ed.* **1981**, *19*, 877.

[25] Brandrup, J.; Immergut, E. H. *Polymer Handbook*; 3rd ed.; John Wiley, Inc.: 1989.

[26] Aharoni, S. M. *n-Nylons: Their Synthesis, Structure, and Properties*; Wiley: Chichester, 1997.

[27] Mandelkern, L. *Crystallization of Polymers*; McGraw-Hill: New York, 1964.

[28] Dole, M.; Wunderlich B. *Makromol. Chem.* **1959**, *34*, 29.

[29] Ubbelohde, A. R. *The Molten State of Matter*; Wiley: Chichester, 1978.

[30] Starkweather Jr., H. W.; Zoller, P.; Jones, G. A. *J. Polym. Sci. Polym. Phys. Ed.* **1984**, *22*, 1615.

[31] Sims, W. M.: German Patent 2,626,273 (1976).

[32] Sims, W. M.; Bliss, A. D.: German Patent 2,225,515 (1972).

[33] Johnson, R.W.; Valdespino, J. M.; Gordon, R.L.; Miller, G.E.; Kight, R.W. *Encyclopedia of Polymer Science and Engineering*; 2nd ed.; John Wiley: New York, 1988; Vol. 11.

[34] Jones, N. A.; Atkins, E. D. T.; Hill, M. J.; Cooper, S. J.; Franco, L. *Polymer* **1997**, *38*, 2689.

[35] Dupont, G.; Champetier, G.; Cohen, J. *J. P. Compt. Rend. Acad. Sci. France* **1957**, *245*, 1542.

[36] Kolbe, H. *Justus Liebigs Ann. Chem.* **1849**, *69*, 257.

[37] Signer, R.; Sprecher, P. *Helv. Chim. Acta* **1947**, *30*, 1001.

[38] Fairweather, D. A. *Proc. Roy. Soc. Edinburgh* **1925**, *45*, 4433.

[39] Ellis, B. A. *Org. Syn., Coll. Vol.* **1941**, *1*, 18.

[40] Bidd, I.; Holdup, D. W.; Whiting, M. C. *J. Chem. Soc., Perkin Trans*. **1987**, *1*, 2455.

[41] Brooke, G. M.; Burnett, S.; Mohammed, S.; Proctor, D.; Whiting, M. C. *J. Chem. Soc., Perkin Trans*. **1996**, *1*, 1635.

[42] Shiio, I.; Uchio, R.: Japanese Patent 51-6750 (1974).

[43] Hata, S.: Japanese Patent 48-26238 (1971).

[44] Seher, A. *Ann. Chem.* **1954**, *589*, 222.

[45] Hünig, S.; Buysch, H.-J.; Hoch, H.; Lendle, W. *Chem. Ber.* **1967**, *100*, 3996.

[46] Hünig, S.; Buysch, H.-J. *Chem. Ber.* **1967**, *100*, 4017.

[47] Schmidt, K. F. *Angew. Chem.* **1923**, *36*, 511.

[48] Wolff, H. *Org. React.* **1946**, *3*, 307.

[49] Zabicky, J. *The Chemistry of Amides*; Wiley: New York, 1970.

[50] Hardy, J. *The Encyclopedia of Basic Materials for Plastics*; Van Nostrand Reinhold: New York, 1967.

[51] Reed, H. W. B. *J. Chem. Soc.* **1954**, 1931.

[52] Shea, K. J.; Walker, J. W.; Zhu, H.; Paz, M. M.; Greaves, J. *J. Am. Chem. Soc.* **1997**, *119*, 9049.

[53] Busch, B. B.; Paz, M. M.; Shea, K. J.; Staiger, C. L.; Stoddard, J. M.; Walker, J. R.; Zhou, X.-Z.; Zhu, H. *J. Am. Chem. Soc.* **2002**, *124*, 3636.

[54] Carothers, W. H. *J. Am. Chem. Soc.* **1929,** *510*, 2548.

[55] Carothers, W. H. *Trans. Faraday Soc.* **1936**, *32*, 39.

[56] Young, R. J.; Lovell, P. A. *Introduction to Polymers*; 2nd ed.;Chapman & Hall: London, 1997.

2. Polyamides 6.24 and 6.34[1]

2.1 Introduction

In Chapter 1, the rationale to produce amphiphilic polyamides by introducing extended aliphatic segments into the polymer backbone has been described. In order to produce high strength fibers, these aliphatic segments should be able to establish a network which consists of their connected aliphatic crystals (see Chapter 1). The latter is most favored to be formed by aliphatic segments which are uniform in length and strictly linear. This is an explicit demand for the synthesis which will be employed to produce the extended aliphatic segments. In addition, these compounds have to be synthesized in high purity in order to use them for polycondensation. Moreover, this chapter focuses upon the extended dicarboxylic acids due to their good synthetic accessibility (cf. Chapter 1). Tetracosanedioic acid (**1**) which was employed for the synthesis of polyamide 6.24 (**PA-6.24**) represents the longest, commercially available linear aliphatic diacid. In order to prepare polyamides with even more extended aliphatic segments, tetratriacontanedioic acid (**2**) was synthesized. As pointed out in Chapter 1 the enamine-coupling route, originally proposed by Hünig *et al.*, was employed for this purpose [1].

In this chapter, the synthesis and certain properties of **PA-6.24** and polyamide 6.34 (**PA-6.34**) are described as examples of a series of polyamides comprising extended aliphatic segments. It will be demonstrated that incorporation of the latter indeed led to polyamides of amphiphilic nature, which potentially made the new materials attractive for a number of potential applications that range from compatibilizers to high strength fibers.

---

[1] This chapter is based on the publication: New Polyamides with Long Alkane Segments: Nylon 6.24 and 6.34: Ehrenstein, M.; Dellsperger, S.; Kocher, C.; Stutzmann, N.; Weder, C.; Smith, P. *Polymer* **2000**, *41*, 3531.

2.2 Results and Discussion

2.2.1 Monomer Synthesis

The tetratriacontanedioic acid (**2**) was synthesized by the enamine-coupling route established by Hünig *et al*. (see Scheme 2.1) [1].

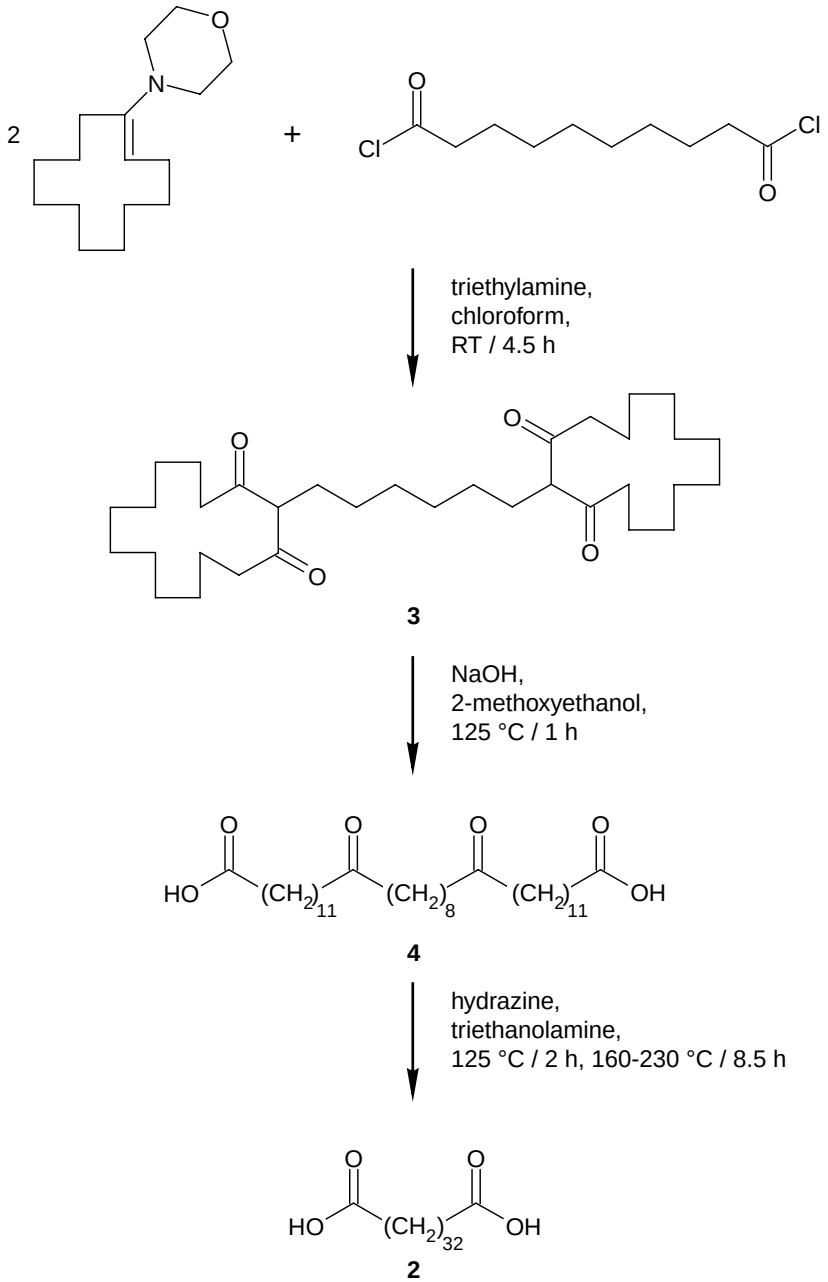

*Scheme 2.1: Synthesis of tetratriacontanedioic acid (**2**).*

The key step is the “chain-extending” cycloaddition of a diketene (which is formed *in situ* from sebacoyl dichloride) with two equivalents of 1-morpholino-cyclododecene. This addition is followed by a ring-opening reaction of 2-hexamethylene-bis-(cyclotetradecanedione-(1,3)) (**3**) with sodium hydroxide. Both keto-functions of the resulting 13,22-dioxo-tetratriacontanedioic acid (**4**) are reduced with hydrazine (Wolff-Kishner reduction). The final overall yield of the best reaction condition was 44 % and was in good agreement with previously published results [1].

2.2.2 Synthesis of Polymers

PA-6.24 and **PA-6.34** were synthesized in a similar way to standard melt-polycondensation of hexamethylenediamine and the appropriate dicarboxylic diacid, as shown in Scheme 2.2 [2].

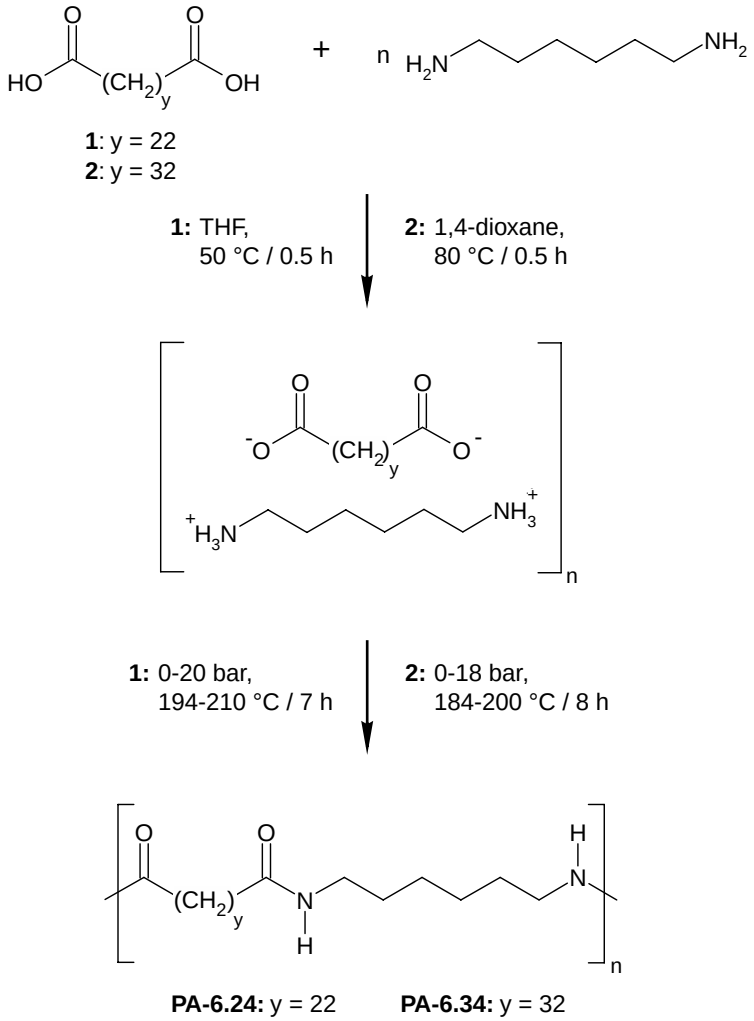

*Scheme 2.2: Synthesis of **PA-6.24** and **PA-6.34**.*

In order to prepare high-molecular weight polymers, first the hexamethylenediamine salts of the dicarboxylic diacids were produced and were thoroughly purified by recrystallization at RT from THF or a (1 : 5 v/v) mixture of dioxane and toluene. Subsequently, these salts were polymerized in an autoclave, which allowed for careful control of the pressure, as well as of temperature during the reaction. Routine application of high pressure (nitrogen) prevented evaporation of hexamethylenediamine at the early stages of the polycondensation. Also, a small excess of the latter was added to the diamine salts of the dicarboxylic diacids to compensate for any potential losses. Typical reaction times were in the range of 7-8 h. Figure shows a typical temperature-pressure-time diagram of the synthesis procedure of **PA-6.34**. The resulting **PA-6.24** and **PA-6.34** were characterized to satisfaction by ^{1}H-NMR and ^{13}C-NMR spectroscopy, and elemental analysis.

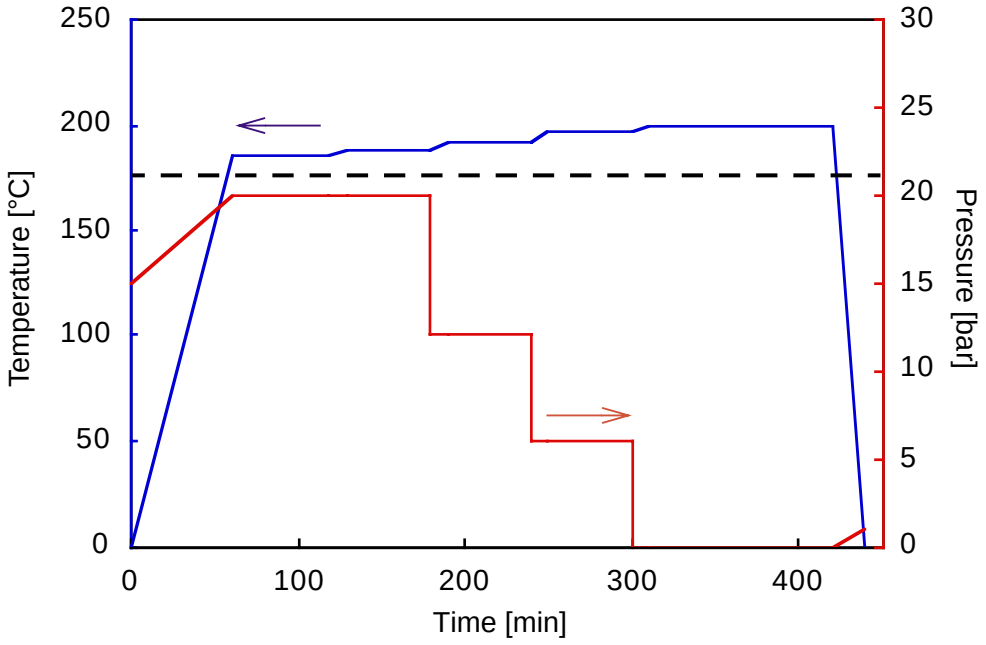

*Figure 2.1: Temperature-pressure-time diagram of the synthesis procedure of **PA-6.34** (blue = temperature; red = pressure; broken line = melting temperature of **PA-6.34** (T_m = 177 °C)).*

2.2.3 Solution Characterization of PA-6.24 and PA-6.34

The solubility of the new polymers was evaluated in a wide range of solvents through visual and optical microscopic examinations. For this purpose, approximately 20

mg of polymer was added under vigorous stirring to 1 mL of selected solvents. The results are summarized in Table 2.1 together with data obtained for common PA-6.6 (Solutia, Vydyne 21). Methanesulfonic acid (MSA) and ethanesulfonic acid (ESA) proved to be good room-temperature solvents for **PA-6.24** and for **PA-6.34**. Classical solvents for common nylons such as *m*-cresol and sulfuric acid, on the other hand, only dissolved **PA-6.24** at ambient temperature and did not dissolve **PA-6.34**. Despite the fact that a substantial aliphatic segment was present in the repeat unit of both **PA-6.24** and **PA-6.34**, common organic solvents such as chloroform or toluene did not dissolve these polymers, not even at elevated temperatures. Also, notorious H-bond-breaking organic solvents such as 1-methyl-2-pyrrolidinone (NMP) and dimethyl sulfoxide (DMSO) did not dissolve **PA-6.24** and **PA-6.34** (cf. Table 2.1).

Table 2.1: Solubility of PA-6.24 and PA-6.34 in various solvents. Key: (-) insoluble; (+) soluble; (G) gel forming, soluble at 80 °C. Experiments were conducted at a concentration of ~ 20 mg polymer per 1 mL of solvent.

Solvent	**PA-6.6**		**PA-6.24**		**PA-6.34**	
	25 ˚C	**50 ˚C**	**25 ˚C**	**50 ˚C**	**25 ˚C**	**50 ˚C**
Toluene	-	-	-	-	-	-
Chloroform	-	-	-	-	-	-
DMF	-	-	-	-	-	-
NMP	-	-	-	-	-	-
DMSO	-	-	-	-	-	-
m-Cresol	+	+	-	+	-	+
Formic acid	+	+	-	-	-	-
Sulfuric acid	+	+	+	+	G	G
Methanesulfonic acid	+	+	+	+	+	+
Ethanesulfonic acid	+	+	+	+	+	+

A most remarkable and interesting phase behavior was observed for **PA-6.34** in H-bonds breaking conc. sulfuric acid (96 - 100 %). **PA-6.34** powder could be suspended in sulfuric acid and during heating the polyamide particles became transparent and started

to stick together. At elevated temperatures, i.e. 80 ˚C, **PA-6.34** seemed to be dissolved, yielding viscous solutions from which fibers could be spun. Upon cooling, a two phase system was formed consisting of a clear (thermo-reversible) gel[2] and residual sulfuric acid. The concentration of **PA-6.34** in the obtained gel depended on the amount of shear stress which was applied during the preparation procedure. Under high shear stress conditions a gel of 7 wt % **PA-6.34** was produced in the cases of lower shear stress a concentration of 20 - 30 wt % **PA-6.34** were found (cf. Experimental Section). These values were determined by measuring the weight of dry **PA-6.34** which was obtained from a corresponding gel after extracting the sulfuric acid with 5 M NaOH solution (30 min), washing twice with 200 mL of distilled water for 24 h, and finally drying under vacuum and at 75 ˚C for 16 h. This procedure was developed by Weenink and has the main advantage that the degradation of the polyamide during the extraction of the sulfuric acid is significant by lower than with distilled water only [3].

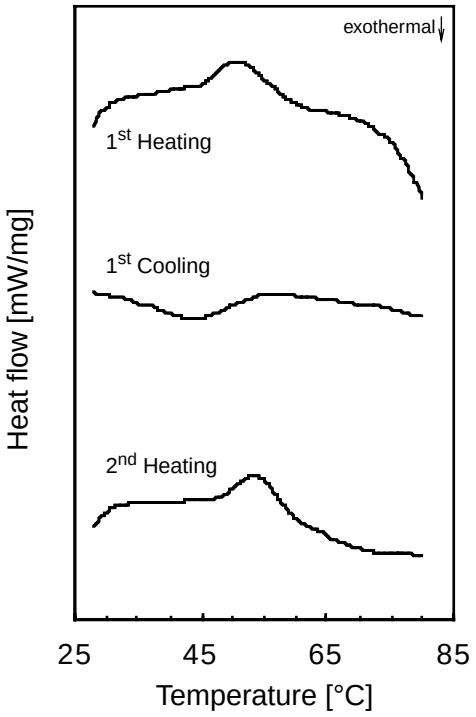

*Figure 2.2: Differential scanning calorimetry scans of **PA-6.34**/sulfuric acid gel (7 wt % **PA-6.34**; heating and cooling rates 10 ˚C/min).*

[2] Gel refers to a solid with no tendency to flow due to formation of a certain network upon cooling, derived from a viscous liquid.

The above gels were also investigated by differential scanning calorimetry (DSC) (cf. Figure 2.2). The DSC scans showed relatively broad endothermal and exothermal signals in the range of 45 to 62 ˚C and 34 to 55 °C, respectively (heating and cooling rate: 10 ˚C/min). The endothermal peak values were determined as a melting temperature of the **PA-6.34**/sulfuric acid gel. Most interestingly, these values matched relatively well with the melting temperatures of *n*-alkanes of a length similar to the aliphatic moiety constituting the polymer as shown in Table 2.2, suggesting that the observed melting transition at around 55 ˚C of these gels corresponds to the melting of the extended aliphatic segments. In addition, the melting temperature of the gel did not depend on the weight concentration of the **PA-6.34**. At higher temperatures (peak value: 89 °C) a strong exothermal signal in the DSC curve was observed which is ascribed to the beginning of the degradation of the polyamides in sulfuric acid.

Table 2.2: Melting temperatures of different n-alkanes [4].

***n*-Alkane**	**$C_{22}H_{46}$**	**$C_{26}H_{54}$**	**$C_{28}H_{58}$**	**$C_{32}H_{66}$**
Melting Temperature [°C]	44.4	56.4	64.5	69.7

In Figure 2.3 a transmission light microscope (interference contrast mode, a) and transmission electron microscopy (TEM) picture (b) of the same **PA-6.34**/sulfuric acid gel is shown. In order to investigate this sample by TEM the sulfuric acid had to be extracted from the sample which was achieved by dipping the sample in liquid ammonia at - 70 ˚C and subsequently washing with distilled water. From these pictures no long range order was observed as known, e.g. for crystalline structures, but a certain kind of structuring. The transmission light microscope of the gel showed areas with disordered fibrous arrangements. Form these arrangements it was concluded that there has to be a certain interaction between this fibrils like, for example, an aliphatic network. This assumption was also supported by TEM pictures. A TEM image showed disordered accumulation of thin filaments. After removing the sulfuric acid with liquid ammonia at - 70 °C the remaining **PA-6.34** polymer chains were not mobile enough to rearrange each other in order to crystallize, for example, in a polyamide typical structure at this low temperature (see Chapter 4, Figure 4.4). Therefore, the observed structure should be

similar to the real structure of the **PA-6.34** in the investigated gel. The filament like structure was, most probably, formed due to the fact that there was a certain short range order established in the former gel based on the aliphatic network.

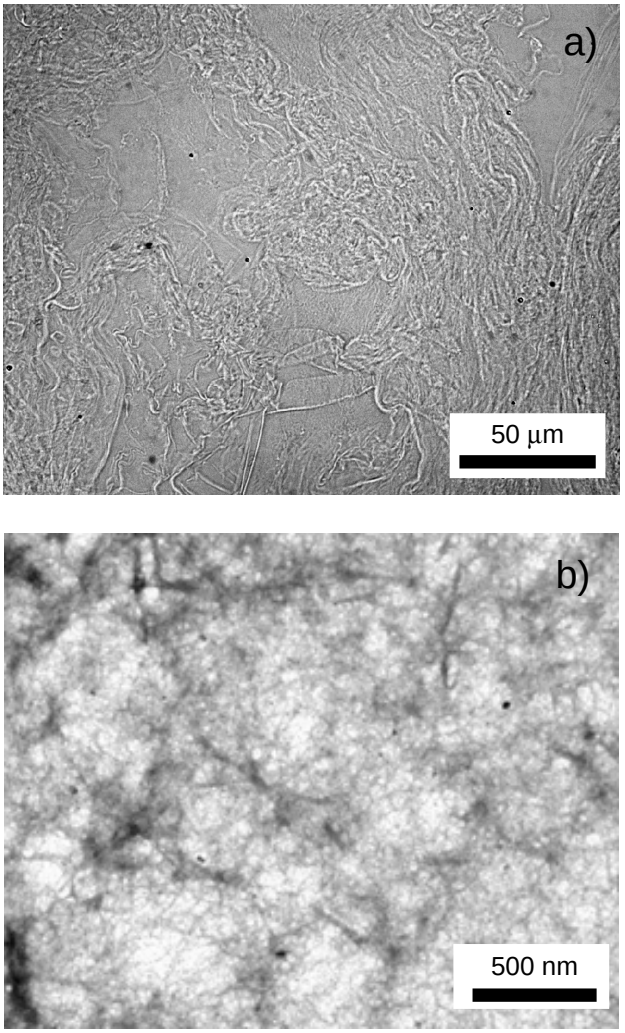

Figure 2.3: a) Transmission light micrograph (interference contrast mode) of a gel of PA-6.34/sulfuric acid. b) Transmission electron microscopy picture of a gel of PA-6.34/ sulfuric acid where the sulfuric acid had been extracted by liquid ammonia.[3]

2.2.4 Molecular Weight

In order to obtain an indication of the molecular weight of the newly synthesized polyamides, the inherent viscosities (η_{inh}) of **PA-6.24** and **PA-6.34** were measured at a polymer concentration of 0.5 g/dL at 25 ˚C in methane sulfonic acid (MSA) and ethane

[3] These pictures were taken by Dr. H. Chanzy visitor from the CERMA V-CNRS, Grenoble.

sulfonic acid (ESA). The results are summarized in Table 2.3. The viscosities measured in ESA (**PA-6.24**: 0.92 dl/g, **PA-6.34**: 0.85 dl/g) appeared to be indicative for the polymeric character of both polyamides in contrast to viscosity measured for **PA-6.34** in MSA which was unexpectedly low (0.09 dl/g). In order to investigate the origin of this deviating behavior in more detail, static light-scattering experiments[4] were carried out on both **PA-6.24** and **PA-6.34** in MSA. These investigations revealed weight-average molecular weights ($\overline{M}_w$) of 35,000 for **PA-6.24** and 30,000 (both ± 5,000) for **PA-6.34**. In addition, light-scattering measurements of **PA-6.34** in MSA revealed a relative small radius of gyration of 260 ± 80 Å in comparison to **PA-6.24** in MSA, which showed a radius of gyration of 350 ± 80 Å. The value of **PA-6.34** was consistent with a small end-to-end distance. This result appeared to explain the unusual low viscosity of this system (η_{inh} = 0.09 dl/g). Unfortunately, fluorescence of ESA prevented comparable experiments in this solvent.

*Table 2.3: Inherent viscosity at RT, c = 0.5 g/dl of **PA-6.24** and **PA-6.34** in MSA and ESA and weight-average molecular weights determined by light scattering in MSA, [b]*

Polyamide	$\overline{M}_w$	η_{inh} **(MSA) [dl/g]**	η_{inh} **(ESA) [dl/g]**
PA-6.24	35,000	0.72	0.92
PA-6.34	30,000	0.09	0.85

2.2.5 Water Absorption and Thermal Properties

The water absorption of the **PA-6.24** and **PA-6.34** was determined by the loss of weight during a TGA measurement at 120 °C under nitrogen atmosphere (see Table 2.4). The investigated polyamide samples were conditioned in a climatic exposure cabinet at 25 °C and 50 % of relative humidity for 24 h.[5] The observed water content of **PA-6.24** and **PA-6.34** were found be located in the expected region based on their amide to methylene group ratio and compared to conventional polyamides.

---

[4] The light-scattering experiments were carried out by Prof. Peter Schurtenberger, Insitute of Polymers, ETH Zürich.

[5] The determination of the water content were conducted by Gaby Riedel, Lehrstuhl für Kunststofftechnik, University of Erlangen-Nürnberg.

Table 2.4: Selected properties of PA-6.24 and PA-6.34 in comparison with those of PA-6.6 and PA-12 [2].

Property	**PA-6.6**	**PA-6.24**	**PA-6.34**	**PA-12**
Melting temperature (DSC)	264 ˚C	189 ˚C	177 ˚C	180 ˚C
Glass transition (DSC)	48 ˚C	54 ˚C	88 ˚C	42 ˚C
Glass transition (DMTA)	80 ˚C	58 ˚C	57 ˚C	62 ˚C
Water content (TGA, 50 % rel. humidity)	2.5 %	1.0 %	0.4 %	0.8 %

Certain thermal characteristics of the present polyamides were investigated using differential scanning calorimetry (DSC), dynamic mechanical thermal analysis (DMTA) and thermogravimetric analysis (TGA) at heating rate of 10 ˚C/min. The results together with data for PA-6.6 and PA-12 are summarized in Table 2.4.

TGA experiments conducted with a heating rate of 10 ˚C/min showed that for both polymers, **PA-6.24** and **PA-6.34,** decomposition set in at around 400 and 420 ˚C in air and nitrogen atmosphere, respectively. DSC scans of **PA-6.24** and **PA-6.34,** recorded at 10 ˚C/min on samples that were once-molten and cooled at a heating rate of 10 ˚C/min, displayed well-defined melting temperatures at 189 ˚C and 177 ˚C (see Figure 2.4), respectively. These values, not surprisingly, were slightly below the melting temperature reported for nylon 6.18 (i.e. 192 ˚C) [5].

In addition, the DSC traces of carefully dried (16 h, 100 ˚C, vacuum) **PA-6.24** showed a glass transition temperature (T_g) at around 54 ˚C; i.e. in the range of the α-relaxation of common nylons [2]. In the case of a melt-pressed film of **PA-6.34** an unexpected high transition was observed at 88 ˚C. In order to investigate the thermal behavior of **PA-6.34** in some more detail, quenching and annealing experiments were performed. In the former, **PA-6.34** was first molten at 205 ˚C for 15 min under inert atmosphere, and subsequently rapidly cooled by immersing the sample in liquid nitrogen. Annealing experiments were conducted in the DSC, in which the samples were tempered at 100 ˚C for 60 h under nitrogen atmosphere. Heating of quenched material was accompanied by a significant recrystallization as can be seen from the DSC heating scan of this sample (Figure 2.5); the latter appeared to indicate a relatively low rate of

crystallization of **PA-6.34**. This observation was not unexpected in view of the very large crystalline unit cell of this polymer and the extensive molecular motion required to form the proper register. The size of the crystalline unit cell will be discussed in Chapter 4. The relative high recrystallization temperature can be explained with the strength of H-bonds. In order to recrystallize, the polyamide chains need a certain mobility. But this mobility was suppressed by the present H-bonds which stayed intact even at elevated temperatures. It is known from IR-spectroscopy that a large number of inter- and intra-molecular H-bonds are still present even in the molten state of aliphatic polyamides [6,7]. Therefore, close to the melting temperature enough H-bonds were broken in order to allow the polyamide chains to recrystallize.

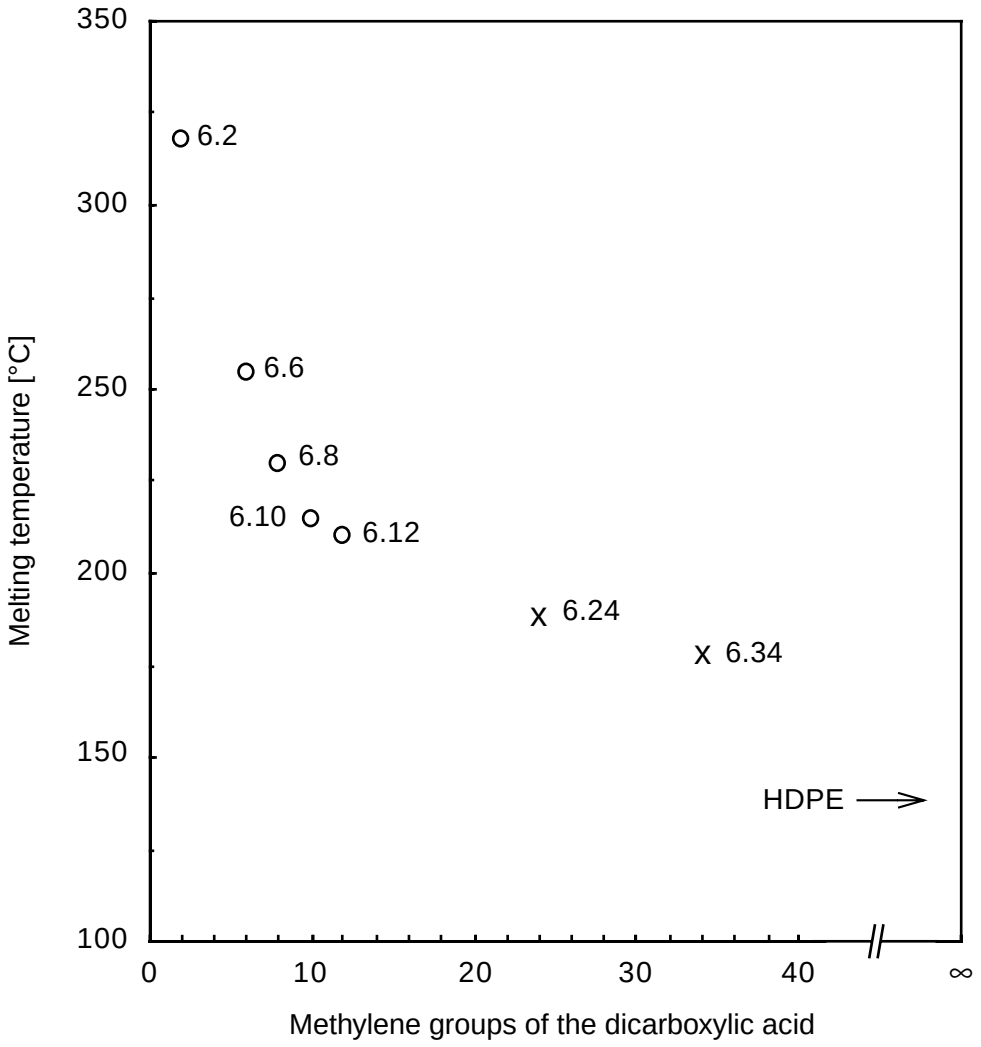

Figure 2.4: Melting temperatures of polyamide series PA-6.y: (o) Refs. [2,8,9]; (x) this work. Also shown is the melting temperature of standard high-density polyethylene (HDPE, 132 ˚C)

DMTA measurements indicated a clear transition at 58 ˚C for **PA-6.24**, which was in good agreement with the T_g found with DSC. For the melt-pressed sample of **PA-6.34**, a transition at 57 ˚C was distinguished, which was lower than the values observed in DSC experiments, but was located in the range of T_g's of common nylons.

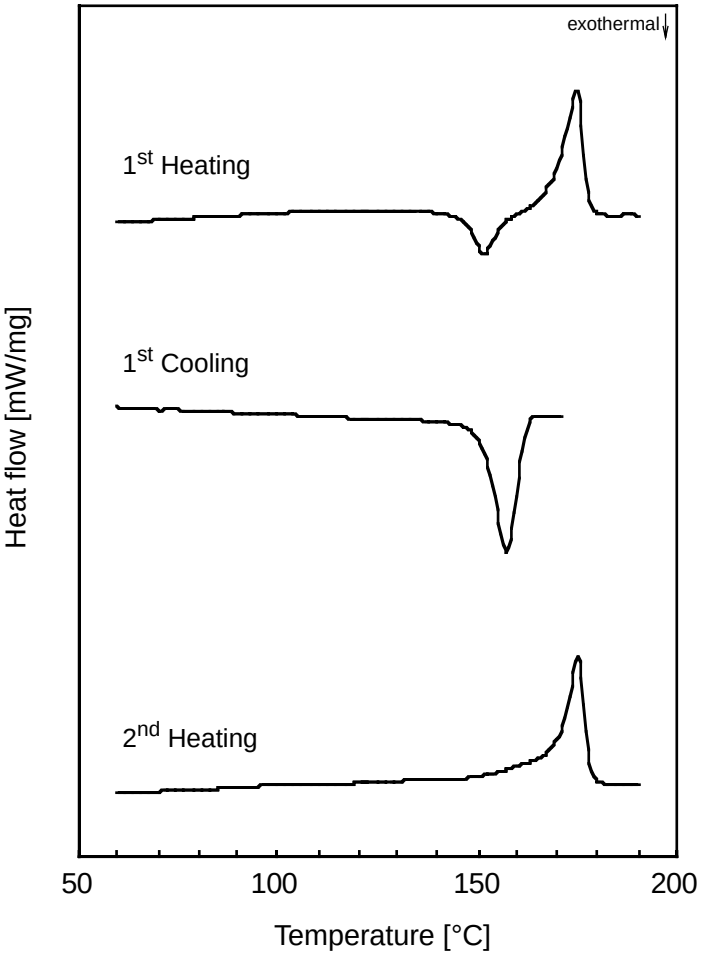

*Figure 2.5: Differential scanning calorimetry scans of **PA-6.34**. The sample was quenched from the melt at 200 ˚C by immersion in liquid nitrogen prior to the first heating scan (heating and cooling rates 10 ˚C/min).*

2.2.6 Mechanical Properties

Dried, melt-pressed polyamide films were prepared and their mechanical properties were investigated by standard tensile tests at different temperatures (Experimental Section). Young's moduli of melt-crystallized, isotropic samples at room temperature were found to be 1.3 GPa for **PA-6.24** and 0.7 GPa for **PA-6.34**; the tensile strengths were 33 and 21 MPa, respectively. In comparison with common nylons, these

values initially appeared to be rather low. However, as illustrated in Figure 2.6, which compares the mechanical properties of the series polyamides 6.y (of comparable molecular weight), the characteristics of **PA-6.24** and **PA-6.34** follow the expected trend, both with respect to mechanical and thermal properties — and indeed in that sense fill the gap between standard polyamides and polyethylene.

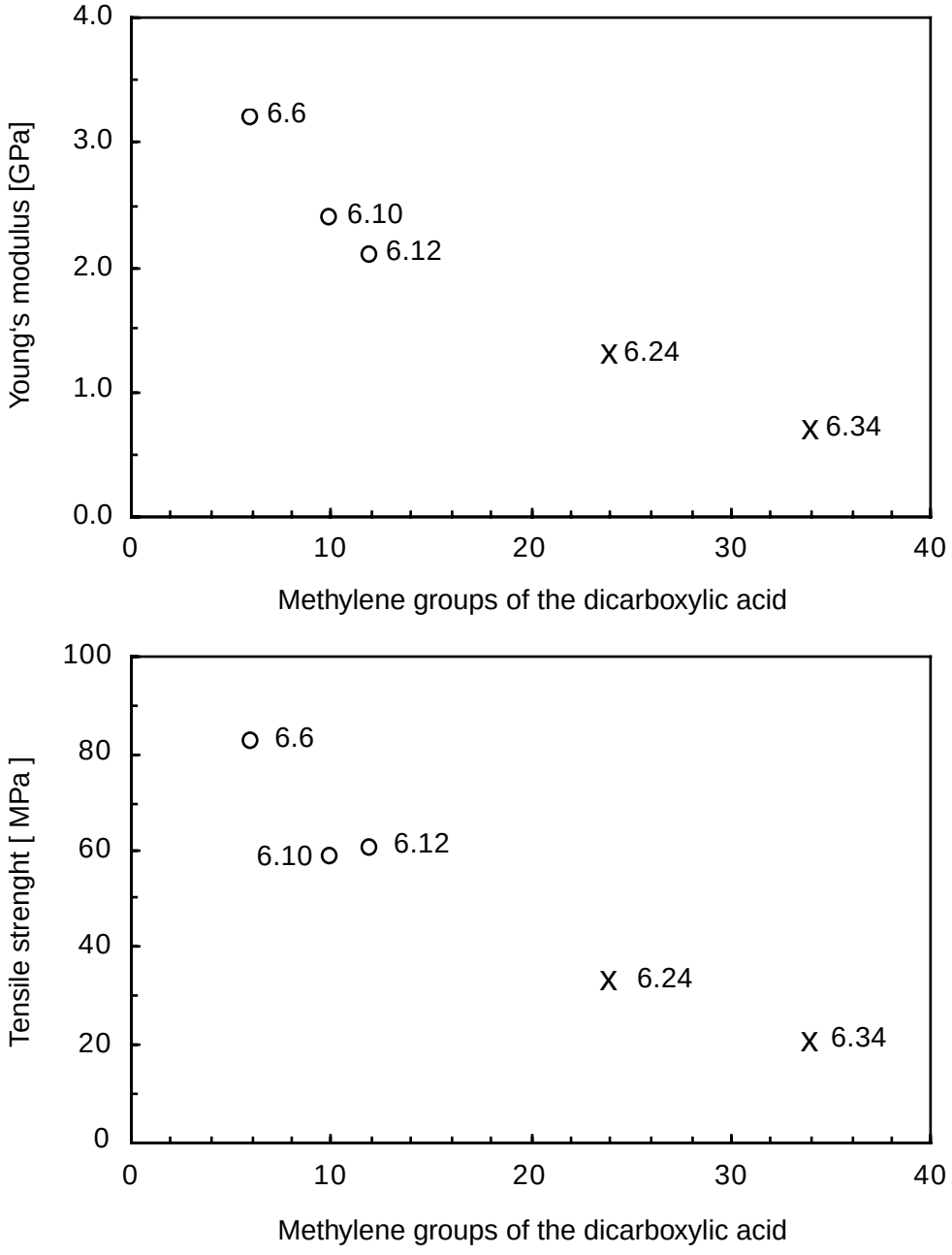

Figure 2.6: Tensile moduli and tensile strengths of melt-crystallized, isotropic, dried samples of polyamides PA-6.y at room temperature: (o) Ref. [2]; (x) this work.

PA-6.34 films were oriented by tensile deformation at a temperature of 150 ˚C, to a maximum draw ratio of up to 5.3 (Figure 2.7). This value is comparable to that observed for standard nylons [10], and is indicative of the reasonable molecular weight of the present materials [11]. Young's modulus of a five times drawn film was determined to be 3.7 GPa. This compared to 5-10 GPa for common 4-5 times drawn nylon 6.6 [3].

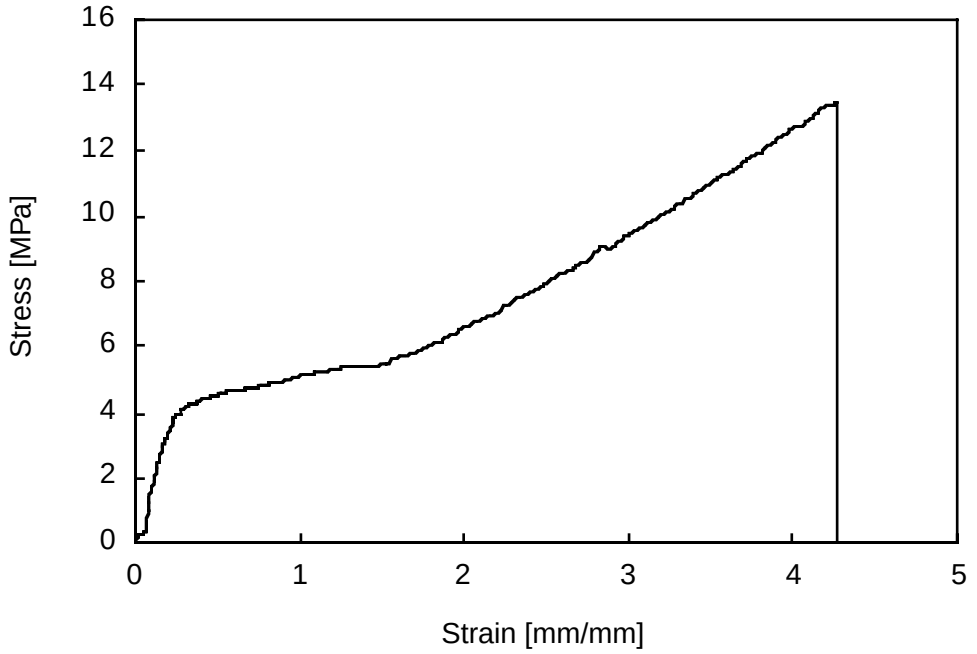

Figure 2.7: Stress-strain curve at 150 ˚C of a dried film of PA-6.34.

2.2.7 Wide-Angle X-ray Diffraction

The X-ray diffraction patterns of **PA-6.24** and **PA-6.34** showed two prominent diffraction signals at 0.44 nm and 0.36 nm (Figure 2.8 a, b), indicative of a significant degree of crystallinity of this material. The X-ray patterns of the oriented **PA-6.24** and **PA-6.34** samples unambiguously show the uniaxial orientation of the drawn films (Figure 2.8 c, d). A detailed analysis of the crystal structure of this polymer and other polyamides is described in Chapter 4.

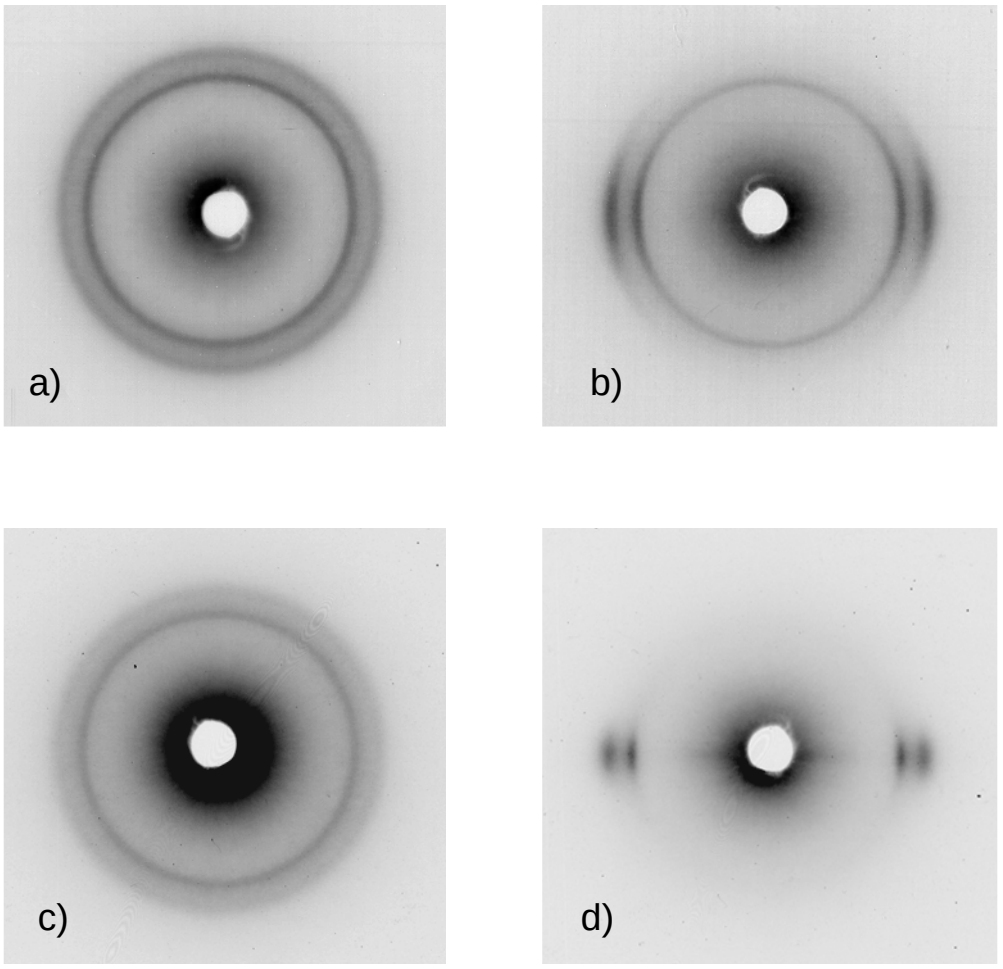

*Figure 2.8: Wide-angle X-ray diffraction patterns of **PA-6.24**: (a) isotropic; (b) drawn at 160 ˚C to a draw-ratio (λ) of 3.8; drawing axis vertical; and **PA-6.34**: (c) isotropic; (d) drawn at 150 ˚C to a draw-ratio (λ) of 5.3; drawing axis vertical.*

2.2.8 Compatibilizing Properties

The (poly-)amphiphilic nature of **PA-6.34** could make this material a potential candidate for application as “compatibilizer” in blends of, for example, polyolefins and nylons. The latter have recently attracted significant interest [12,13], not the least because of recycling of carpet waste. In initial experiments, two different polymer blends were prepared and examined, comprising PA-6, and polyethylene and isotactic polypropylene, respectively. These incompatible blends contained equal weight-fractions of the hydrophilic PA-6 and the hydrophobic polymer, and 5 wt % **PA-6.34** (based on

overall weight). The blends were produced in a mini-twin-screw extruder (see Experimental Section for details). Light-microscopy photomicrographs of melt-compression molded films of the different blends are shown in Figure 2.9, together with the respective reference experiments (no added **PA-6.34**). As is evident from these micrographs, the addition of **PA-6.34** to both blend systems investigated here dramatically decreased the size of the PA-6 and polyolefin domains (cf. Table 2.5).

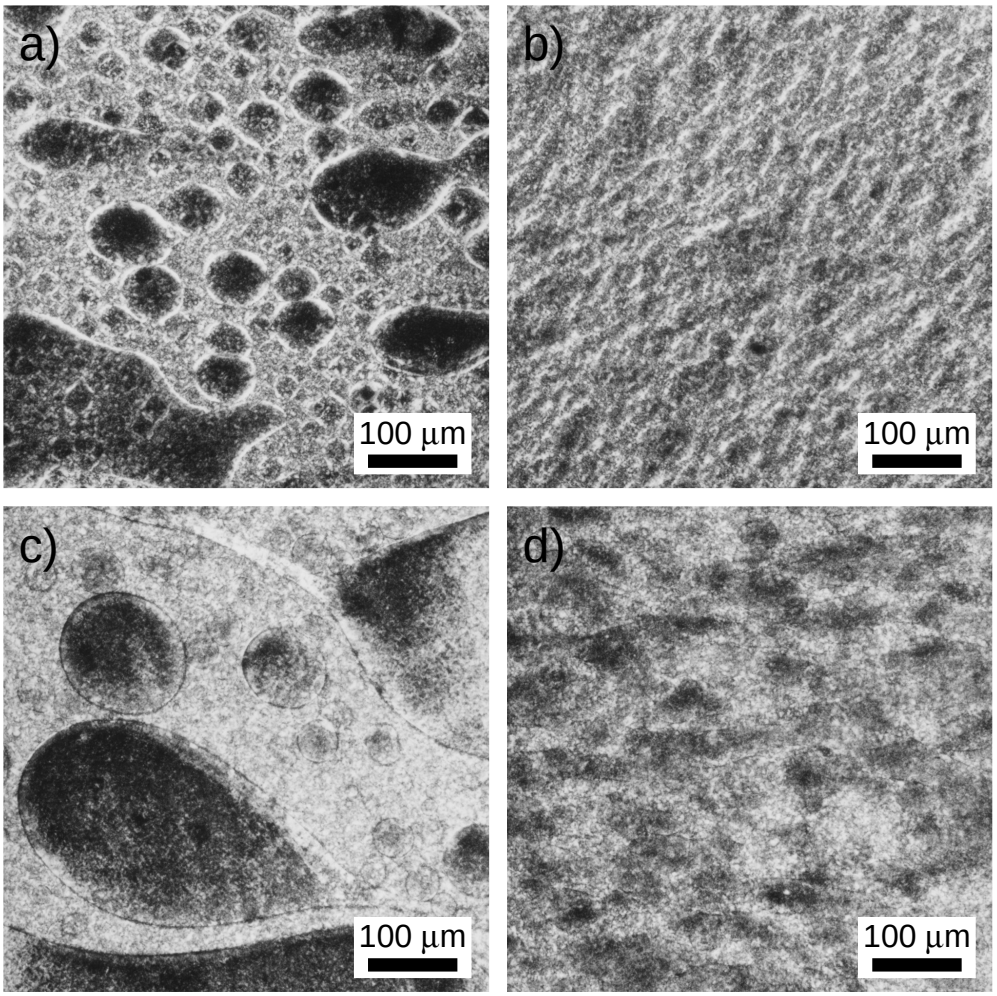

*Figure 2.9: Optical micrographs (phase contrast) of different polymer blends: (a) PA-6/ HDPE (50/50 wt %); (b) PA-6/HDPE/**PA-6.34** (47.5/47.5/5.0 wt %); (c) PA-6/i-PP (50/ 50 wt %); (d) PA-6/i-PP/**PA-6.34** (47.5/47.5/5.0 wt %).*

*Table 2.5: Effect of **PA-6.34** on the domain size of different blends.*

Blend	**Typical Domain Size**	**Domain Size Distribution**
PA-6/HDPE	200 μm	very broad, connected domains
PA-6/HDPE/PA-6.34	5 μm	very narrow, almost homogeneous
PA-6/*i*-PP	200 μm	very broad, connected domains
PA-6/*i*-PP/PA-6.34	50 - 100 μm	broad, some connected domains

2.3 Conclusions

The (melt-polycondensation) synthesis and characterization of **PA-6.24** and **PA-6.34** was presented. The weight-average molecular weights of these new polymers were in the range 30,000–35,000. The thermal and mechanical properties of **PA-6.24** and **PA-6.34** were found to be a new combination of those of common polyamides and polyethylene. **PA-6.34** displayed a most interesting gelation behavior in sulfuric acid, which offered the possibility of new fiber spinning processes. The potentially useful "compatibilizing" property of **PA-6.34** in, e.g. blends of PA-6 and polyolefins was demonstrated.

2.4 Experimental Section

General Methods. All reagents and solvents were purchased from Fluka, Aldrich and Merck, except tetracosanedioic acid (**1**), which was obtained from Acros. Only analytical grade quality chemicals were used. DSC and TGA measurements were performed with a Netzsch DSC 200 and a TG 209 instrument with a heating and cooling rate of 10 ˚C/min, respectively. Melting temperatures (T_m) were determined by DSC

measurements and taken as the peak values of endothermal in the scans. The DMTA measurements were carried out under nitrogen atmosphere with a DMTA 3e Rheometric Scientific instrument. ^{1}H-NMR and ^{13}C-NMR spectral data are expressed in ppm relative to internal TMS standard and were obtained on various Bruker NMR spectrometers. All viscosity measurements were made at 25 ˚C and a concentration of 0.5 g polymer per dL using Ubbelhode capillaries from Schott (type 53020 / II) in combination with a Schott AVS 410 viscometer. Elemental analyses and mass spectra were carried out by the Microanalysis and Mass Spectra Laboratories of the Department of Chemistry of ETH Zürich. X-ray measurements were performed on a Seifert ISO-Debeyflex 2002, using Ni-filtered Cu-K_α radiation (conditions: 12 h or 24 h, 30 mA, 35 kV). All mechanical measurements were carried out on an Instron 4464 tensile tester equipped with a load cell of 10 N. The static light-scattering measurements were carried out with a Malvern 4700 PS/MW spectrometer, equipped with an argon ion laser (Coherent, Innova 200-10, wavelength λ_0 = 488 nm), a digital autocorrelator (Malvern 7032ES/136C), and a computer-controlled and stepping-motor driven variable-angle detection system. Light scattering experiments were performed according to the procedures given elsewhere [14]. Unless otherwise stated, all polyamide samples were dried for at least 12 h at 80 ˚C under vacuum (10 mbar) before they were used for any experiment.

2-Hexamethylene-bis(cyclotetradecanedione-(1,3)) (3). In argon atmosphere, a solution of 1-morpholino-1-cyclododecene (60.02 g, 238.7 mmol), triethylamine (35 mL) and chloroform (30 mL) was cooled to - 6 ˚C. A solution of sebacoyl chloride (21.29 g, 88.6 mmol) in chloroform (30 mL) was added over a period of 16 min in drops to the stirred and cooled solution; the temperature of the reaction mixture was kept below 15 ˚C. After the addition was completed, chloroform (20 mL) was added and the reaction mixture was stirred for 4.5 h at room temperature. The resulting suspension was subsequently homogenized by the addition of chloroform (460 mL). Hydrochloric acid (2.5 M, 250 mL) was added to the clear, yellow solution, and the mixture was stirred for 20 h. The two phases were separated and the aqueous layer was extracted with chloroform (2 x 150 mL). The combined organic phases were washed with diluted, aqueous HCl (3 x 500 mL), dried with $MgSO_4$, and evaporated *in vacuo*. The resulting off-white solid was extracted in boiling methanol for 1 h; and the product was isolated by

filtration at 35 ˚C. The product was recrystallized at RT from ethyl acetate (1200 mL) to yield pure 2-hexamethylene-bis-(cyclotetradecanedione-(1,3)) (**3**) as a white powder (23.7 g, 50.3 %); T_m: 120.9 ˚C and 151.4 ˚C. ^{1}H-NMR (500 MHz, $CDCl_3$, 300 K): δ 3.59 (t, *J* = 7.23 Hz, 2H), 2.50-2.36 (m, 8H), 1.80-1.75 (m, 4H), 1.72-1.64 (m, 4H), 1.62-1.55 (m, 4H), 1.40-1.13 (m, 36H). ^{13}C-NMR (125 MHz, $CDCl_3$; 300 K): δ 206.25 (*C*=O), 68.67 (O=C-*C*H-C=O), 39.67, 29.12, 27.98, 27.37, 26.33, 25.55, 25.36, 24.97, 21.03 (all aliphatic -*C*H_2-). Mass spectrum: m/e 530.3 (M^+ parent). Anal. Calcd for $C_{34}H_{58}O_4$: C, 76.93; H, 11.01; O, 12.06; Found: C, 77.04; H, 11.22; O, 11.86.

13,22-Dioxo-tetratriacontanedioic acid (4). 2,2-Hexamethylene-bis-(cyclotetra-decanedione-(1,3)) (**3**) (23.7 g, 44.6 mmol) was dissolved in 2-methoxyethanol (250 mL) at 125 ˚C, and a hot (115 ˚C) solution of NaOH (11.9 g, 296.9 mmol) in 2-methoxyethanol (155 mL) was added quickly to the rapidly stirred solution. A white solid formed immediately, and stirring became difficult. After stirring for 1 h at 125 ˚C, the reaction mixture was allowed to cool to room temperature, the product was isolated by filtration and washed with 2-methoxyethanol and ethanol. Recrystallization at RT from acetic acid (100 %, 700 mL) yielded 13,22-dioxo-tetratriacontanedioic acid (**4**) (24.33 g, 96.2 %) as a slightly pink powder; T_m: 146.1 ˚C. ^{1}H-NMR (500 MHz, DMSO-d_6, 353 K): δ 2.36 (t, *J* = 7.28 Hz, 8H), 2.17 (t, *J* = 7.36 Hz, 4H), 1.54-1.45 (m, 12H), 1.29-1.19 (m, 36H). ^{13}C-NMR (125 MHz, DMSO-d_6; 353 K): δ 209.77 (CH_2-*C*O-CH_2), 173.68 (-CH_2-*C*OOH), 41.42, 41.40 (-*C*H_2-CO-*C*H_2-), 33.34 (-*C*H_2-COOH), 28.39, 28.34, 28.26, 28.17, 28.15, 28.12, 28.09, 24.07, 22.89, 22.85 (all aliphatic -*C*H_2-). Anal. Calcd for $C_{34}H_{62}O_6$: C, 72.04; H, 11.02; O, 16.93; Found: C, 72.29; H, 11.21; O, 16.66.

Tetratriacontanedioic acid (2). Hydrazine monohydrate (100 mL) was added to a solution of 13,22-dioxo-tetratriacontanedioic acid (**4**) (24.12 g, 42.55 mmol) in triethanolamine (200 mL) and the reaction mixture was stirred for 2 h at 125 ˚C. After cooling to 80 ˚C, a hot solution of KOH (13.2 g, 235.2 mmol) in triethanolamine (70 mL) was added to the reaction mixture. The resulting solution was vigorously stirred, heated to 160 ˚C and, after stirring for 20 min at this temperature, carefully heated to 230 ˚C during 105 min. The solution was stirred at 230 ˚C for 6.5 h, cooled to RT during that cooling a solid precipitated. Water (350 mL) was added, the mixture was heated to 100 ˚C and the resulting suspension was filtered while hot. The resulting solid was first

recrystallized at RT from acetic acid (100 %, 600 mL) and then from a mixture of 1,4-dioxane (4500 mL) and 12 M HCl (75 mL). Tetratriacontanedioic acid (**2**) was obtained as white powder (21.10 g, 92 %); T_m: 133.0 ˚C. ^{1}H-NMR (300 MHz, DMSO-d_6, 353 K): δ 2.17 (t, J = 7.30 Hz, 4H), 1.54-1.47 (m, 4H), 1.37-1.24 (m, 58H). ^{13}C-NMR (125 MHz, DMSO-d_6; 353 K): δ 173.61 (-*C*OOH), 33.36 (-*C*H_2-COOH), 28.51, 28.24, 28.15, 24.10 (all aliphatic -*C*H_2-). Anal. Calcd for $C_{34}H_{66}O_4$: C, 75.78; H, 12.34; O, 11.88; Found: C, 75.33; H, 12.53; O, 12.33.

Polyamide 6.24. Tetracosanedioic acid (**1**) (2.17 g, 5.45 mmol) was dissolved in THF (110 mL) at 50 ˚C and a solution of hexamethylenediamine (0.66 g, 5.65 mmol) in THF (15 mL) was added under vigorous stirring. The hexamethylenediamine-tetracosanedioic acid salt immediately precipitated. The mixture was stirred for another 30 min at 50 ˚C, allowed to cool to room temperature, and the white product was collected by filtration. The hexamethylenediamine-tetracosanedioic acid salt was recrystallized at RT from a mixture of ethanol (130 mL) and water (40 mL), and was obtained as white powder (2.30 g, 86 %); T_m: 161.4 ˚C.

A glass tube was charged with hexamethylenediamine-tetracosanedioic acid salt (1.68 g, 3.42 mmol) and a slight excess of hexamethylenediamine (22 mg, 0.19 mmol) was added. The glass tube was snugly fitted into an autoclave. After the autoclave was evacuated and flushed with nitrogen and after this cycle had been repeated three times, a nitrogen pressure of 15 bar was applied. The reaction was subsequently started by quickly raising the autoclave temperature to 194 ˚C; an increase in pressure to about 20 bar was observed. After keeping the autoclave for 2 h at 194 ˚C, the temperature was increased to 202 ˚C. After 1.5 h under these conditions, the pressure was decreased (10 bar) and the autoclave was kept for 2 h. In a last step, a vacuum (< 0.1 mbar) was applied, the temperature was increased to 210 ˚C, and the reaction was continued for another 2 h. The autoclave was then cooled to room temperature. The resulting **PA-6.24** was obtained as a white solid (1.29, 83 %) and was pulverized in a freezing mill; T_m: 189.0 ˚C. ^{1}H-NMR (300 MHz, phenol-d_6, 353 K): δ 3.17 (t, J = 7.20, 4H), 2.16 (t, J = 7.60, 4H), 1.64 (t, J = 7.00, 4H), 1.26-1.45 (m, 40H), 1.05-1.16 (m, 4H). ^{13}C-NMR (300 MHz, phenol-d_6, 300 K): δ 176.32 (-*C*ONH-), 40.13 (-CONH-*C*H_2-), 36.97 (-*C*H_2-CONH-), 29.90, 29.83, 29.77, 29.61, 29.38, 29.24, 26.39, 26.11 (all aliphatic -*C*H_2-). Anal. Calcd for

$C_{30}H_{58}N_2O_2$: C, 75.26; H, 12.21; N, 5.85; O, 6.68; Found: C, 75.06; H, 12.11; N, 5.89; O, 7.07.

Polyamide 6.34. Tetratriacontanedioic acid (**2**) (5.39 g, 10.00 mmol) was dissolved in 1,4-dioxane (400 mL) at 90 ˚C and a solution of hexamethylenediamine (1.16 g, 10.00 mmol) in 1,4-dioxane (50 mL) was added under vigorous stirring. The hexamethylenediamine-tetratriacontanedioic acid salt immediately precipitated. The mixture was stirred for another 30 min at 100 ˚C, allowed to cool to room temperature, and the white product was collected by filtration. The hexamethylenediamine-tetratriacontanedioic acid salt was recrystallized at RT from a mixture of 1,4-dioxane (200 mL) and toluene (1000 mL), and was obtained as white powder (5.44 g, 83 %); T_m: 157.7 ˚C.

A glass tube was charged with hexamethylenediamine-tetratriacontanedioic acid salt (5.25 g, 8.01 mmol) and a slight excess of hexamethylenediamine (19 mg, 0.16 mmol) was added. The glass tube was snugly fitted into an autoclave. After the autoclave was evacuated and flushed with nitrogen and this cycle had been repeated three times, a nitrogen pressure of 16 bar was applied. The reaction was subsequently started by quickly raising the autoclave temperature to 184 ˚C; an increase in pressure to about 18 bar was observed. The temperature was gradually increased to 192 ˚C over a period of 3.5 h. The pressure was then decreased, and the polycondensation was continued at a pressure of 6 bar and temperature of 192 ˚C for 2 h. Finally, a vacuum (< 0.1 mbar) was applied, the temperature was increased to 200 ˚C, and the reaction was continued for another 2.5 h. The autoclave was then cooled to room temperature. The resulting **PA-6.34** was obtained as a white solid (4.21 g, 85 %) and was pulverized in a freezing mill; T_m: 177.0 ˚C. ^{1}H-NMR (300 MHz, phenol-d_6, 353 K): δ 3.17 (t, *J* = 7.20, 4H), 2.16 (t, *J* = 7.60, 4H), 1.64 (t, *J* = 7.00, 4H), 1.21-1.50 (m, 60H), 1.06-1.18 (m, 4H). ^{13}C-NMR (300 MHz, phenol-d_6, 300 K): δ 176.31 (-*C*ONH-), 40.12 (-CONH-*C*H_2-), 36.97 (-*C*H_2-CONH-), 29.89, 29.77, 29.62, 29.38, 29.24, 26.39, 26.11 (all aliphatic -*C*H_2-). Anal. Calcd for $C_{40}H_{78}N_2O_2$: C, 77.61; H, 12.70; N, 4.53; O, 5.17; Found: C, 77.61; H, 12.63; N, 4.68; O, 5.14.

Gel Preparation. All these experiments were conducted in a glove-bag filled with nitrogen.

Gel preparation for the transmission light microscope and TEM investigations. 0.7 mg of **PA-6.34** (dried for 16 h at 75 ˚C under vacuum) were dissolved in 1.355 g of ESA. 10 mL of 99.999 % sulfuric acid were added to this solution and subsequently shaken for just a moment. After 14 h a white precipitation appeared at the top of this mixture. For TEM investigation, a small drop from the top was placed on a carbon coated gold grid. This grid was washed in liquid ammonia at - 70 ˚C for a minute and subsequently washed in distilled water for a few minutes in order to remove the sulfuric acid and potential salts.

Gel preparation for the estimation of the polyamide concentration in the gel and the DSC investigations. Three different mixtures of **PA-6.34** powder and sulfuric acid (99.999 %, concentrations see Table) were manually stirred at 65 ˚C for 5 min in a special glass-KPG-stirrer in order to applied shear. During that procedure the heterogeneous mixtures became clear and optically homogeneous. It was stirred until the mixture was cooled down to RT (see Figure 2.10). Two gels with a different **PA-6.34** content were found in each mixture. The reason was the different shear force due to the construction in the special glass-KPG-stirrer. The force between the walls of the KPG-stirrer-inliner and the KPG-stirrer tubular jacket was much stronger than at the bottom of the special glass-KPG-stirrer due to the very distance between the walls. Consequently, the mixing of the **PA-6.34**/sulfuric acid mixture at walls was more intensive than at the bottom at the same time.

Table 2.6: Preparation of the PA-6.34/sulfuric acid-gels.

Mixture	PA-6.34 (g)	Sulfuric Acid (99.999 %, g)	PA-6.34 in Gel (bottom, wt %)	PA-6.34 in Gel (between, wt %)
A	0.053	0.385	27.1	-
B	0.054	0.500	28.1	6.9
C	0.054	0.736	26.1	6.8

The **PA-6.34** content in the gels was determined by washing the corresponding gel sample three times with 200 mL water for 72 h. Subsequently, the obtained polymer was dry under vacuum (< 0.1 mbar) at 80 °C for 24 h.

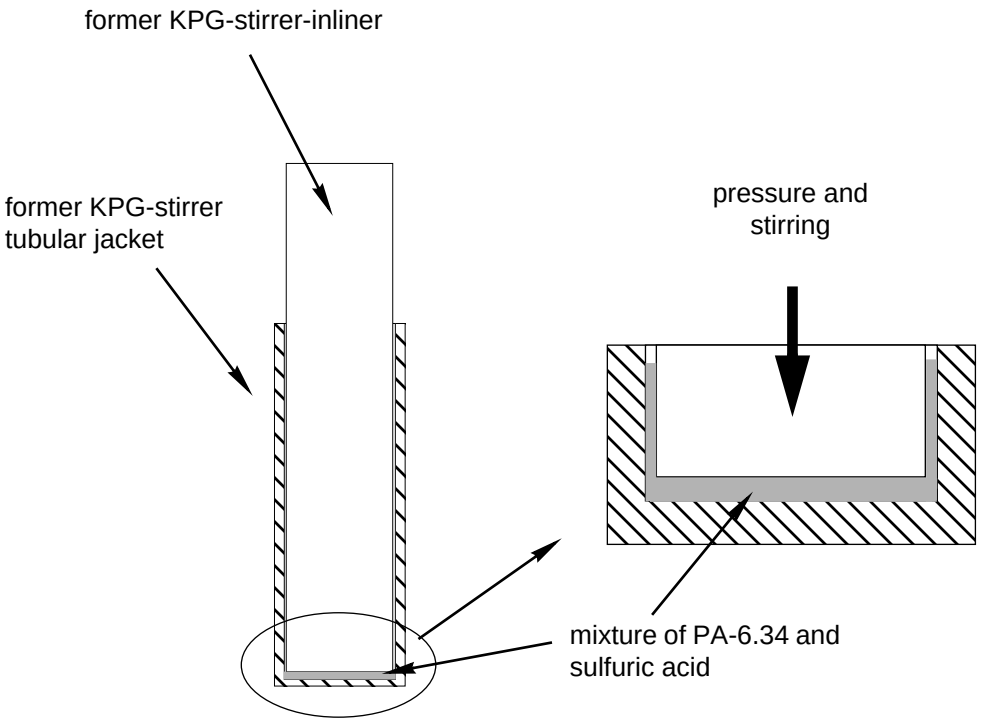

Figure 2.10: Special glass-KPG-stirrer with a mixture of PA-6.34 and sulfuric acid.

Film Preparation. Polyamide film samples were produced by compression molding the polymers between two poly(tetrafluoroethylene) (PTFE) sheets of a thickness of 0.4 mm. **PA-6.24** and **PA-6.34** powders were filled into a mold (length/ width/thickness 40.00/37.00/0.05 mm), and heated at 205 ˚C and 195 ˚C, respectively. After 5 minutes a force of 1.0 ton was applied for 2 min.; subsequent quenching to ambient resulted in films of a thickness of about 80 μm.

Mechanical Characterization. Mechanical tensile testing of the films was performed in a temperature range of 25 ˚C to 150 ˚C and at a strain rate of 100 %/min on dog-bone shaped samples (test area = 12.7 mm x 2 mm). For this purpose a tensile tester (Instron 4464) equipped with a controlled atmosphere chamber was employed.

Blend Preparation. A twin-screw co-rotating mini-mixer (commercially available from DACA Instruments, Santa Barbara, CA) was used for all blending experiments. In order to prevent degradation of the polymers, the entire process of feeding, mixing, and extrusion was carried out under a constant flow of nitrogen (5 L/min). The mixer was

preheated to a temperature of 240 ˚C before adding the polymers in the following order: polyethylene (DSM, $\overline{M}_w$ = 100,000) or isotactic polypropylene (Polysciences, $\overline{M}_w$ = 220,000), respectively, polyamide 6 (Polysciences, $\overline{M}_w$ = 35,000), and,finally, **PA-6.34**. All blends investigated comprised a 1:1 w/w ratio of the polyolefin and PA-6, and in the case of the compatibilized blends a total weight-fraction of 5 wt % of **PA-6.34** was used. The mixer drive was set to 50 rpm for the filling process. The blends were extruded in recycling-mode for 10 min at speed of 150 rpm. Before discharging, the speed of the mixer was reduced to 50 rpm. Thin films of a thickness of approximately 100 μm were prepared as described above, and pressed at a temperature of 240 ˚C as detailed above.

Blend Characterization. A Leica DMRX light microscope in transmitted light mode (phase contrast) was used for optical investigation of the polymer blend films. The prepared polymer films were placed on a glass slide, immersed with paraffin oil and covered with a cover glass. The paraffin oil was found to increase the depth of focus to a large extent and give a better contrast.

2.5 References

[1] Hünig, S.; Buysch, H.-J. *Chem. Ber.* **1967**, *100*, 4017.

[2] Kohan, M. I. *Nylon Plastics Handbook*; Carl Hanser Verlag: Munich, 1995.

[3] Weenink, W. D. *Nylon-Sulfonic Acid Systems*; Diss. ETH No. 13037, Zürich, 1999.

[4] Lide, D. R. *CRC Handbook of Chemistry and Physics*; CRC Press: Boca Raton, 1995-1996.

[5] Jones, N. A.; Atkins, E. D. T.; Hill, M. J.; Cooper, S. J.; Franco, L. *Polymer* **1997**, *38*, 2689.

[6] Skrovanek, D. J.; Howe, S. E.; Painter, P. C.; Coleman, M. M. *Macromolecules* **1985**, *18*, 1676.

[7] Skrovanek, D. J.; Painter, P. C.; Coleman, M. M. *Macromolecules* **1986**, *19*, 699.

[8] Brandrup, J.; Immergut, E. H. *Polymer Handbook*; 3rd ed.; John Wiley, Inc.: 1989.

[9] Vasile, C. *Handbook of Polyolefines*, Marcel Dekker: New York, 2000.

[10] Postema, A. R.; Smith, P.; English, A. D. *Polymer Commun.* **1990**, *31*, 444.

[11] Smith, P.; Matheson, R. R.; Irvine, P. A. *Polymer Commun.* **1984**, *25*, 294.

[12] Tang, T.; Lei, Z.; Huang, B. *Polymer* **1996**, *37*, 3219.

[13] Ohlsson, B.; Hassander, H.; Törnell, B. *Polymer* **1998**, *39*, 4715.

[14] Grob, M. C.; Schurtenberger, P.; Suter, U. W. *Macromol. Chem. Phys.* **1995**, *196*, 1391.

3. Polyamides x.34: Synthesis and Characterization

3.1 Introduction

In Chapter 2 the synthesis of first examples of a new class of linear aliphatic polyamides which contain extended aliphatic segments, PA-6.24 and PA-6.34, was reported. Their thermal and mechanical properties were, not unexpectedly, found to be between those of common linear aliphatic AABB polyamides and polyethylene. In the case of PA-6.34 a most interesting thermo-reversible gelation behavior in sulfuric acid was found, which among other things offered the possibility of new fiber spinning processes (see Chapter 1, Figure 1.3). In addition, it was possible to demonstrate the potentially useful “compatibilizing” property of PA-6.34 in, e.g., blends of PA-6 and polyolefins. In view of the most interesting properties of PA-6.34, other members of the polyamides x.34 were synthesized, in order to systematically study their properties.

Thus, in this chapter the synthesis and certain properties of **PA-2.34, PA-4.34**, **PA-8.34, PA-10.34** and **PA-12.34** are discussed. It will be demonstrated that these new polyamides show similar amphiphilic characteristics as PA-6.34 which complete and broaden the scope of the presently investigated novel polyamides.

3.2 Results and Discussion

3.2.1 Synthesis of Polymers

PA-2.34, **PA-4.34**, **PA-8.34**, **PA-10.34** and **PA-12.34** were synthesized by the standard melt-polycondensation of tetratriacontanedioic acid and the appropriate diamine, as shown in Scheme 3.1. The diacid had been prepared by the methods described in Chapter 1. As discussed before, in order to prepare adequate molecular weight polymers, the diamine salts of the dicarboxylic diacids were produced. Typical reaction times were in the range of 7-8 h, except for the **PA-2.34** which was reacted for

12 h. In case of the latter, the differences between the monomers (with respect to molecular weight and polarity) were most pronounced among the systems, possibly leading to problems of mixing during the polymerization. Thus, in order to achieve a high-molecular weight polyamide, the polycondensation was conducted with a slightly modified polymerization protocol which included a longer reaction time (cf. Experimental Section for details). The chemical structures of all polyamides prepared were characterized to satisfaction by ^{1}H-NMR spectroscopy and elemental analysis.

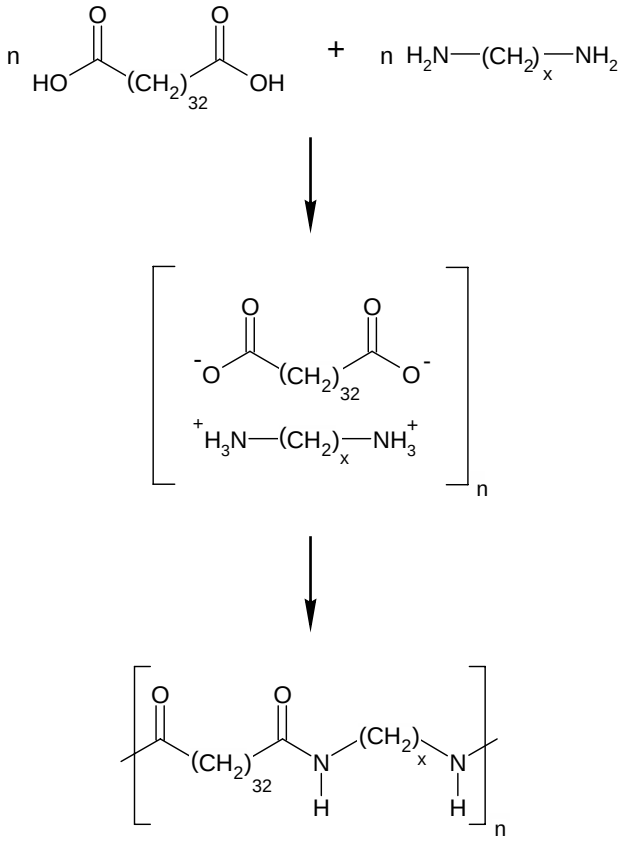

*Scheme 3.1: Synthesis of **PA-x.34** (x = 2, 4, 6, 8, 10, 12).*

3.2.2 Solution Characterization of the Series PA-x.34.

The solubility in a wide range of solvents of the new polymers was evaluated through visual examinations. For this purpose, approximately 2 wt % of polymer were added under vigorous stirring to 1 mL of a selected solvent. The results are summarized in Table 3.1, together with data obtained with common PA-6.6 (Solutia, Vydyne 21) and PA-6.34. Methanesulfonic acid (MSA) and ethanesulfonic acid (ESA) proved to be good

Table 3.1: Solubility of PA-x.34 in various liquids. Key: (-) insoluble; (+) soluble; (G) forms gel; [1] soluble at 150 °C; [2] soluble at 80 °C.

Solvent	**PA-2.34**		**PA-4.34**		**PA-6.34**		**PA-8.34**		**PA-10.34**		**PA-12.34**	
	25 ˚C	**50 ˚C**	**25 ˚C**	**50 ˚C**	**25 ˚C**	**50 ˚C**	**25 ˚C**	**50 ˚C**	**25 ˚C**	**50 ˚C**	**25 ˚C**	**50 ˚C**
n-Heptane	-	-	-	-	-	-	-	-	-	-	-	-
Toluene	-	-	-	-	-	-	-	-	-	-	-	-
1,2,3,4-Tetrahydronaphthalene	G[1]	G[1]	G[1]	G[1]	G[1]	G[1]	G[1]	G[1]	G[1]	G[1]	G[1]	G[1]
DMF	-[1]	-[1]	-[1]	-[1]	-[1]	-[1]	-[1]	-[1]	-[1]	-[1]	-[1]	-[1]
DMSO	-	-	-	-	-	-	-	-	-	-	-	-
m-Cresol	-	+	-	+	-	+	-	+	-	+	-	+
Formic acid	-	-	-	-	-	-	-	-	-	-	-	-
Sulfuric acid	G[2]	G[2]	G[2]	G[2]	G[2]	G[2]	G[2]	G[2]	G[2]	G[2]	G[2]	G[2]
Methanesulfonic acid	+	+	+	+	+	+	+	+	+	+	+	+
Ethanesulfonic acid	+	+	+	+	+	+	+	+	+	+	+	+

room-temperature solvents for the whole series of polyamides containing tetratriacontanedioic acid. Classical solvents for common nylons such as sulfuric acid and *m*-cresol, on the other hand, did not dissolve the present polymers at ambient temperature. Except at 50 °C, the latter dissolved PA-x.34. Common non-polar organic solvents such as toluene did neither dissolve these polymers, nor caused swelling, not even at elevated temperatures. Also, notorious H-bond-breaking organic solvents such as 1-methyl-2-pyrrolidinone (NMP) and dimethyl sulfoxide (DMSO) did not dissolve the new polyamides at room temperature and 50 ˚C. But, high boiling solvents like *n,n*-dimethylformamide (DMF) and 1,2,3,4-tetrahydronaphthalene were proven to be high temperature (above 150 °C) solvents, whereas dodecane was not able to do so. However, the entire series of polyamides x.34 showed the same remarkable thermo-reversible gelation in sulfuric acid as already described for PA-6.34 in Chapter 2. Figure 3.1 shows the differential scanning calorimetry scans of **PA-2.34**/sulfuric acid gel (a) and **PA-12.34**/sulfuric acid gel (b) at heating and cooling rates of 10 ˚C/min. Melting temperatures of these gels ranged from 41 to 68 ˚C, which fitted well with the observed values of PA-6.34 described in Chapter 2. **PA-2.34** represents a particularly interesting material in this context. The gel based on this polymer and sulfuric acid did not only show the highest melting temperature, but was also found to recrystallize upon the heating as it is evident from the DSC scan shown in Figure 3.1

This phenomenon of **PA-2.34** is well-known in the literature for polymer gels, and is ascribed to the enhanced mobility of the chains at the beginning of the melting process enabling them to recrystallize at this temperature [1,2]. A possible explanation, why only **PA-2.34** showed this behavior, could be that the mobility of the **PA-2.34** polymer chains were quite limited due to the ethylenediamine segment in comparison to the other PA-x.34 polymers. Consequently, the ability to form perfect crystals was reduced. Therefore, the gain of mobility at the melting temperature had, most probably, a more significant effect upon the **PA-2.34** chains than on the others.

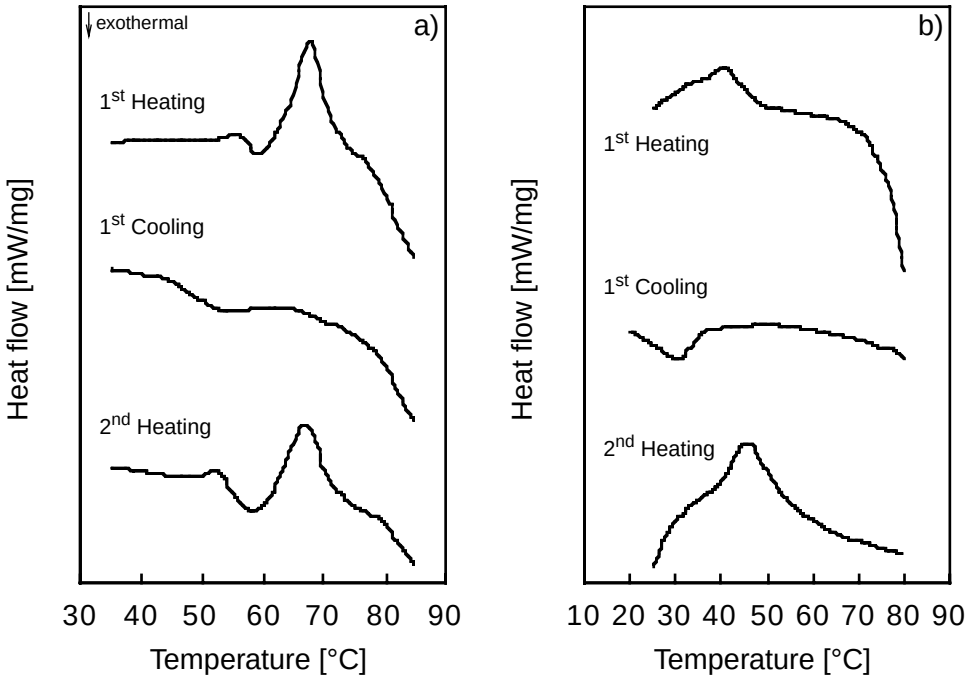

*Figure 3.1: Differential scanning calorimetry scans of **PA-2.34**/sulfuric acid gel (12 wt % **PA-2.34**) a) and **PA-12.34**/sulfuric acid gel (12 wt % **PA-2.34**) b) (heating and cooling rates 10 ˚C/min).*

Interestingly, it was also possible to dissolve the new polyamides in high boiling apolar solvents which favorable interact with the polymer‘s aliphatic segments. For example, above 150 ˚C, all PA-x.34 dissolved in 1,2,3,4-tetrahydronaphthalene. Upon decreasing the temperature, the polyamide/1,2,3,4-tetrahydronaphthalene solution started to form a gel. This effect could be attributed to the reformation of hydrogen bonds between the amide groups, while the aliphatic parts of the dicarboxylic acid remained “dissolved” in the hydrocarbon solvent. Accordingly, the gelation temperature depended on the concentration of the amide groups in the investigated polyamide x.34 as shown in the Figure 3.2. The melting temperatures were measured on gels prepared from 37.5 wt % PA-x.34 and 1,2,3,4-tetrahydronaphthalene, and are based on the second heating of a DSC measurement (10 ˚C/min). These gelation properties were significant evidence of the amphiphilic character for the novel polyamides x.34.

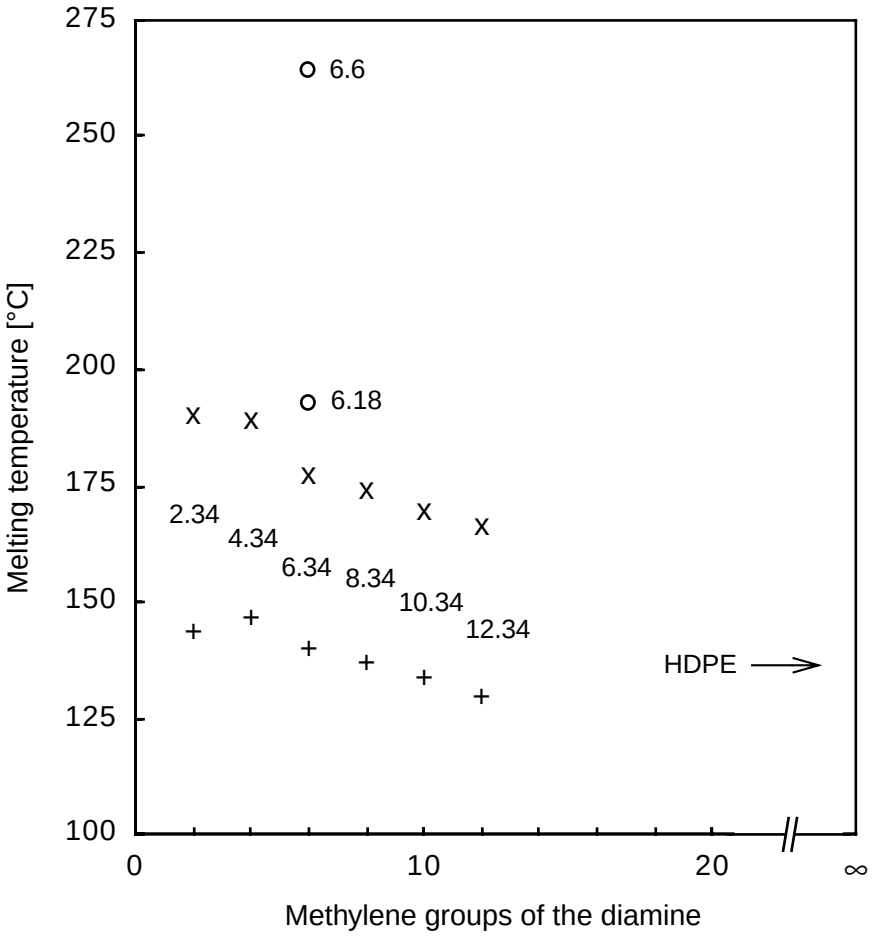

Figure 3.2: Melting temperatures of polyamides PA-x.34 (x) and of PA-x.34 / 1,2,3,4-tetrahydronaphthalene gel (37.5 wt % polyamide) (+); For the propose of comparison, the values of PA-6.6, PA-6.18 (o) and high-density polyethylene are also included [3-5].

In order to obtain an indication of the molecular weight of the newly synthesized polyamides, the inherent viscosities of **PA-2.34, PA-4.34**, **PA-8.34, PA-10.34** and **PA-12.34** were measured at a polymer concentration of 0.5 g/dL at 25 ˚C in ESA. The results are summarized in Table 3.1. The inherent viscosities were in the range of 0.44 – 0.52 dl/g. In Chapter 2, it was shown that an inherent viscosity of 0.85 of PA-6.34 in ESA corresponds to a weight-average molecular weight ($\overline{M}_w$) of 30,000 ± 5,000. Thus, the observed inherent viscosities of **PA-2.34, PA-4.34**, **PA-8.34, PA-10.34** and **PA-12.34** indicate, in comparison with the inherent viscosity of PA-6.34, the polymeric character of these polyamides.

Table 3.1: Viscosity of PA-x.34 in ethanesulfonic acid, measured at RT, and with c = 0.5 g/dL.

Polyamide	**η_{inh}(ESA), dL/g**
PA-2.34	0.44
PA-4.34	0.52
PA-6.34	0.85
PA-8.34	0.48
PA-10.34	0.51
PA-12.34	0.47

3.2.3 Thermal Properties

Thermal characteristics of the present polyamides were investigated using differential scanning calorimetry (DSC), dynamic mechanical thermal analysis (DMTA) and thermogravimetric analysis (TGA) at heating rates of 10 or 20 ˚C/min. The results, together with data for PA-6.34 are summarized in Table 3.2.

Table 3.2: Thermal properties of PA-x.34.

Property	**PA-2.34**	**PA-4.34**	**PA-6.34**	**PA-8.34**	**PA-10.34**	**PA-12.34**
Melting temperature (DSC, peak)	190 ˚C	189 ˚C	177 ˚C	174 ˚C	169 ˚C	166 ˚C
Solid transition (DMTA, tan δ, peak)	38 ˚C	37 ˚C	57 ˚C	54 ˚C	45 ˚C	47 ˚C
Thermal stability (TGA, air, onset)	448 ˚C	434 ˚C	450 ˚C	438 ˚C	438 ˚C	445 ˚C

TGA experiments showed that for all five polymers, **PA-2.34, PA-4.34**, **PA-8.34, PA-10.34** and **PA-12.34** decomposition sets in at around 430 and 450 ˚C (onset) under nitrogen and air. DSC scans of the new polyamides recorded at a heating rate of 10 ˚C/ min on samples that were once-molten and cooled, displayed well-defined melting temperatures between 190 ˚C and 166 ˚C (see Figure 3.2). As expected, the melting temperatures linearly decreased with increasing length of the diamine moiety (see below). Unfortunately, the determination of glass transition temperatures (T_g) from DSC traces of carefully dried **PA-2.34, PA-4.34**, **PA-8.34, PA-10.34** and **PA-12.34** samples was stifled due to the extremely small heat flow associated with this transition. Consequently, DMTA measurements were conducted, in order to carefully investigate the secondary thermal transitions. The DMTA measurements of dry, melt-pressed films indicated clear transitions in the range of 37 to 47 ˚C (max. of the tan δ peak) for **PA-2.34, PA-4.34**, **PA-8.34, PA-10.34** and **PA-12.34** (Table 3.2), thus, in a regime which was in good agreement with the glass transitions of common nylons [3]. Furthermore, quenching experiments were carried out in order to investigate the thermal behavior in some more detail. The polyamides were first molten and kept for 15 min under inert gas atmosphere at 20 ˚C above their melting temperature, and subsequently rapidly cooled by immersing the sample in liquid nitrogen. Heating of quenched samples was accompanied by significant recrystallization effects, as was evident from the DSC heating scans of these samples (see Figure 3.3); the latter appeared to indicate relatively low rates of crystallization for this new class of polyamides, a finding which was already reported for PA-6.34. This observation was not unexpected in view of the very large crystalline unit cell of this polymer and the extensive molecular motion required to form the proper register. The crystal structure of PA-x.34 will be discussed in Chapter 4.

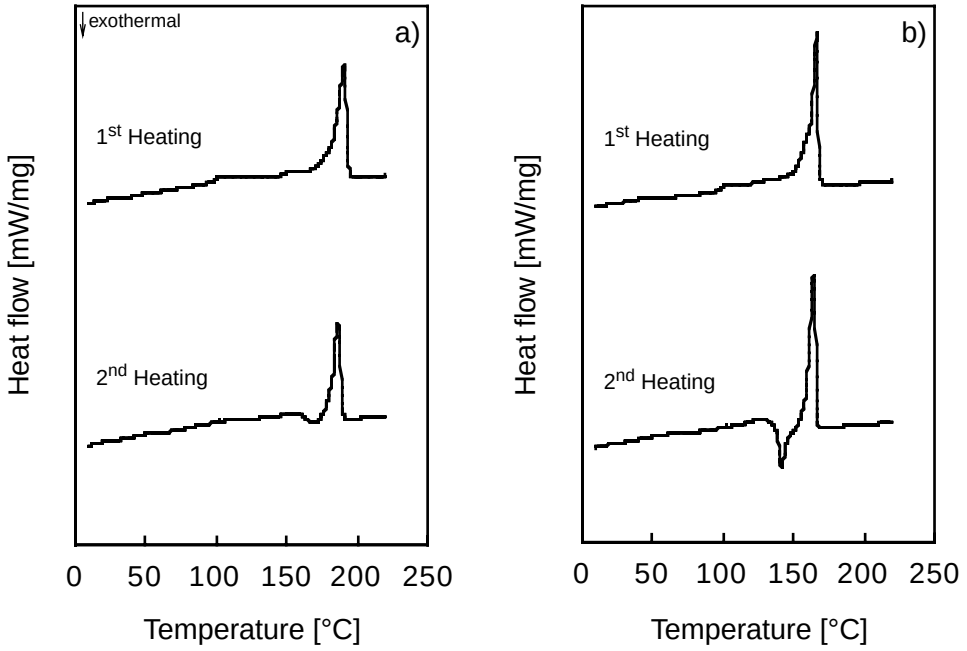

*Figure 3.3: Differential scanning calorimetry scans of **PA-2.34** a) and **PA-12.34** b) quenched in the DSC at a cooling rate of 100 °C/min (heating rates 10 ˚C/min).*

3.2.4 Investigation of Melting Temperatures of Polyamides x.34

Steiger *et al*. developed a semi-empirical approach to estimate the melting temperatures (T_m) of a homologous series of polymers of the general formula of a copolymer ~~*(-A—(CH$_2$)$_f$-)$_n$*~~ [6]. T_m was found to scale linearly with 1/*f*, and thus, this method can be applied to extrapolate the melting temperature of any member of a given series, if T_m of at least two members of the series are known. The approach was proven to result accurate predictions for linear aramides and *n*-nylons with odd as well as even numbers of methylene groups in the polymer backbone [6]. Thus, it is used here to compare the experimentally determined melting temperatures of the new polyamides and to extrapolate the values of other members of this series. Figure 3.4 shows a plot of T_m versus 1*/f*, which demonstrates that this semi-empirical method indeed describes the melting temperatures of the homologous series of polyamides x.34 very well. Therefore, it was possible to predict the melting temperatures of other members of this series (see Table 3.3). This prediction allows the assumption that even polyamides of this class with very extended aliphatic segments (PA-100.34: $T_m \approx 156$ °C) still should exhibit a higher

melting temperature than HDPE (T_m = 135 °C). Therefore, these kind of polyamides could be interesting, for example, to produce “high melting” polyethylene.

However, it should be noted that **PA-2.34** displayed a rather deviating behavior. Its melting temperature was substantially lower than expected from the extrapolation (190 °C instead of 220 °C, cf. Figure 3.4). This fact maybe explained by the well-known limited mobility of the small diamine segment, which decreases the ability to crystallize and results in a different crystal structure (cf. Figure 3.6, Chapter 4) [7].

Table 3.3: Extrapolated melting temperatures of certain polyamides x.34.

Polyamide	**PA-16.34**	**PA-24.34**	**PA-32.34**	**PA-34.34**	**PA-100.34**
T_m (extra.)	164 ˚C	161 ˚C	160 ˚C	160 ˚C	156 °C

Most interesting, the approach is also applicable to PA-x.34/1,2,3,4-tetrahydronaphthalene gels, as is evident from Figure 3.4b. Therefore, the above assumption that the aliphatic segments of the dicarboxylic acid were dissolved and only the H-bonds remained intact, is supported by this observation. **PA-2.34** was again an exception due to the limited mobility in the ethylenediamine segment.

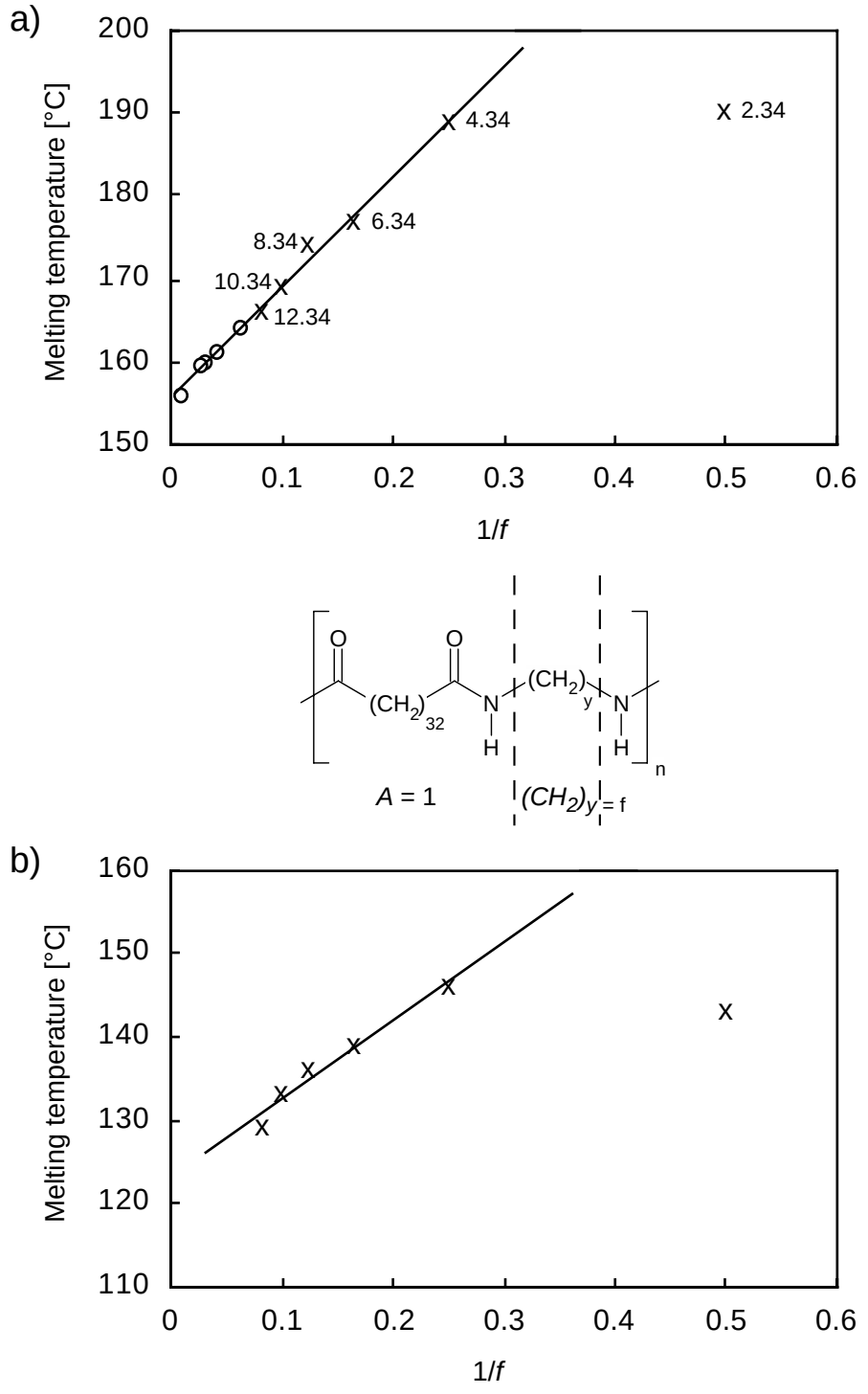

Figure 3.4: Melting temperatures of PA-x.34 (a) and of the PA-x.34/1,2,3,4-tetrahydronaphthalene gel (37.5 wt% PA-x.34), (b) versus 1/f ((x) experimentally determined, (o) extrapolated).

3.2.5 Mechanical Properties

Dry, melt-pressed polyamide films were prepared and their mechanical properties were investigated by standard tensile tests at different temperatures (Experimental Section). Young's moduli of melt-crystallized, isotropic samples at room temperature were found to be in the range of 500 - 700 MPa at 25 °C for the entire polyamide x.34 series; and the tensile strengths were 20 - 30 MPa at 25 °C, respectively (Figure 3.5).

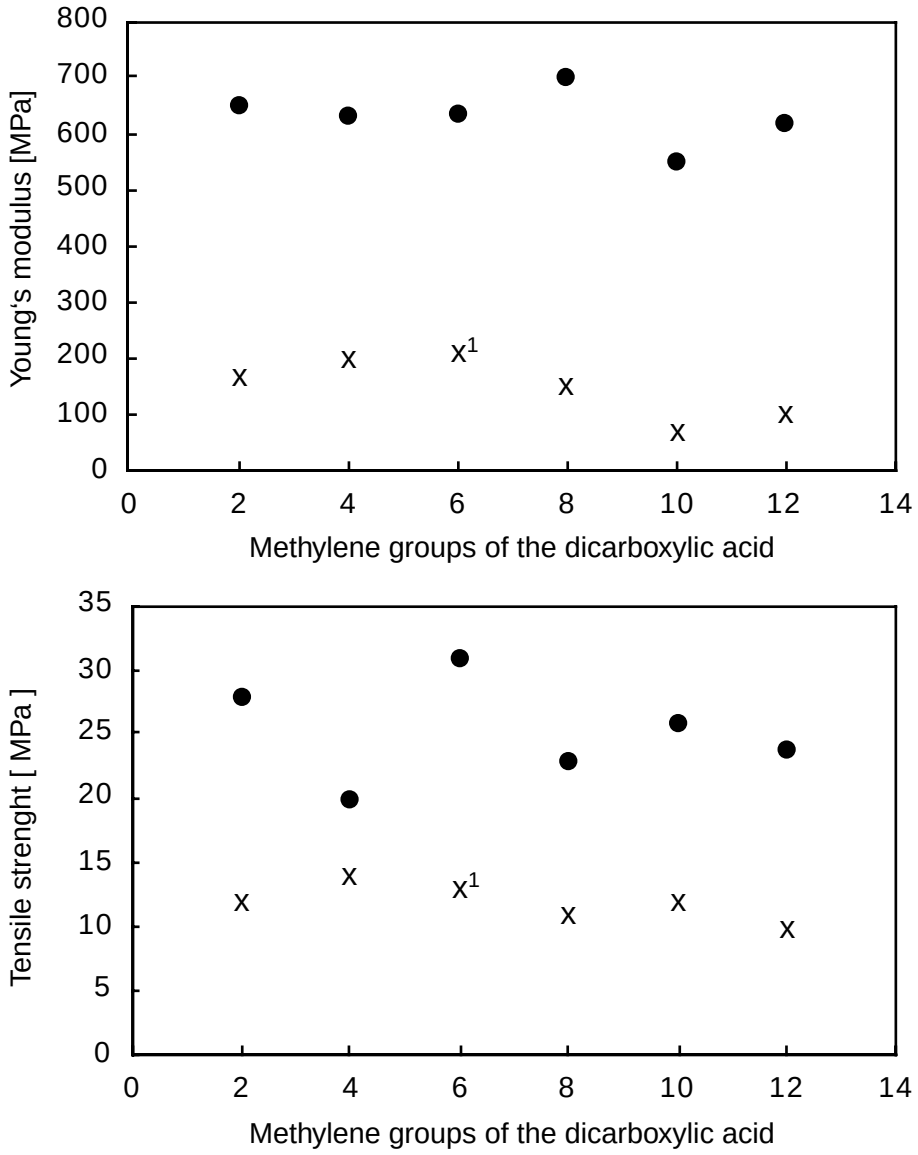

Figure 3.5: Tensile moduli and tensile strength of melt-crystallized, isotropic, dried samples of polyamides PA-x.34 at 25 ˚C (●) and at 100 °C ([1] 75 °C) (x), respectively.

3.2.6 X-ray Diffraction

Wide-angle X-ray diffractograms of **PA-4.34**, **PA-8.34, PA-10.34** and **PA-12.34** showed two prominent reflections, indicative of a significant degree of crystallinity of these materials. Exemplarily shown in Figure 3.6 a) is the diffractogram of an unoriented sample of **PA-12.34**, which is representative for the present series. The exceptional position of **PA-2.34** in the group of polyamides x.34 was also confirmed by X-ray investigations. It showed, in contrast to the others, a diffuse reflection ring, which is well-known in the literature for polyamides 2.y (Figure 3.6 c)) [7]. X-ray patterns of oriented samples, e.g. of **PA-12.34** as well as **PA-2.34**, unambiguously showed the uniaxial orientation of the drawn films (Figure 3.6 b),d)). Detailed analysis of the crystal structures of the new polymers will be discussed in Chapter 4.

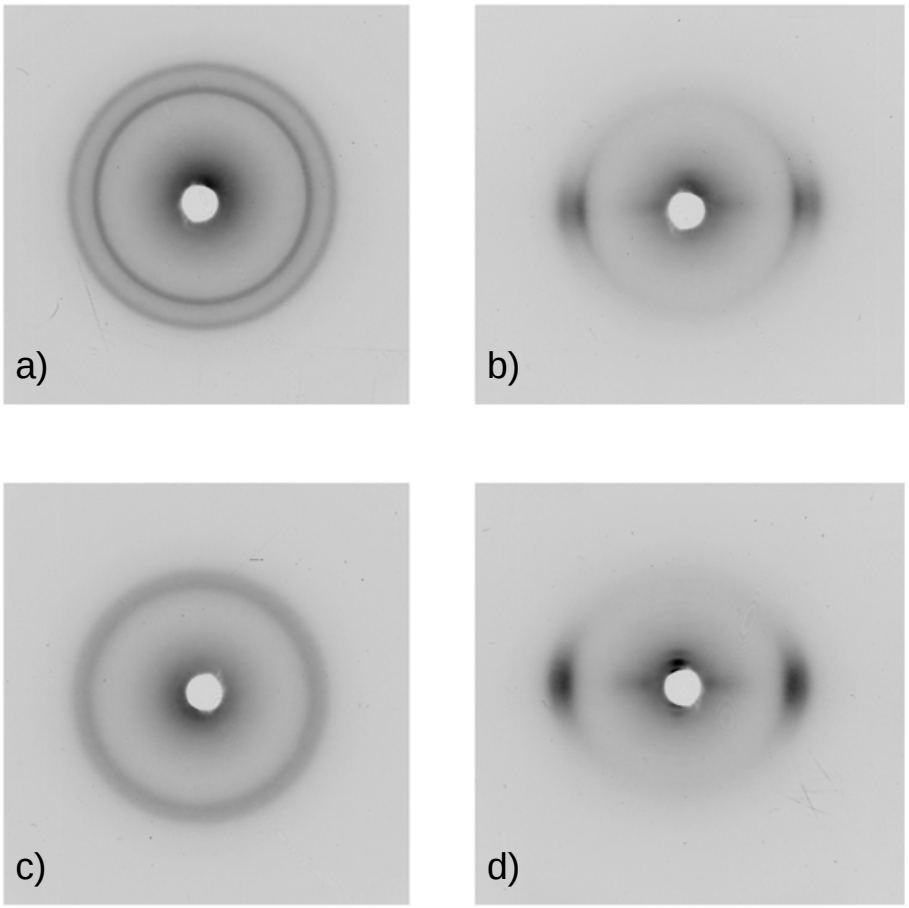

Figure 3.6: Wide-angle x-ray diffraction patterns of PA-12.34 (a: isotropic; b: drawn at 120 ˚C to a draw-ratio (λ) of 4) and PA-2.34 (c: isotropic; d: drawn at 120 ˚C to a draw-ratio (λ) of 3.5).

3.3 Conclusions

In this chapter the synthesis and characterization of a new series of polyamides containing tetratriacontanedioic acid was presented. The thermal and mechanical properties of **PA-2.34, PA-4.34**, **PA-8.34, PA-10.34** and **PA-12.34** were found to be in between those of common polyamides and polyethylene. All these new polyamides displayed a most interesting thermo-reversible gelation behavior in sulfuric acid. In addition, 1,2,3,4-tetrahydronaphthalene could also be used as a gelation solvent. But in this case, the network consisted, most probably, of the H-bonds between the amide groups and did not consist of "crystallites" formed by the extended aliphatic segments as it was the case for the PA-x.34/sulfuric acid gels.

3.4 Experimental Section

General Methods. All reagents and solvents were purchased from Fluka and Aldrich, except tetratriacontanedioic acid, which was synthesized according to the procedure in Chapter 2. Only analytical grade quality chemicals were used. ^{1}H-NMR spectral data are expressed in ppm relative to internal TMS standard and were obtained on various Bruker NMR spectrometers. All viscosity measurements were made at 25 ˚C and at a concentration of 0.5 g/dL using Ubbelohde capillaries from Schott (type 53020 / II) in combination with a Schott AVS 410 viscometer. Elemental analyses and mass spectra were carried out by the Microanalysis and Mass Spectra Laboratories of the Department of Chemistry of ETH Zürich. X-ray measurements were performed on a Seifert ISO-Debyeflex 2002, using a Ni-filtered Cu-K_{α} as ray source (conditions: 12 h and 24 h, 30 mA, 35 kV). All mechanical measurements were carried out on an Instron 4464 tensile tester equipped with a load cell of 10 N. Unless otherwise stated, all polyamide samples were dried for at least 16 h at 75 ˚C under vacuum (10 mbar) before used for any experiment.

Polyamide 2.34. Tetratriacontanedioic acid (0.754 g, 1.40 mmol) was dissolved in boiling 1,4-dioxane (55 mL) and a solution of 1,2-diaminoethane (0.090 g, 1.50 mmol)

in 1,4-dioxane (15 mL) was added under vigorous stirring at 85 ˚C, causing the immediate precipitation of the white 1,2-diaminoethane-tetratriacontanedioic acid salt. The mixture was allowed to cool to room temperature, and the product was collected by filtration. The 1,2-diaminoethane-tetratriacontanedioic acid salt was obtained as a white powder (0.784 g, 93 %); T_m: 160 ˚C.

A closed-bottom glass tube was charged with 1,2-diaminoethane-tetratriacontanedioic acid salt (0.777 g, 1.30 mmol), and snugly fitted into an autoclave. After the autoclave was evacuated and flushed with nitrogen and this cycle had been repeated three times, a nitrogen pressure of 18 bar was applied. The reaction was subsequently started by quickly raising the autoclave temperature to 180 ˚C; an increase in pressure to about 27 bar was observed. The temperature was gradually increased to 195 ˚C over a period of 4.5 h. The pressure was then decreased in four steps to vacuum and the temperature was increased also in four steps to 210 ˚C (1^{st} step: 200 ˚C, 15 bar, 1 h; 2^{nd} step: 205 ˚C, 10 bar, 1 h; 3^{rd} step: 210 ˚C, 5 bar, 1 h; 4^{th} step: 210 ˚C, 2.5 x 10^{-2} mbar). The polycondensation was continued under the latter conditions for 12 h. The autoclave was then slowly cooled to room temperature. The resulting **PA-2.34** was obtained as a white solid (0.721 g, 93 %) and was pulverized in a freezing mill; T_m: 187 ˚C. ^{1}H-NMR (300 MHz, phenol-d_6, 373 K): δ 3.24 (s, 4H), 2.14 (t, J = 7.64, 4H), 1.61 (t, J = 7.10, 4H), 1.20-1.50 (m, 58 H). Anal. Calcd for $C_{36}H_{70}N_2O_2$: C, 76.81; H, 12.53; N, 4.98; O, 5.68; Found: C, 76.33; H, 12.82; N, 5.19; O, 5.58.

Polyamide 4.34. A solution of 1,4-diaminobutane (0.124 g, 1.41 mmol) and 1,4-dioxane (10 mL) at 60 ˚C was added under vigorous stirring to a solution of tetratriacontanedioic acid (0.741 g, 1.38 mmol) in 1,4-dioxane (55 mL) at 85 ˚C. After the addition was complete, the mixture was stirred for 16 h at room temperature, and the white product was collected by filtration. The 1,4-diaminobutane-tetratriacontanedioic acid salt was obtained as white powder (0.744 g, 86 %); T_m: 150 ˚C.

The procedure and set-up for the melt-polycondensation of polyamide 4.34 was similar to the one of **PA-2.34** described above except a modified pressure-temperature protocol, and employing 1,4-diaminobutane-tetratriacontanedioic acid salt (0.589 g, 0.94 mmol) for the polymerization. A nitrogen pressure of 19 bar was initially applied and the autoclave was heated to 175 ˚C; an increase in pressure to about 26 bar was observed. The temperature was gradually increased to 180 ˚C over a period of 3.5 h. The pressure

was then decreased and the polycondensation was continued at a pressure of 10 bar and temperature of 190 ˚C for 1.5 h. Finally, a vacuum (2.5 x 10^{-2} mbar) was established, and after another 1h, the temperature was increased to 200 ˚C and the reaction was continued for another 2 h. The autoclave was then cooled to room temperature. The resulting **PA-4.34** was obtained as a white solid (0.556 g, 94 %) and was pulverized in a freezing mill; T_m: 186 ˚C. ^{1}H-NMR (300 MHz, phenol-d_6, 373 K): δ 3.13 (s, 4H), 2.13 (t, *J* = 7.59, 4H), 1.62 (t, *J* = 6.77, 4H), 1.21-1.50 (m, 62 H). Anal. Calcd for $C_{38}H_{74}N_2O_2$: C, 77.23; H, 12.62; N, 4.74; O, 5.41; Found: C, 76.70; H, 12.63; N, 4.89; O, 5.80.

(Polymers **PA-8.34**, **PA-10.34**, and **PA-12.34** were prepared in analogy to PA-4.34, using the detailed reaction conditions compiled in Table 3.4.)

Polyamide 8.34. ^{1}H-NMR (300 MHz, phenol-d_6, 373 K): δ 3.20 (t, *J* = 7.14, 4H), 2.15 (t, *J* = 7.54, 4H), 1.64 (t, *J* = 6.99, 4H), 1.25-1.50 (m, 62 H), 1.19 (s, 8 H). Anal. Calcd for $C_{42}H_{82}N_2O_2$: C, 77.95; H, 12.77; N, 4.33; O, 4.94; Found: C, 77.31; H, 12.37; N, 4.67; O, 5.30.

Polyamide 10.34. ^{1}H-NMR (300 MHz, phenol-d_6, 373 K): δ 3.23 (t, *J* = 7.16, 4H), 2.15 (t, *J* = 7.51, 4H), 1.63 (t, *J* = 6.97, 4H), 1.20-1.50 (m, 74 H). Anal. Calcd for $C_{44}H_{86}N_2O_2$: C, 78.27; H, 12.84; N, 4.15; O, 4.74; Found: C, 77.70; H, 12.44; N, 4.39; O, 5.11.

Polyamide 12.34. ^{1}H-NMR (300 MHz, phenol-d_6, 373 K): δ 3.22 (t, *J* = 6.84, 4H), 2.14 (t, *J* = 7.49, 4H), 1.63 (m, 4H), 1.25-1.50 (m, 78 H). Anal. Calcd for $C_{46}H_{90}N_2O_2$: C, 78.57; H, 12.90; N, 3.98; O, 4.55; Found: C, 78.63; H, 13.09; N, 4.23; O, 4.22.

*Table 3.4: Synthesis of different Polyamides (procedure similar to **PA-4.34**): Reagents and results.*

	Polyamide 8.34	**Polyamide 10.34**	**Polyamide 12.34**
Diamine	1,8-diaminooctane	1,10-diaminodecane	1,12-diaminododecane
	0.193 g, 1.34 mmol	0.186 g, 1.08 mmol in	0.319 g, 1.58 mmol in
	in 1,4-dioxane	1,4-dioxane	1,4-dioxane
	50 mL at 85 °C	50 mL at 85 °C	50 mL at 85 °C
Tetratriacontane-	0.704 g, 1.31 mmol	0.572 g, 1.06 mmol in	0.843 g, 1.56 mmol in
dioic acid	in 1,4-dioxane	1,4-dioxane	1,4-dioxane
	55 mL at 85 °C	55 mL at 85 °C	55 mL at 85 °C
T_m	157 °C	153 °C	152 °C
Yield	0.828 g, 93 %	0.711 g, 94 %	1.077 g, 93 %
		Polycondensation	
Acid/Diamine-Salt	0.822 g, 1.20 mmol	0.701 g, 0.99 mmol	1.068 g, 1.45 mmol
Initial N_2-pressure	16 bar	16 bar	15 bar
Starting Temp.	180 °C	180 °C	175 °C
Pressure, observed	24 bar	20 bar	23 bar
Temp. increase/ Time period	190 °C / 3.5 h	190 °C / 4.0 h	185 °C / 4.0 h
Pressure/Temp./ Time (1.step)	15 bar / 190 °C / 1 h	10 bar / 195 °C / 1 h	10 bar / 190 °C / 1 h
Pressure/Temp./ Time (2.step)	5 bar / 195 °C / 1 h	-	-
Pressure/Temp./	0.025 mbar /	0.025 mbar /	0.025 mbar /
Time (3.step)	200 °C / 3 h	200 °C / 3 h	195 °C / 4 h
T_m	171 °C	166 °C	163 °C
Yield	0.774 g, 99 %	0.639 g, 95 %	0.935 g, 92 %

Thermal Analysis. DSC (under nitrogen) and TGA measurements (under nitrogen and air) were performed on a Netzsch DSC 200 and a TG 209 instrument, respectively. Melting temperatures (T_m) were determined by DSC measurements with a heating rate of 10 ˚C/min, taking the peak of the endothermal transition as T_m. The DMTA

measurements were carried out under air on a DMTA Mk11 Polymer Laboratories instrument, operated in tensile testing mode with an enforced oscillation of 1 Hz and 10 Hz. The dimensions of the standard film samples were 10.00 mm x 12.00 mm x 0.07 mm.

Mechanical Characterization. Polyamide film samples were produced by melt compression molding between two poly(tetrafluoroethylene) (PTFE) sheets of a thickness of 0.4 mm. The polyamide powders were filled into the mould and heated in a melt press (applied temperature = melting temperature + 15 ˚C). After 10 minutes a force of 1.5 tons was applied for 5 minutes; subsequent quenching to ambient temperature resulted in films of a thickness of about 80 µm. Mechanical tensile testing of the films was performed in a temperature range of 25 ˚C to 120 ˚C and at a strain rate of 100 %/ min on dog-bone shaped samples (test area = 12.7 mm x 2 mm). For this purpose a tensile tester (Instron 4464) equipped with a controlled atmosphere chamber was employed.

3.5 References

[1] Wunderlich, B. *Macromolecular Physics*; Academic Press: New York, 1976; Vol. 2, p. 390.

[2] Smith, P.; Lemstra, P. J. *J. Mater. Sci.* **1980**, *15*, 505.

[3] Kohan, M. I. *Nylon Plastics Handbook*, Carl Hanser Verlag: Munich, 1995.

[4] Peacock, A. J. *Handbook of Polyethylene*, Marcel Dekker: New York, 2000.

[5] Jones, N. A.; Atkins, E. D. T.; Hill, M. J.; Cooper, S. J.; Franco, L. *Polymer* **1997**, *38*, 2689.

[6] Steiger, D.; Tervoort, T.; Weder, C.; Smith, P. *Macromol. Rapid Commun.* **2000**, *21*, 405.

[7] Jones, N. A.; Cooper, S. J.; Atkins, E. D. T.; Hill, M. J.; Franco, L. *J. Polym. Sci. Part B:Polym. Phys.* **1997**, *35*, 675.

4. Crystal Structures of the Polyamides x.34[1]

4.1 Introduction

The polyamides x.34 are a new group of aliphatic polyamides. The implantation of extended linear alkyl segments has led to the introduction of novel and interesting properties, as already discussed in Chapters 2 and 3. The introduction of these elongated alkyl segments raises the question: do the crystal structures of these polyamides x.34 still resemble, for example, that of PA-6.6 or is the structure more similar to the crystal structure of high density polyethylene (HDPE). Scale models of the six polyamides x.34 in the all-tans conformation, and a comparison with PA-6.6 and an appropriate segment of poly(m)ethylene are shown in Figure 4.1 to graphically illustrate the frequency and relative positions and orientations of the amide units within the backbone.

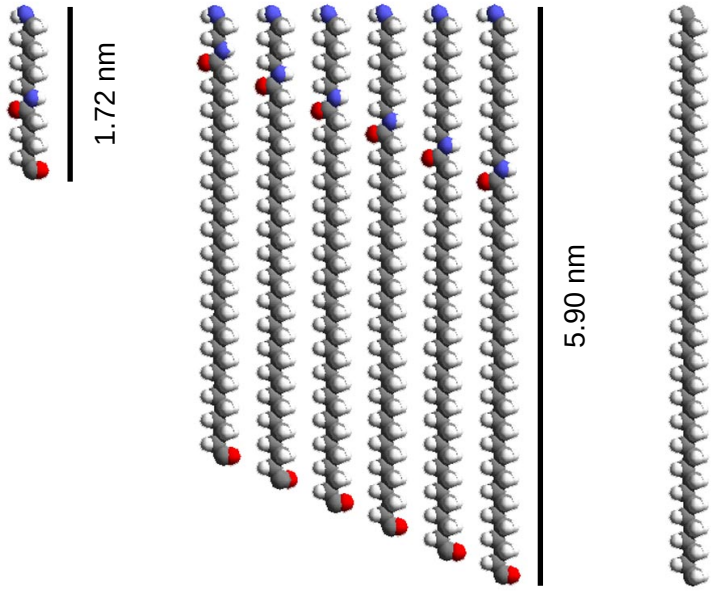

Figure 4.1: Color model of the polyamide x.34 series showing the relative frequency and distribution of amide units; PA-6.6 and C_{48}-alkane (poly(m)ethylene-segment) added for comparison. Color code: red - oxygen; blue - nitrogen; grey - carbon; white - hydrogen.

---

[1] This chapter is based on the publication: Structures of x 34-Nylons in Chain-Folded Lamellae and Gel-Spun Fibers: Ehrenstein, M.; Sikorski, P.; Atkins, E.; Smith, P. submitted to *J. Polym. Sci. Polym. Phys.* on May 2002.

The thermal properties (melting temperature (T_m): 166 - 190 °C; glass transition temperature (T_g): ~ 45 °C) led to the assumption that the crystal structure of these polymers resembles more the one of classical polyamides. The reason of these enhanced properties can be attributed to hydrogen bonds (H-bonds). The strongest H-bonds occur when the three H-bond forming atoms (O—H—N) are positioned in a straight line. A small deviation would already lead to a decrease of the bond strength. Consequently, the amide groups will have to be arranged in a way that this demand is fulfilled. For example, this optimum arrangement occurs in PA-6.6. PA-6.6 is able to crystallize in different structures depending on the crystallization conditions, e.g. temperature or pressure, and the most common and well-known structure is the so called α-structure. In this structure the polymer chains are in the fully extended all trans conformation and form planar sheets of H-bonded molecules which, in turn, are stacked upon each other. The crystal symmetry is triclinic with one chemical repeat unit per unit cell, as is shown in Figure 4.2 [1].

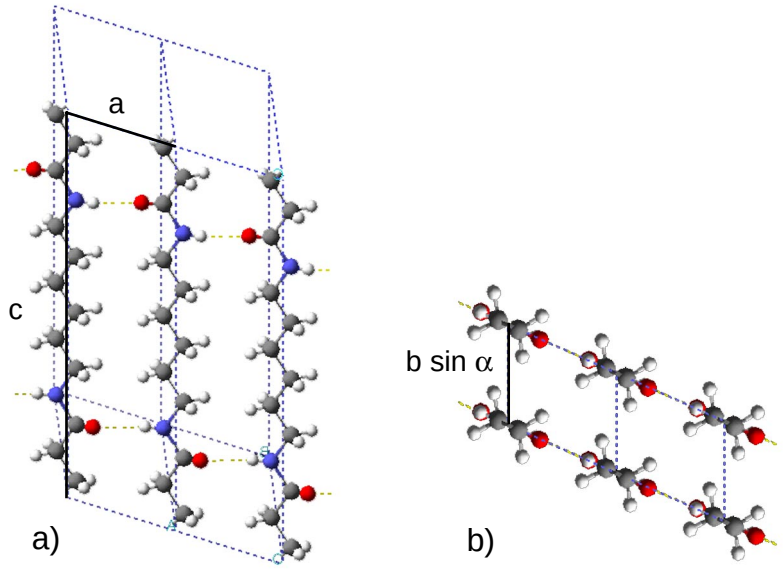

Figure 4.2: Triclinic unit cell of PA-6.6 [1]. a) Orthogonal view to the H-bonded sheet (projection along the b-direction showing the a-c faces). b) View parallel to chain axis (Projection along the c-direction showing the a-b faces).

So, in order to form also strong H-bonds, the polyamides x.34 should crystallize in a similar way to PA-6.6. However, there are some indications why this could not be the case. First of all, the polyamides x.34 exhibit a different solubility behavior compared to

standard AABB polyamides in, for example, concentrated sulfuric acid (see Chapters 2 and 3). Secondly, the difference in size of the chemical repeat unit plays an important role for chain length between two reentry-folds in a crystalline lamella. A chain-folded lamella of PA-6.6 contains between two folds four chemical repeat units (56 atoms) and that actually leads to 8 H-bonds forming amide groups. In comparison PA-6.34 has already 42 atoms per chemical repeat unit, and consequently, the distance between two reentry-folds would consist of only one chemical repeat unit and, therefore, only of two amide groups. It might be considered to be unrealistic to expect that these two H-bond forming amide groups can force the whole polymer chain to crystallize in a manner similar to PA-6.6. On the other hand, a crystallization like polyethylene is also not likely. Polyethylene can crystallize with three types of unit cell, i.e. orthorhombic (most common), monoclinic, and hexagonal. The conformation of the polymer chain is trans-trans and a unit cell contains one ethylene group in the center and four ethylene groups on each corner, leading to a total of two ethylene groups per unit cell (Figure 4.3) [2]. But this orthorhombic packaging of polyethylene is very compact and there is not enough space for relatively big amide groups in order to force the PA-x.34 polymer chains to crystallize in this kind of structure and to form H-bonds at the same time.

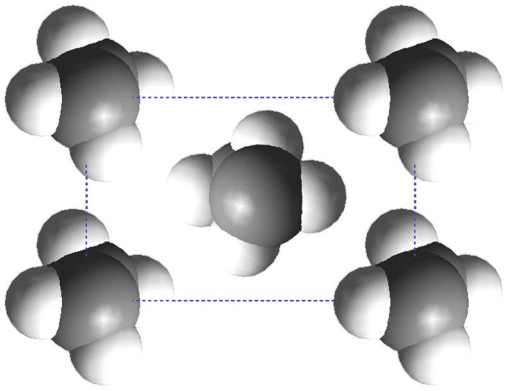

Figure 4.3: View parallel to chain axis of the orthorhombic crystal unit cell of polyethylene [2].

In this chapter the crystal structure of polyamides x.34 was investigated using transmission electron microscopy (TEM) and X-ray diffraction.

4.2 Results and Discussion

4.2.1 Transmission Electron Microscopy

The polyamide x.34 crystals were prepared under self-seeding conditions and by isothermal crystallization from *n*,*n*-dimethylformamide (DMF) solutions at temperatures in the region of 128 - 135 ˚C (see Experimental Part and Table 4.2).

Figures 4.6 and 4.7 shows the transmission electron microscopy (TEM) images of crystallites of the polyamides x.34. The shape of these crystals are like the ones of the even-even polyamides without the extended aliphatic segments and this suggests that the structure of the PA-x.34 crystals might be similar to, e.g. PA-6.6 [3].

The estimated thicknesses from metal shadowing experiments are ≥ 20 nm. The shape of the (roughly) elliptical lamellae, as measured by the ratio of the minor to major elliptical axes, increases linearly with increasing x value, as shown in Figure 4.5. Figure 4.6 shows the change, from long ribbon-like crystals for PA-2.34, to the steadily widening lamellae for PA-4.34 and PA-6.34. This trend continues for polyamides 8.34, 10.34 and 12.34, as shown in Figure 4.7.

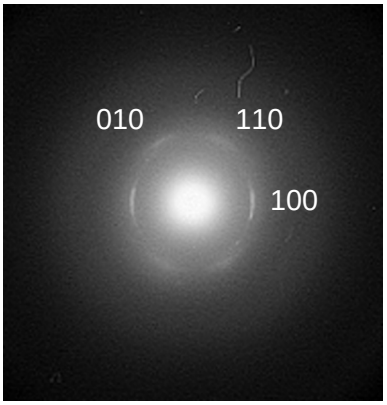

Figure 4.4: Electron diffraction pattern from a lamellar crystal of PA-4.34.

Figure 4.4 shows a typical electron diffraction (ED) pattern of a PA-4.34 as a representative of the PA-x.34 series. The pattern was obtained when the lamellae was tilted 41°, so that the electron beam is parallel to the chain axis (c-direction). This kind of ED pattern is well known for the triclinic unit cell of even-even polyamides with the characteristic strong diffraction spots at 0.44 nm spacing (a-axis projected interchain/ intrasheet spacing) indexes as the 100 and the two diffraction pairs at 0.37 nm spacing

(b-axis projected intersheet spacing) indexes as the 010 and 110. In addition, it was also concluded from the ED data that the a-axis (H-bond direction), and therefore the H-bonded sheet(s), is parallel to the long axis (a_1 in Figure 4.5) of the lamellar crystals and the b-axis (intersheet normal) is parallel to a_2 in Figure 4.5. The observed different crystal sizes can be explained on one hand by the relatively different crystallization conditions. Dimethylformamide does not have the same dissolution ability for all these PA-x.34 polymers (e.g. PA-12.34 does not behave in the same way as PA-2.34 in this solvent because it is more hydrophobic and the longer diamine segment leads to higher flexibility in this segment). Additionally, the melting temperature (T_m) is significantly lower which also has an influence on the chain mobilities at similar crystallization temperatures for this polyamide. On the other hand, it can be concluded from Figure 4.5 that, the higher the frequency of amide units the faster the chain-folded H-bonded sheets grow (a_1-direction) relative to the intersheet stacking (a_2-direction).

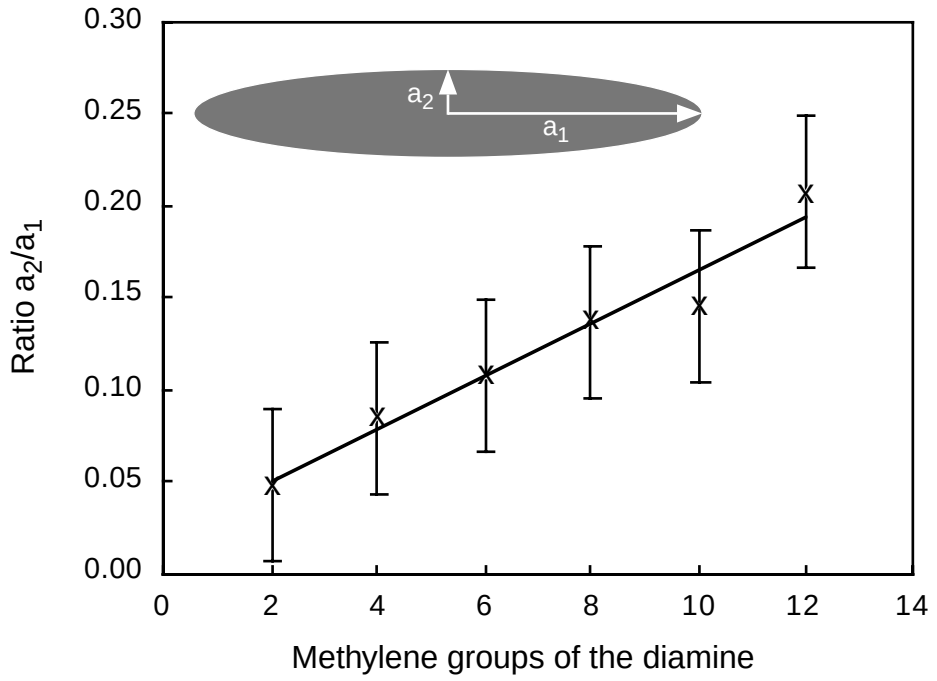

Figure 4.5: Relationship of crystal shape, as expressed by the ratio a_2/a_1 to the number of methylene groups of the diamine.

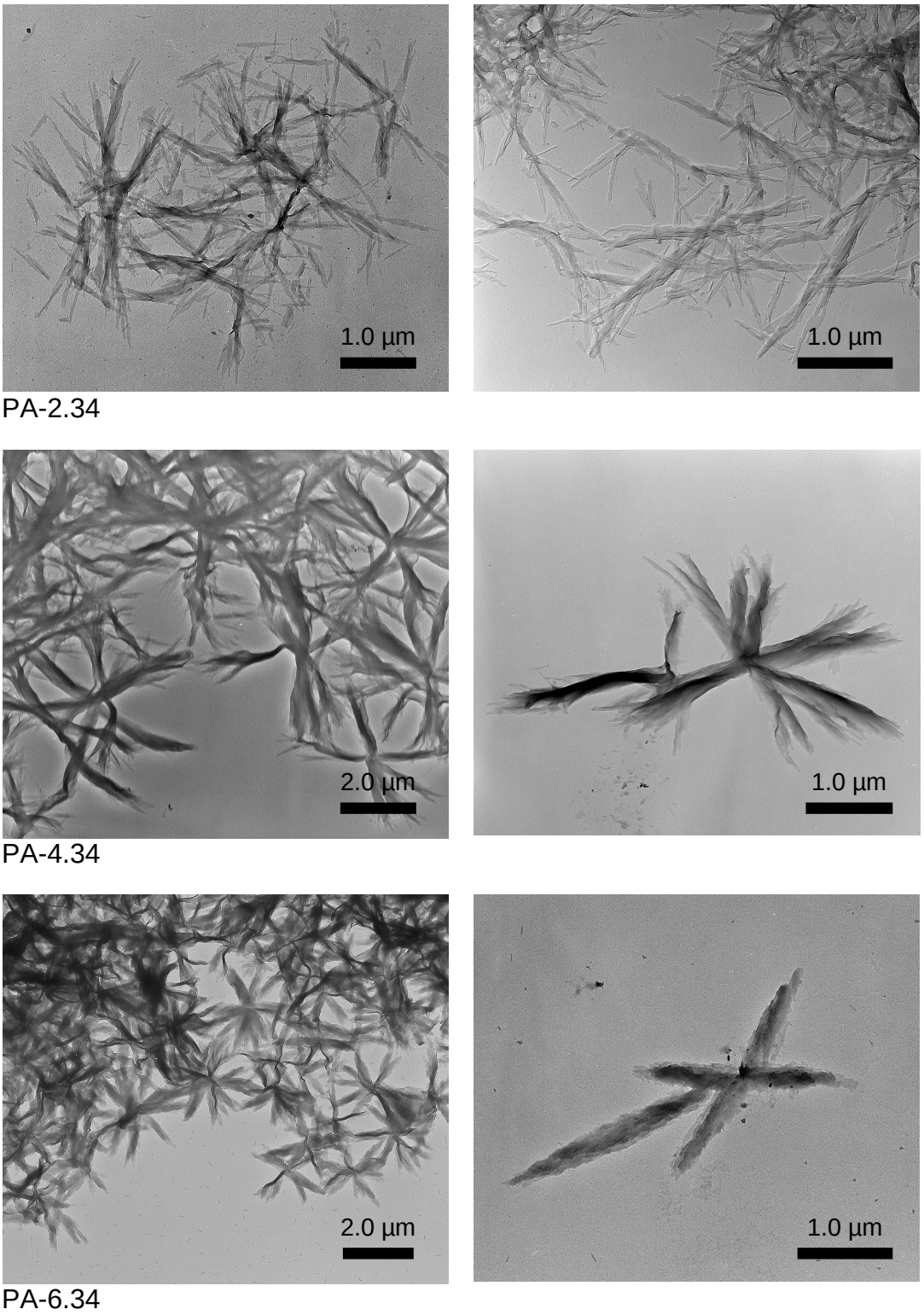

Figure 4.6: TEM images of chain-folded PA-2.34, PA-4.34 and PA-6.34, respectively, of polyamide lamellae isothermally crystallized from DMF solution (PA-2.34 (T_m = 190 ˚C); PA-4.34 (T_m = 189 ˚C); PA-6.34 (T_m = 177 ˚C)).

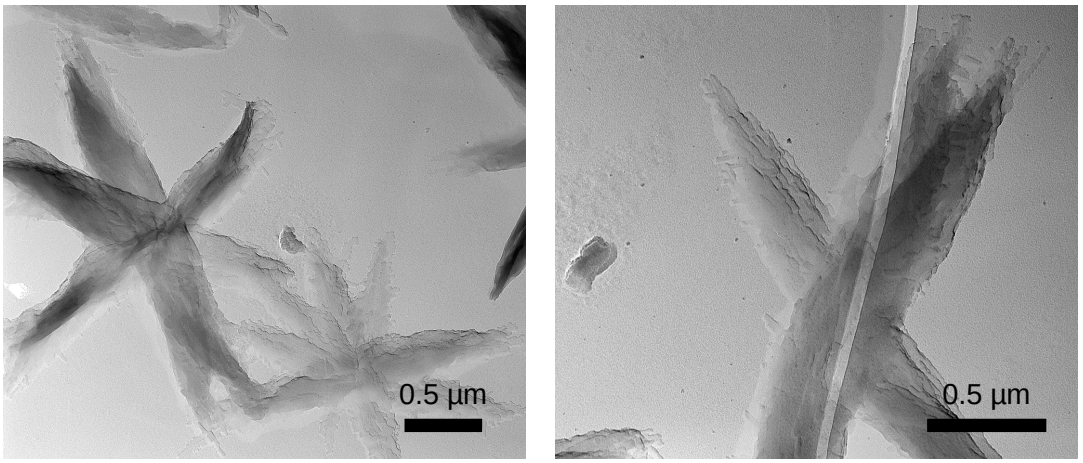

PA-8.34

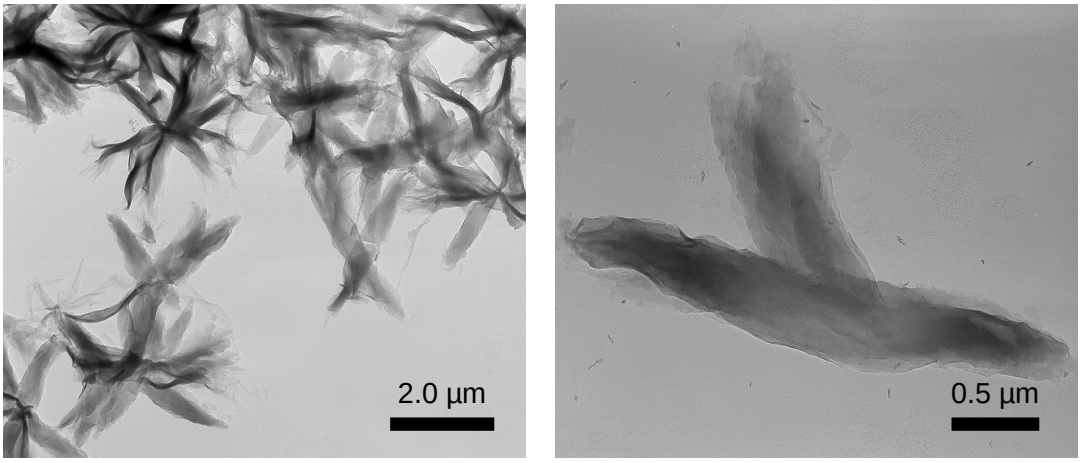

PA-10.34

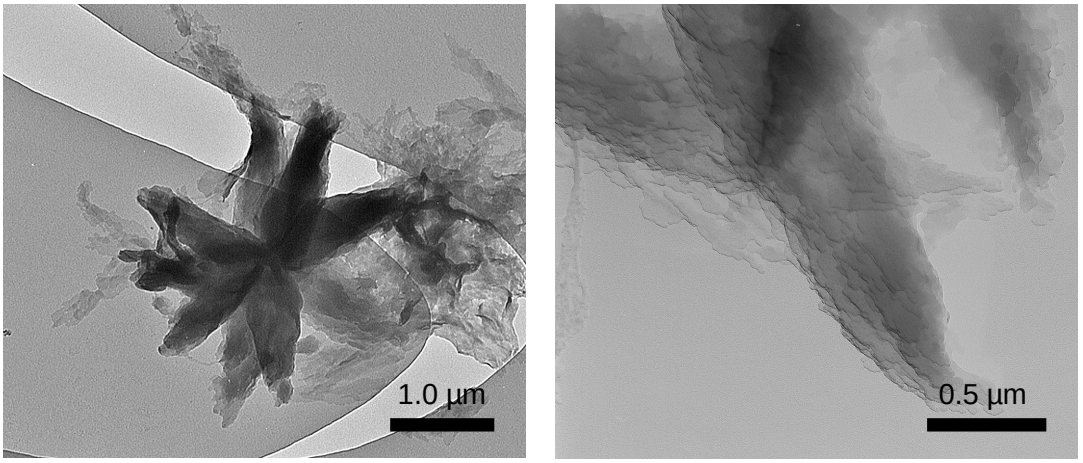

PA-12.34

Figure 4.7: TEM images of chain-folded PA-8.34, PA-10.34 and PA-12.34, respectively, of polyamide lamellae isothermally crystallized from DMF solution (PA-8.34 (T_m = 174 ˚C); PA-10.34 (T_m = 169 ˚C); PA-12.34 (T_m = 166 ˚C)).

4.2.2 X-ray Diffraction

X-ray diffraction studies were conducted on sedimented polyamide x.34 mats. These mats were produced from the corresponding polyamide by isothermal crystallization from hot DMF solution and subsequent filtration of this mixture at RT (see Experimental Section). During this filtration the crystals slowly sedimented. The sedimentation was important in order to produce oriented samples suitable for X-ray diffraction, enabling more easily the assignment of the detected diffractions signals to the corresponding structural unit. The medium- and wide-angle diffraction patterns were taken from the sedimented mats with the incident X-ray beam parallel to the mat surface and mat normal (cf. Figure 4.12 in Experimental Section). The X-ray diffraction patterns recorded are shown in Figures 4.8 and 4.9. The spacings and azimuthal positions of the principal diffraction signals are given in Table 4.1. Two obvious conclusions can already be drawn from this data without further inspection. First, all shown diffraction patterns are similar to those known from the whole group of even-even polyamides [1,3,4]. Secondly, the PA-2.34 patterns are different from the patterns of the other polyamides x.34.

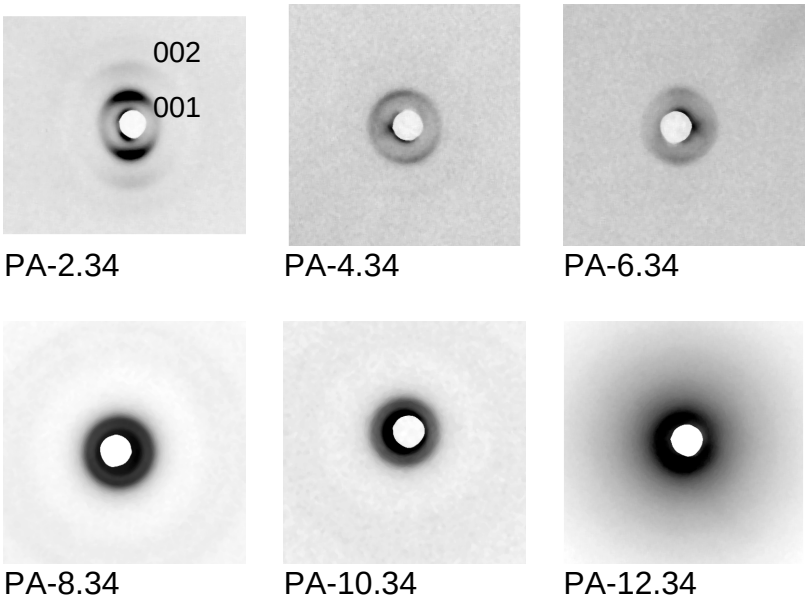

Figure 4.8: Medium angle X-ray diffraction patterns of polyamide x.34 mats.

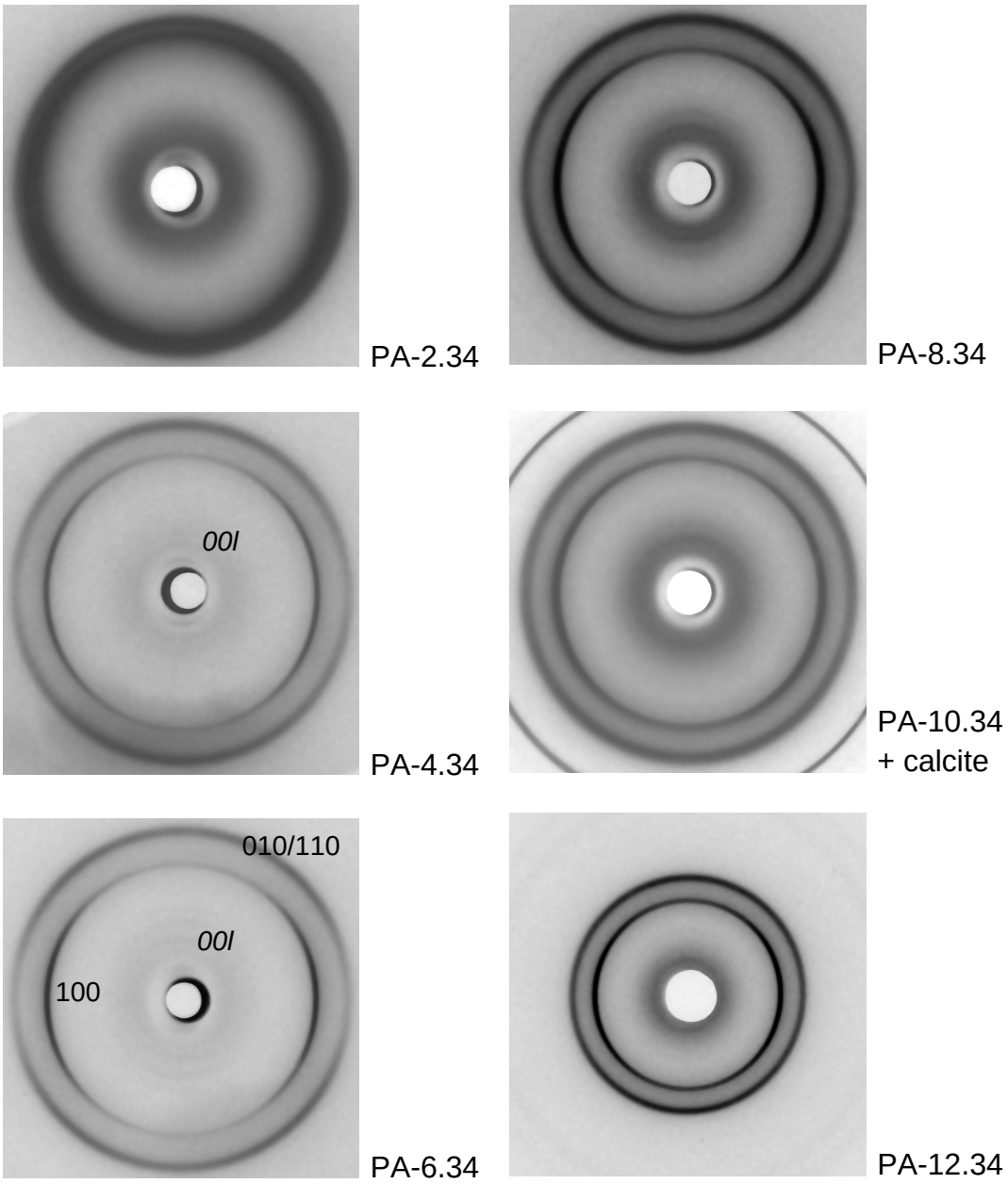

Figure 4.9: Wide angle X-ray diffraction patterns of polyamide x.34 mats (calcite was added for calibration).

4.2.3 Crystal Structure of PA-x.34 (x > 2)

In general, polyamide chains crystallize in order to form as many, strong hydrogen bonds as possible. The H-bonds favor a linear arrangement of the hydrogen bond forming atoms, because deviation form this linear arrangement will lead to a decrease of the strength of these bonds. Due to this fact, the even-even polyamides crystallize with a progressive shear of the fully extended polyamide chains within the hydrogen-bonded sheet. Hence, the chains are tilted at an angle of 13˚ to the lamellar normal (*c**-direction), as illustrated in Figure 4.10 a [1]. These H-bonded sheets can stack to each other in two possible ways. In the so-called α-phase they are arranged with a progressive shear which was established first by Bunn and Garner (see Figure 4.10 b) [1], and in the β-phase they are adjoined in an alternating order (see Figure 4.10 c) [1]. Both, α- or β-phase structures show two strong and characteristic diffraction signals with spacings of 0.44 and 0.37 nm, respectively. These signals represent a projected inter-chain distance within a hydrogen bonded-sheet and the inter-sheet spacing, respectively. However, the α-phase structure is the most common one found experimentally for single crystals of PA-6.6, PA-6.10, and other even-even polyamides [1,3,6-8].

In the case of the lamellae of the crystalline α-phase the 100 diffraction signal (0.44 nm) should occur ± 6˚ above and below the equator, and the 010 and 110 diffraction signal (0.37 nm) at ± 40˚ and ± 33˚, respectively. For the lamellae of the crystalline β-phase the respective angles are ± 14˚, ± 6˚, and ± 6˚. If there are mixtures of both phases in the lamellae the obtained arcs will, consequently, be broader. In Table 4.1 the spacings of all polyamides x.34 are summarized.

The X-ray diffraction patterns of the five family members with x > 2 are all similar (the PA-12.34 mat is so well oriented), and closely resemble those of PA-6.6 and other even-even polyamide sedimented mats [3,6]. The above mentioned two prominent and characteristic polyamide diffraction signals at 0.44 nm and 0.37 nm match the 100 and 010 interchain spacings of the established single-chain, triclinic PA-6.6 α-structure [1]. The azimuthal splitting of the two prominent diffraction arcs, in particular the outer 010 (0.37 nm) confirm that the chains are tilted at a substantial angle (≈ 42°) to the lamellar normal as previously explained by Atkins *et al* [6].

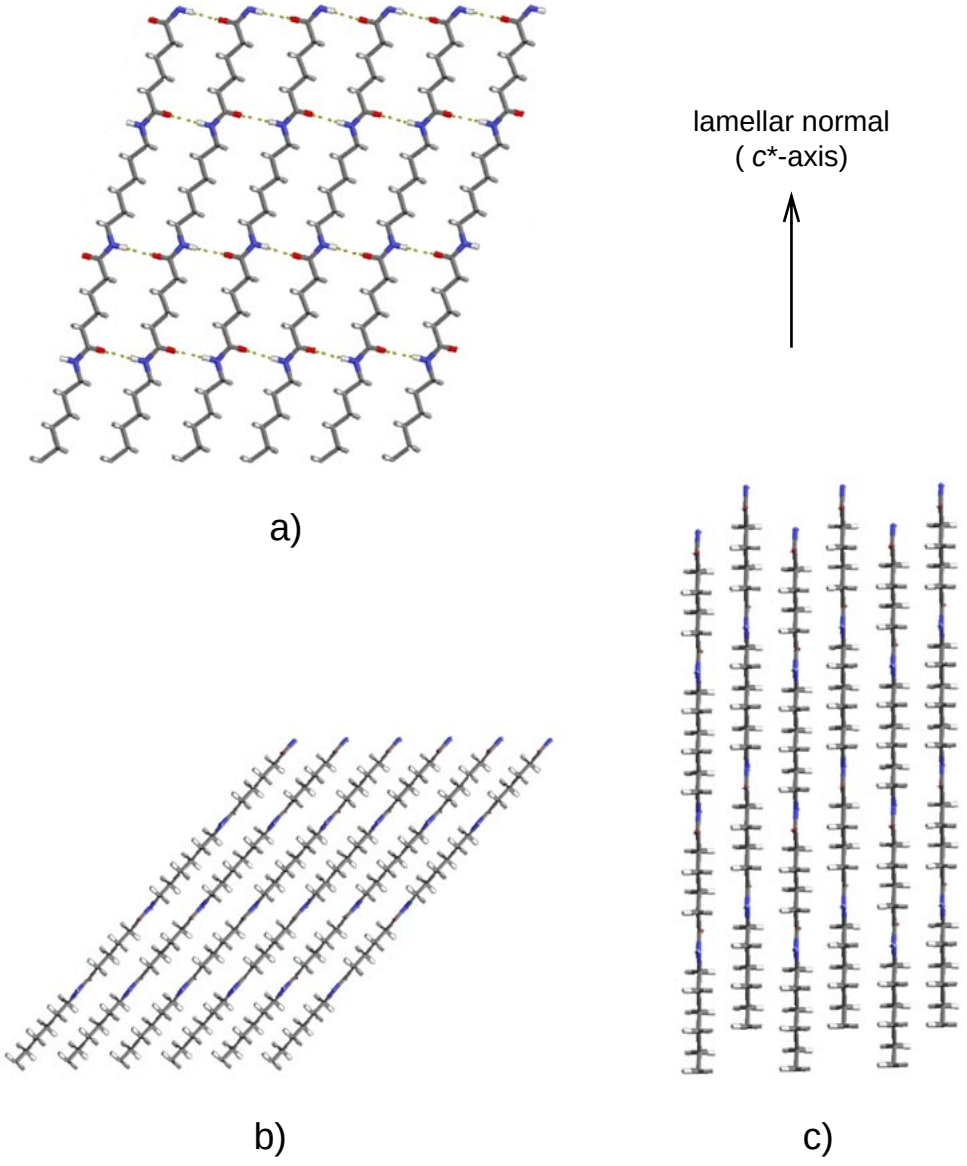

Figure 4.10: Projections of the polyamide 6.6 structures. a) Orthogonal view of a single hydrogen-bonded sheet (along the b-axis). b) Parallel view of the hydrogen-bonded sheets (along the projected a-axis) with a progressive shear between the H-bonded sheets, illustrating the α-phase structure. c) Parallel view of the hydrogen-bonded sheet (along the projected a-axis) with an alternate shear in c-direction, illustrating the β-phase structure [4].

The medium low-angle X-ray diffraction patterns obtained from sedimented mats of the six polyamides x.34 are shown in Figure 4.8 and the measured spacings are given in Table 4.1. The 00*l* diffraction arcs occur on the meridian. Unfortunately, it was not possible to measure the low-angle lamellar stacking periodicities of PA-x.34 crystals with the X-ray apparatus available in order to determine the lamellar thickness. However, the lamellar thickness of PA-x.34 crystals was estimated by means of TEM to be in excess of 20 nm which is at least 4 times the length of the measured 001 diffraction signal (projected c-axis). But with diffraction spacings (d-spacings) of the 00*l* diffraction signals, as in the case of PA-6.6 lamellar α-phase crystals [1,6], it is possible to directly calculate the chain tilt angle with respect to the lamellar normal (*c*^*c**), assuming an all-trans backbone conformation [1,9]. For example, for the PA-6.34 lamellar crystals a d001 = 3.83 nm was measured (see Table 4.1), the calculated length of the c-repeat is 5.16 nm, consequently, the chain tilt angle is 42.1° ($\cos^{-1}$(3.83 nm/5.16 nm) = 42.1°) which is close to the value of 41.3° found for the triclinic α-structure of PA-6.6 [1]. These chain tilt angles are given in Table 4.1 together with unit cell dimension and indexing.

It is also known from diffraction patterns of the α-structures of other chain-folded even-even polyamides that the corresponding 100 and 010 diffraction signals are angularly split ± 6° and ± 40°, respectively, either side of the equator [9]. The present X-ray diffraction results of the PA-x.34 crystals mats are consistent with these values.

Thus, the X-ray diffraction data favor the established PA-6.6-like triclinic α-structure [1], i.e., with chains in the all-trans conformation, H-bonded sheets and stacking with progressive intersheet shear in the ac-plane, in both the chain direction (c-axis) and the hydrogen bond array direction (a-axis) [9]. In order to demonstrate that the basic structures described above for the crystalline lamellae of PA-x.34 are sound, the computer generated X-ray diffraction pattern, using the Cerius2 program, for the PA-6.34 lamellar crystal structure is shown in Figure 4.11 b). It matches the basic features of the composite experimental X-ray diffraction pattern of PA-6.34 shown in Figure 4.11 a). Note in particular the good match of the intensity of the meridional 00*l* diffraction signals with strong 004, 005, and 006 in Figures 4.11 a) and 4.11 b).

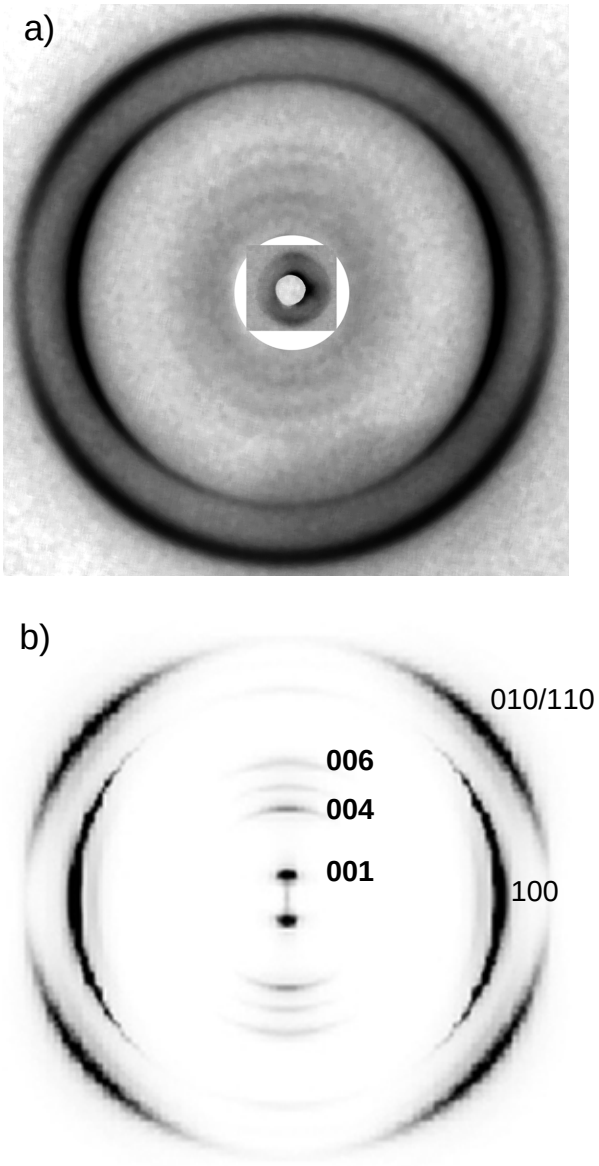

Figure 4.11: X-ray diffraction pattern from PA-6.34 lamellar crystals. a) experimental (photomontage of wide- and medium-angle X-ray diffraction pattern); b) calculated.

It is of interest to note that just two amide groups in a chemical repeat unit, a total of 38 to 48 atoms, force the whole chain into the typical polyamide crystal lattice. This is additional evidence for the strong influence of the amide groups, and consequently of the hydrogen bonds, on the properties of these novel polyamides x.34.

Table 4.1: X-ray Diffraction d_{hkl}-Spacings and Other Structural Parameters. The unit cell parameters for PA-6.6 are: a = 0.49 nm, b = 0.54 nm, c = 1.72, α = 48.5°, β = 77°, γ = 63.5° [1]. The unit cell parameters for the PA-x.34 (x ≥ 4) are almost the same, except of course, the value of the structural repeat c. The unit cell parameters for PA-2.12 are: a = 0.49 nm, b = 0.51 nm, c = 1.98, α = 60°, β = 75°, γ = 59° [5]. Key: [1] Calculated for the backbone in all-trans conformation.

d_{hkl} (Error limits)	**PA-2.12** [5]	**PA-2.34**	**PA-6.6**	**PA-4.34**	**PA-6.34**	**PA-8.34**	**PA-10.34**	**PA-12.34**
100 (± 0.003 nm)	0.414	0.414	0.440	0.443	0.442	0.443	0.444	0.445
010/110 (± 0.003 nm)	0.388	0.386	0.366	0.364	0.364	0.365	0.365	0.365
200 (± 0.003 nm)	-	-	0.220	0.216	0.216	0.218	0.218	0.219
210 (± 0.003 nm)	-	-	0.234	0.234	0.234	0.237	0.236	0.239
001 (± 0.05 nm)	1.71	3.75	1.30	3.68	3.83	4.07	4.22	4.41
002 (± 0.05 nm)	0.86	1.87	0.65	1.87	1.87	-	-	2.15
003 (± 0.05 nm)	-	-	0.43	1.25	1.24	1.38	1.47	1.44
004 (± 0.05 nm)	-	-	0.32	-	0.96	1.04	1.09	1.10
005 (± 0.05 nm)	-	-	0.26	-	0.75	0.82	0.87	-
006 (± 0.05 nm)	-	-	0.22	-	0.63	0.63	-	-
c-repeat[1]	1.98	4.67	1.72	4.91	5.16	5.41	5.65	5.90
c^c*	30.3°	36.6°	41.3°	41.6°	42.1°	41.2°	41.7°	41.6°

4.2.4 Crystal Structure of PA-2.34

PA-2.34 was a special case in the series of polyamides x.34 which has already been discussed in Chapter 3. This special case could also be observed in the X-ray diffraction pattern. The two principal diffraction signals are now at a spacing of 0.42 nm and 0.39 nm, respectively, and the chain tilt angle (c^c*) is reduced to 36.6° (see Table 4.1). These features are similar to typical diffraction pattern of the even-even polyamides 2.y [5,10]. The 100, 010, and 110 signals of this polyamide group appeared to be closer to each other (e.g. for PA-2.12: 100: 0.414 nm; 010/110: 0.388 nm) than in the case of other even-even polyamides like PA-6.6 (100: 0.440 nm; 010/110: 0.366 nm) [1,5]. The difference in spacing of these 100/010 signals can be explained by means of the high temperature crystal structure of even-even polyamides. At higher temperatures even-even polyamides display a transition of the crystal structure from the triclinic phase to a pseudo-hexagonal phase. This transition can be detected by the slowly converging of the 100 and 010/110 diffraction signals upon heating. At a certain temperature between the T_g and T_m, the so-called *Brill* temperature, the merging is finished and the signals remain unchanged until the crystals are going to melt [8,9]. For example, the *Brill* temperature of PA-6.6 is located in the region of 220 ˚C [11,12]. However, upon cooling molten PA-6.6 crystallized again in the usual chain-folded, hydrogen-bonded sheets held together by van der Waals forces. In contrast, the polyamides 2.y do not seem to be able to give the triclinic structure on cooling from the melt, most probably, due to the limited flexibility of the short diaminoethane segment. Therefore, they crystallize in crystal structure resembles the structural changes that occur on heating PA-6.6, prior to the Brill temperature [5].

4.2.5 Folding of the Polyamide Chain in the Crystal Lamella

A priori, it is well established that the folds in even–even polyamides *cannot* entertain an amide unit and maintain α-structure. Unless they are polyamides of the PA-2N.2(N+1) group, e.g. PA-8.10 or PA-10.12, which is not the case for PA-x.34 series [9]. The PA-x.34 have the possibility to fold in either the long (32 alkyl units) diacid alkane segment or the shorter and variable length diamine alkyl segments, or an orchestrated combination. Only the occurrence and measurement of subsidiary maxima from limited

lattice effects, or precise LSP values for annealed samples, can firmly delineate the detailed folding pattern [6,13]. The diamine dimethylene segment in the PA-2.34 is too short to make an adjacent re-entry fold which is necessary to form the observed H-bonded sheets and, therefore, it is assumed that the PA-2.34 should fold *via* the diacid alkyl segments, which is reported in the literature for series of polyamides 2.y [5],

4.3 Conclusions

The TEM pictures and the X-ray diffraction patterns verified the polyamide crystal structure of the novel polyamides x.34. All the new polyamides x.34 crystallize in the typical triclinic or pseudo-hexagonal similar crystal structure of the corresponding even-even polyamides, except of course, for the difference in the distance of the diffraction signals on the meridian of the 00*l* series. This fact points out the marked influence of the amide groups on the crystal structure and, consequently, also on the properties of the novel polyamides x.34. The reason of this strong influence is the energetic requirement of the H-bonds to be linear in order to be as strong as possible. Therefore, the PA-x.34 favor the above discussed crystal structure with the tilted H-bonded sheets.

4.4 Experimental Part

Lamellar Crystal Samples. The synthesis of the used polyamides 2.34, 4.34, 6.34, 8.34, 10.34, and 12.34 is described in Chapters 2 and 3. The typical preparation of lamellar crystals is described with PA-2.34 as an example. Specific conditions for the other polyamides x.34 are shown in Table 4.2.

5.8 mg of polyamide 2.34 was dissolved in 14.3 mL of DMF at 150 ˚C and the resulting solution was kept at this temperature for 30 min. Subsequently, the polymer was precipitated by cooling the solution to RT. The polymer lamellae were redissolved at 146 ˚C (self-seeding temperature). Immediately after the solution became clear it was kept at 135 ˚C. After 10 min the polyamide crystallized forming a suspension with some

aggregates. In order to destroy this aggregation the solution was ultrasonicated until the polymer crystals were finely suspended. The obtained crystals were used for both TEM as well as X-ray diffraction. The sedimented mats of chain-folded lamellar crystals for X-ray investigations were obtained by filtration of 5 mL of this suspension through a PTFE syringe filter. The mat obtained was carefully dried and annealed at 145 ˚C under vacuum for 14 h.

Transmission Electron Microscopy. Samples for TEM were prepared according to the following procedure. A carbon-coated TEM copper grid was placed on a filter paper. A small drop of the above described crystal suspension was dropped on this grid after which the solvent was allowed to evaporate. TEM micrographs were taken at a magnification between 2,000 and 26,000 using a Philips EM400T at 100 kV.

X-ray Diffraction. X-ray diffraction patterns were taken on a Philips PW2213 sealed beam X-ray generator using a Ni-filtered Cu Kα (conditions: 35 kV, 40 mA, wavelength: 0.1542 nm). The diffraction photographs were recorded on a film using a flat-plate camera. Selected polyamide samples were calibrated with calcite (d_B equals 0.3035 nm) which was dusted onto the crystal mats. The surface of the sedimented crystal mats were placed parallel to the point-collimated X-ray beam; normal to the projected c-axis (cf. Figure 4.12). All wide- and medium-angle X-ray diffraction patterns were obtained at room temperature and vacuum.

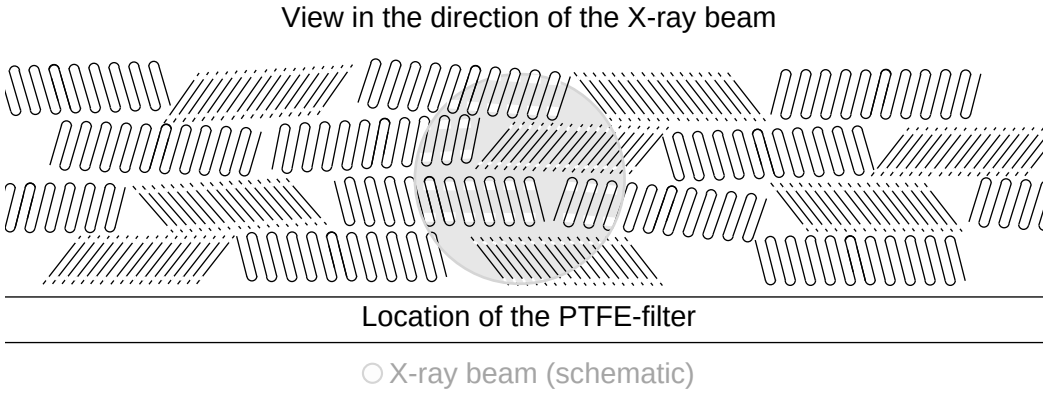

Figure 4.12: Schematic illustration of the position of the crystal mats to the X-ray beam.

Table 4.2: Crystallization conditions of the polyamides x.34.

Polyamide	Polymer (mg)	Solvent (DMF, mL)	Polymer/ Solvent (mg/mL)	1st Dissolving Temp. (˚C)	Self-Seeding Temp. (˚C)	Crystallization Temp. (˚C)	Crystallization Time (min)	Annealing Temp. (˚C) & Time (h)
PA-2.34	5.8	14.3	0.41	150	146	135	10	145, 14
PA-4.34	6.4	15.8	0.41	150	146	135	10	145, 14
PA-6.34	1.8	4.0	0.45	146	146	130	10	-
PA-8.34	6.9	16.8	0.41	150	145	132	23	-
PA-10.34	4.4	10.0	0.44	145	145	129	20	128, 14
PA-12.34	2.6	15.0	0.19	148	147	128	20	125, 14

Model Building. The software package Cerius2, version 3.8 (MSI) was used in structural modeling.

4.5 References

[1] Bunn, C. W.; Garner, E. V. *Proc. R. Soc. (Lond.)* **1947**, *189A*, 39.

[2] Peacock, A. J. *Handbook of Polyethylene*; Marcel Dekker, Inc.: New York, 2000.

[3] Jones, N. A.; Atkins, E. D. T.; Hill, M. J. *J. Polym. Sci. Phys. Ed.* **2000**, *38*, 1209.

[4] Jones, N. A.; Atkins, E. D. T.; Hill, M. J.; Cooper, S. J.; Franco, L. *Polymer* **1997**, *38*, 2689.

[5] Jones, N. A.; Cooper, S. J.; Atkins, E. D. T.; Hill, M. J.; Franco, L. *J. Polym. Sci. Phys. Ed.* **1997**, *35*, 675.

[6] Atkins, E. D. T.; Keller, A.; Sadler, D. M. *J. Polym. Sci. Part: A-2* **1972**, 10, 863.

[7] Dreyfuss, P.; Keller, A. J. *J. Macromol. Sci. Phys.* **1970**, *B4*, 811.

[8] Jones, N. A.; Atkins, E. D. T.; Hill, M. J. *Macromolecules* **2000**, *33*, 2642.

[9] Jones, N. A.; Atkins, E. D. T.; Hill, M. J.; Cooper, S. J.; Franco, L. *Macromolecules* **1997**, *30*, 3569.

[10] Atkins, E. D. T.; Hill, M. J.; Jones, N. A.; Cooper, S. J. *J. Polym. Sci. Polym. Phys. Ed.* **1998**, *36*, 2401.

[11] Brill, R. J. *Prakt. Chem.* **1942**, *161*, 49.

[12] Brill, R. J. *Physik Chem.* **1943**, *61*, 1353.

[13] Magill, J. H.; Girolamo, M.; Keller, A. *Polymer* **1981**, *22*, 43.

5. Fibers of Polyamide 6.34

5.1 Introduction

Interest in high-strength / high-modulus polymer fibers arises from the observation that polymers may combine good mechanical properties with low weight. Figure 5.1 compares the specific (i.e. per unit density) modulus and strength of various high-performance materials [1].

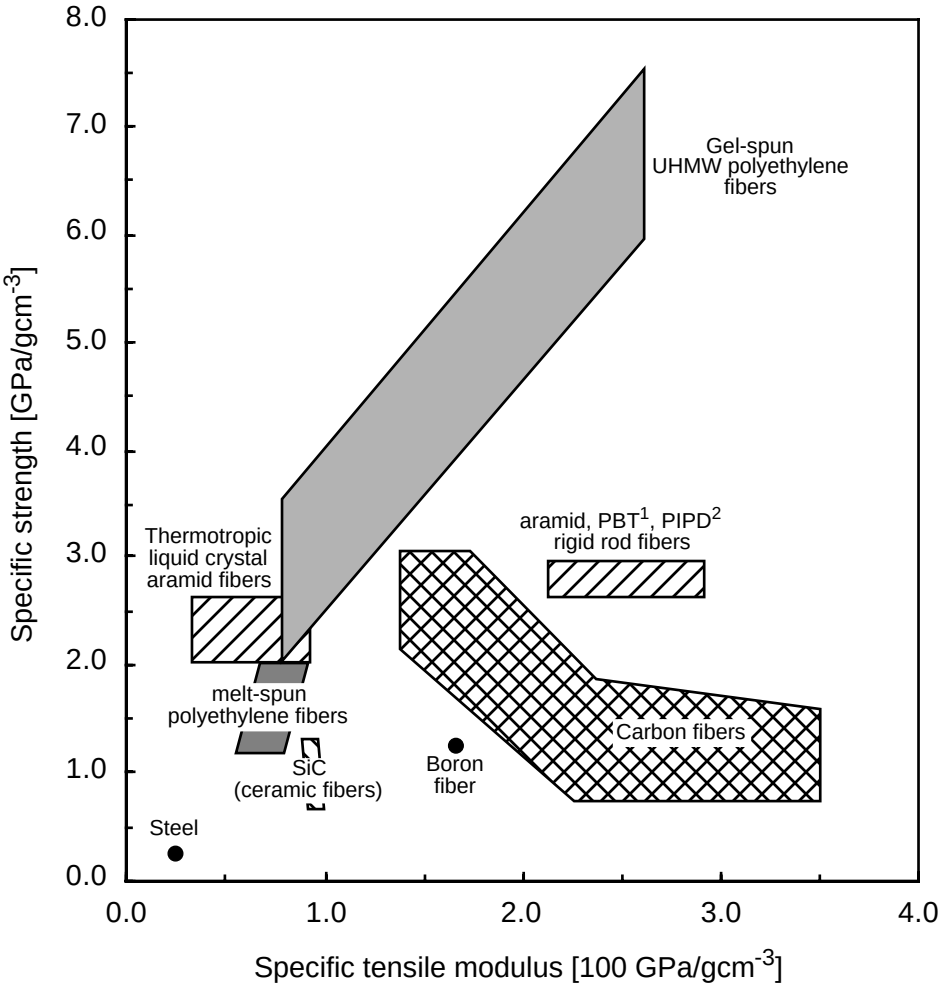

Figure 5.1: Specific strength vs. specific modulus for a variety of high performance materials. Key: Specific strength = strength/density, specific tensile modulus = modulus/ density [1]PBT = poly(butylenterephthalate, [2]PIPD = poly{2,6-diimidazo[4,5-b4‘,5‘-e]pyridinylene-1,4(2,5-dihydroxy)phenylene} = M5 (Akzo-Nobel) [1-5].

From a property-weight point of view, polymers with high specific strengths are clearly superior to metals and ceramics [1,3,6,7].

A precondition for making high-strength polymer fibers is that the constituent macromolecular chains be highly extended and oriented in the direction of the fiber axis. There are essentially two ways of preparing high-strength polymer fibers. The first is to synthesize stiff, planar molecules which exhibit liquid crystal behavior between their solid state and their melting temperature (thermotropic) or in solution (lyotropic) and form highly oriented, extended-chain structures in the solid state. Typical polymers of the latter are aramides. For example, in 100% sulfuric acid, poly(*p*-phenylene terephthalamide) forms nematic structures which can be easily oriented in the direction of the fiber by dry-jet wet-spinning [8]. The second involves flexible-chain polymers, such as polyethylene, that can be oriented into extended-chain structures in the solid state by either solid-state extrusion or super-drawing. The most successful example of this approach is the gel spinning of ultra-high-molecular-weight polyethylene [9,10].

The production of high-strength polymer fibers requires a high degree of chain orientation. The eventual orientation is a product of the attainable draw ratio, which is controlled by three factors: chain length and therefore molecular weight [10,11], entanglement density in the polymer [10], and movement in the solid (crystalline) phase [13,14].

The weight-average molecular weight ($\overline{M}_w$) of the synthesized PA-6.34 was observed to be around 30,000 (cf. Chapter 2). This $\overline{M}_w$ value limits the maximum draw ratio attainable for this material by plastic deformation [11,15]. Entanglement density, the second factor, has a bearing on deformation if the molecular weight of the polymer is relatively high and can be avoided by crystallization from solution [9,10,16-19]. In addition, the molecular weight of around 30,000 of here discussed PA-6.34 is below the critical molecular weight which would effect the draw ratio of polyamides due to entanglement [15,20,21]. The third factor in the case of polyamides is movement in the solid (crystalline) phase. A high draw ratio requires a certain level of movement in the crystalline phase so that the polymer chains may be drawn out of the crystals without breaking. Drawing is quite easy in the case of polyethylene, where the relatively weak van der Waals bonds do not hinder the necessary movement of individual chains through the crystalline phase, especially at elevated temperatures (cf. Figure 5.2) [14,22]. On the contrary polyamides, the energy required to draw a polyamide chain out of a PA-6.6

crystal corresponds to the dissociation energy of approx. 20 hydrogen bonds or nearly that of a covalent bond [23]. Consequently, the chain is likely to break before it can slip out of the crystal. English *et al.* demonstrated with ^{2}H-NMR experiments that strong hydrogen bonds can limit the draw ratio [14]. Not even elevated temperatures can significantly reduce the number of hydrogen bonds in the crystalline lattice. Consequently, it is not possible to exceed the maximum attainable draw ratio of 4 - 5 (see Figure 5.2) – the production of high-strength polyamide fibers is therefore primarily hampered by the strong hydrogen bonds in the crystalline phase [15].

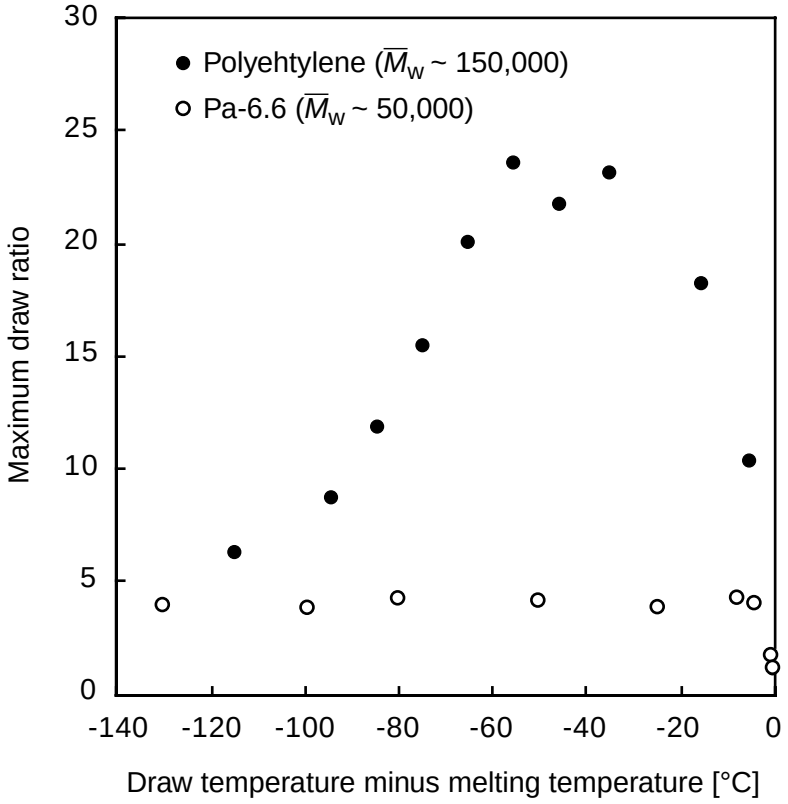

Figure 5.2: The maximum observed draw ratios of polyethylene and polyamide 6.6 versus the draw temperature [14].

In this chapter the possibility of making high-modulus polyamide fibers of the novel PA-6.34 will be discussed. It was the ability of PA-6.34 to form an aliphatic network in conc. sulfuric acid which led to the assumption that a polyethylene-like gel process could be devised for the PA-6.34/sulfuric acid system. The conc. sulfuric acid was able to break the hydrogen bond between the amide groups without dissolving the aliphatic segments of PA-6.34 (see Chapter 2). Other encouraging factors were the far

fewer hydrogen bonds in the crystalline phase of PA-6.34 compared with PA-6.6, and the low crystallization rate (see Chapters 2 and 4). Consequently, it seemed that a temperature window might exist in which it is possible to produce PA-6.34 fibers with a crystalline phase contained just enough hydrogen bonds to form the network necessary for orienting the polymer chains in tensile deformation while still allowing movement. These prepared PA-6.34 fibers should lead to high modulus PA-6.34 fibers by a tensile deformation process at elevated temperatures.

5.2 Gel Processing

5.2.1 Methods to Produce a PA-6.34/Sulfuric Acid Gel

PA-6.34 was able to form a thermoreversible gel in concentrated sulfuric acid (concentration: 99.999 %.). At temperatures above 80 °C, this gel turned into a viscous solution from which fibers could be spun (see Figure 5.3).

Figure 5.3: Solution spun PA-6.34/sulfuric acid fiber at 80 ˚C.

There were two ways to make the PA-6.34/sulfuric acid gel. It was important that the outcome be a completely homogeneous gel, i.e., that all H-bonds between intra- and interchain amide groups were broken. The first method (A) consisted in simultaneously applying heat and mechanical shear force to a PA-6.34/sulfuric acid mixture. The PA-6.34/sulfuric acid gel used for tensile testing was prepared by stirring 0.5 g of dried PA-6.34 powder with 2.5 mL conc. sulfuric acid at 95 °C with a magnetic bar (see

Experimental Section). The search for a stirring system capable of supplying a higher shear force to the PA-6.34/sulfuric acid mixture led to the investigation of a special glass-KPG stirrer (see Chapter 2 where this stirrer was used to produce PA-x.34/sulfuric acid gels). But this stirrer was only effective with a small amount of material (~ 50 mg). A double-helix mixing-screw stirrer was used for larger batches, but this was unsuccessful too, since the Weissenberg effect caused the “partial” polyamide gel to creep out of the sulfuric acid before the mixture was homogeneous [24].

The idea behind the second method (B) was to make a solution of PA-6.34 in a certain solvent, which would then be washed out with conc. sulfuric acid (for dilute systems, see also Experimental Section in Chapter 2). The advantage of this method would be that no polyamide crystals should be theoretically capable of existing in a solution of PA-6.34. The resultant PA-6.34/sulfuric acid gel would therefore not contain any direct hydrogen bonds between amide groups. The solvent chosen was ethanesulfonic acid (ESA), which was capable of dissolving PA-6.34 at room temperature – the ESA not only broke the hydrogen bonds, but it also influenced van der Waals’ interactions between aliphatic moieties of the PA-6.34 and improved the solubility (see Chapter 2). In addition, ESA also proved to be miscible with sulfuric acid over a wide range of compositions. A concentrated solution of PA-6.34 and ESA was therefore prepared at room temperature (10 wt % PA-6.34). The ESA was extracted five times with an excess of conc. sulfuric acid. The PA-6.34 started to gel when the conc. sulfuric acid was added. The resultant PA-6.34/sulfuric acid gel consisted of 14 wt % PA-6.34, sulfuric acid and traces of ESA (around 0.05 wt %, calculated from the preparing procedure). The melting temperature (T_m) was 50 - 60 °C and thus in the expected melting range of the other PA-6.34/ sulfuric acid gels investigated (see Chapter 2). Aside from the fact that all hydrogen bonds formed with the amide groups were presumably broken, method (B) offered the important advantage of not requiring additional heating to produce the PA-6.34/sulfuric acid gel. Degradation of the polyamide in conc. sulfuric acid was significantly slower at room temperature than at elevated temperatures.

5.2.2 Mechanical Properties of PA-6.34/Sulfuric Acid Gel (Method (A))

The network-forming moiety was most likely the extended aliphatic segment of the dicarboxylic acid, because all hydrogen bonds formed by the amide groups were removed by the conc. sulfuric acid which was present in at least five-fold excess compared with the polyamide concentration (see Chapter 2 and Experimental Section). In theory, these residual aliphatic "crystallites" should have undergone deformation similar to that of high-density polyethylene on account of their aliphatic nature. Consequently, it should be possible to draw this PA-6.34/sulfuric acid fiber to draw ratios above the usual value of $\lambda = 4 - 5$ [15], especially since there are no longer any hydrogen bonds to hinder movement in the crystalline phase and since the residual aliphatic crystallites form the network needed to transmit the applied tensile force across the entire sample. Subsequent experiments bore out this assumption. The solution-spun fibers of PA-6.34/sulfuric acid gel prepared by method (A) exhibited significant necking under stress at RT; this is evidence of plastic deformation, which is a prerequisite for orienting the polymer chains. Furthermore, the draw area displayed a significant dependence of birefringence in cross-polarized light on the applied angle (0°, 90°: dark; 45°: bright); this is highly indicative of uniaxial orientation (cf. Figure 5.4) [25]. These two observed effects support the presence of a limited network in the investigated polyamide/sulfuric acid fiber.

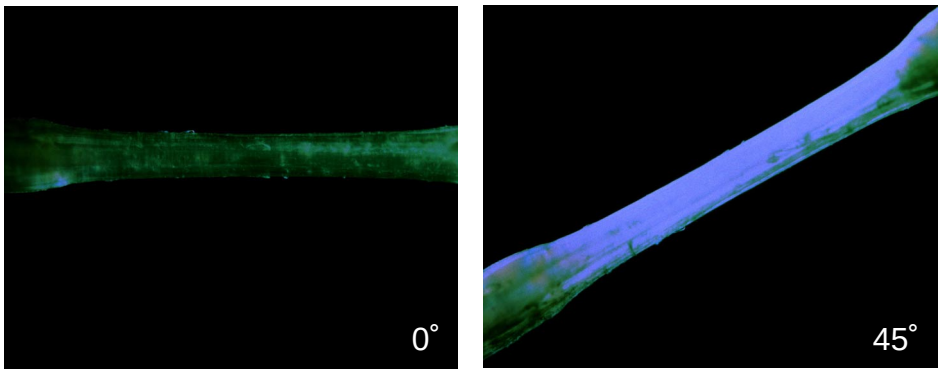

Figure 5.4: A PA-6.34/sulfuric acid fiber in cross-polarized light after drawing at RT (draw ration = 2 to 3).

Figure 5.5 shows the stress-strain curves, measured at different temperatures, for melt-pressed tensile bars of PA-6.34/sulfuric acid gel made by method (A).

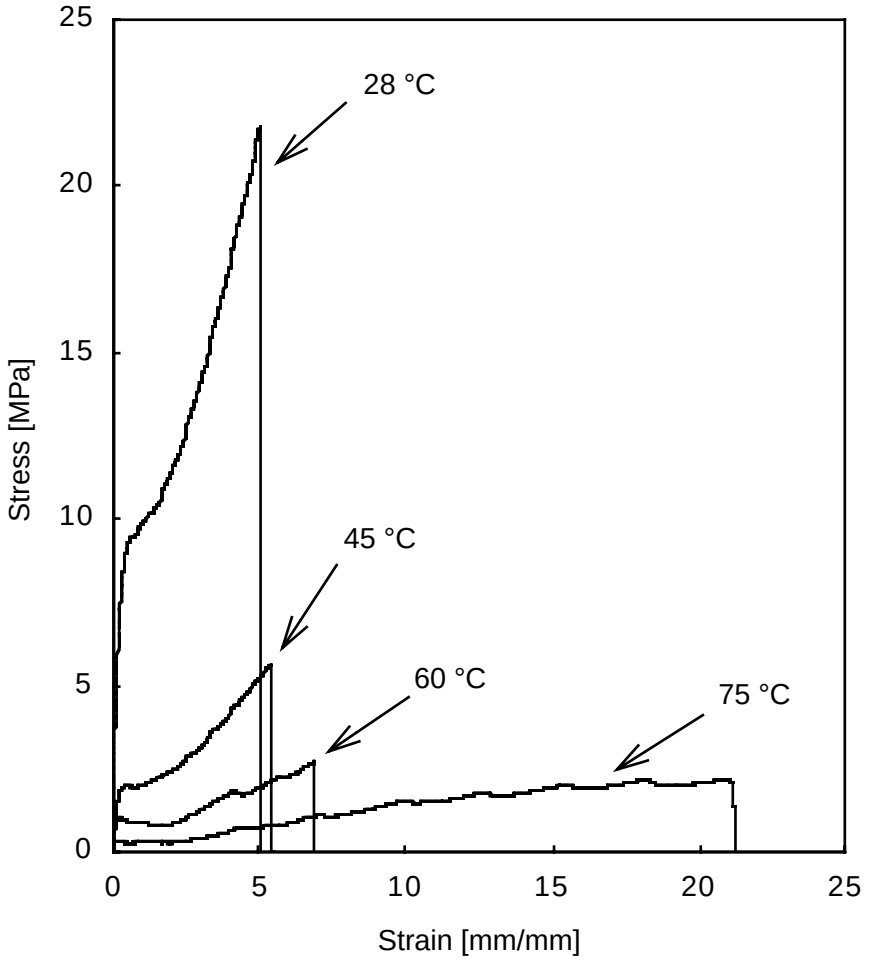

Figure 5.5: Stress-strain curves of the PA-6.34/sulfuric acid gel (procedure A) at different temperatures (strain rate: 12.7 mm/min).

There is a certain error in the shown stress-strain curves due to the difficulty of determining the exact dimensions of the tensile bar. In addition, the stretched samples were elastic to a certain degree and, therefore, the observed strain was always higher than the "true" strain. The "waves" in the stress-strain curves at elevated temperatures (60 and 75 °C) were attributed to temperature instability within the chamber of the tensile tester (duration of experiment between 7 to 25 min.). Nevertheless, the observed stress-strain curves showed a significant increase in draw ratio with increase in drawing temperature. In particular, a λ of around 20 at 75 °C was very promising in respect of achieving high orientation. This value was roughly four times that for neat PA-6.34. In addition, the stress-strain curves of tensile tests performed at lower temperatures, for example 28 °C and 45 °C, show only a point of inflection instead of a definite yield point (see Figure

5.5). This deformation response is similar to the one of PA-6.6 draw at high temperatures (above 80 °C) or PA-6.34 at 150 °C (see Figure 2.7) and indicates an increase of chain mobility in the amorphous phase [26]. However, during the tensile tests, a yield point indicative of plastic deformation was observed at temperatures above the melting temperature of the aliphatic “crystallites” (cf. Figure 5.5). The drawing temperature of 75 °C is above the determined melting temperature of the PA-6.34/sulfuric acid gel, consequently, there was the possibility that this drawing was actually taking place from a high-viscosity melt and not from a gel. To investigate this possibility, the tensile test at 75 °C was repeated with a small modification. This time, two tensile bars were tested simultaneously and the test was stopped as soon as the first tensile bar broke. The second, intact test bar was kept under stress while the system was cooled to RT. At RT, this sample no longer exhibited the aforementioned elasticity. The sulfuric acid was extracted from the sample with 5 M NaOH under constant stress. The resulting fiber was washed with distilled water and dried under stress at 75 °C for 14 h (see Experimental Section). The stress-strain curve for this produced PA-6.34 fiber at RT is shown in Figure 5.6.

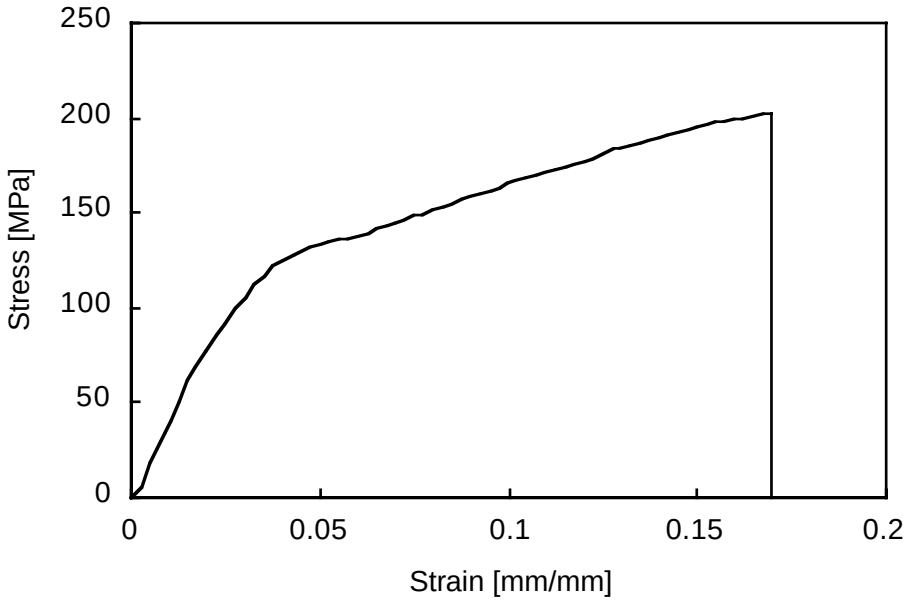

Figure 5.6: Stress-strain curve at RT of a PA-6.34 fiber which was produced by the gel process at 75 ˚C with a draw ratio of 20 (Gel preparation: procedure (A); strain rate: 12.7 mm/min).

The tensile modulus of this PA-6.34 fiber was 4.0 GPa, a value roughly equivalent to tensile modulus of an untreated PA-6.34 fiber drawn five times (3.7 GPa; see Chapter 2), for which plastic deformation was observed. It was therefore concluded that plastic deformation had occurred during the tensile test, because tensile modulus increased greatly compared to an isotropic PA-6.34 sample (0.7 GPa; see Chapter 2). The same applied to the tensile strength. In addition, the orientation achieved in the test bar was supported by the X-ray diffraction pattern of the PA-6.34 sample discussed here and shown in Figure 5.7. This pattern revealed a substantial degree of uniaxial orientation, as can be seen from the equatorial reflections. Consequently, the drawing of the PA-6.34/ sulfuric acid gel fiber at 75 °C was most likely not drawing from a viscous melt. As the temperature (75 °C) was above T_m of the gel, most probably a type of network other than the aliphatic network was formed in the PA-6.34/sulfuric acid gel fiber. It is possible that, due to the method of preparing the gel, the sulfuric acid did not break all the hydrogen bonds between the amide groups in the PA-6.34 crystals and, therefore, the gel contains both very small remaining H-bonded PA-6.34 crystals and aliphatic “crystallite” segments. Thus, the residual polyamide crystals are able to act as the network which transmits the applied tensile force to orient the polymer chains and, consequently, leading to a drawing situation similar to that for a virgin PA-6.34 fiber.

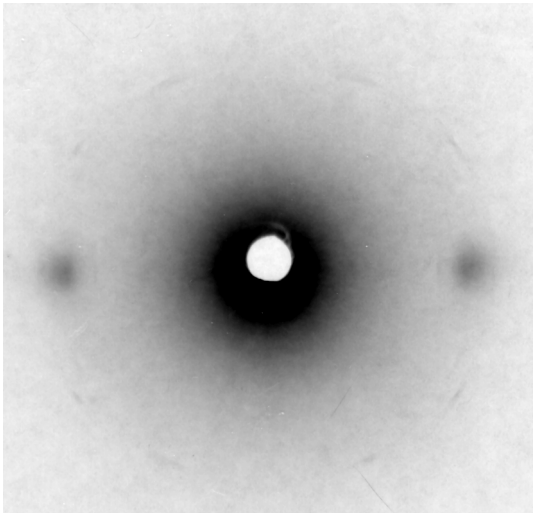

Figure 5.7: X-ray diffraction pattern of a PA-6.34 fiber which was produced by the gel process at 75 ˚C with a draw ratio of 20 (Gel preparation: procedure (A)).

5.2.3 Mechanical Properties of PA-6.34/Sulfuric Acid Gel (Method (B))

To rule out the possibility of the aforementioned polyamide network, tensile tests were performed on a PA-6.34/sulfuric acid gel made by method (B). The maximum draw ratio attained was 9.5 at 70 °C (see Figure 5.8), which was less than for the PA-6.34/ sulfuric acid gels used above, and the samples already showed signs of melting. Most likely, the observed draw ratio was lower than during the first measurements because higher humidity during the measurements led to much greater absorption of water by the hygroscopic sulfuric acid and caused damage to the gel. The existence of water dilute the concentrated sulfuric acid, which leads to an acceleration of the degradation of the polyamide and also the polyamide starts to "precipitate" from the gel due to the fact that dilute sulfuric acid is not capable to break the H-bonds between the amide groups in PA-6.34. However, the tensile test exhibited a yield point and that was indicative of the same kind of plastic deformation in the other tensile tests at elevated temperatures (cf. Figure 5.5). But, unfortunately, these tests did not yield better results, and so this method was abandoned.

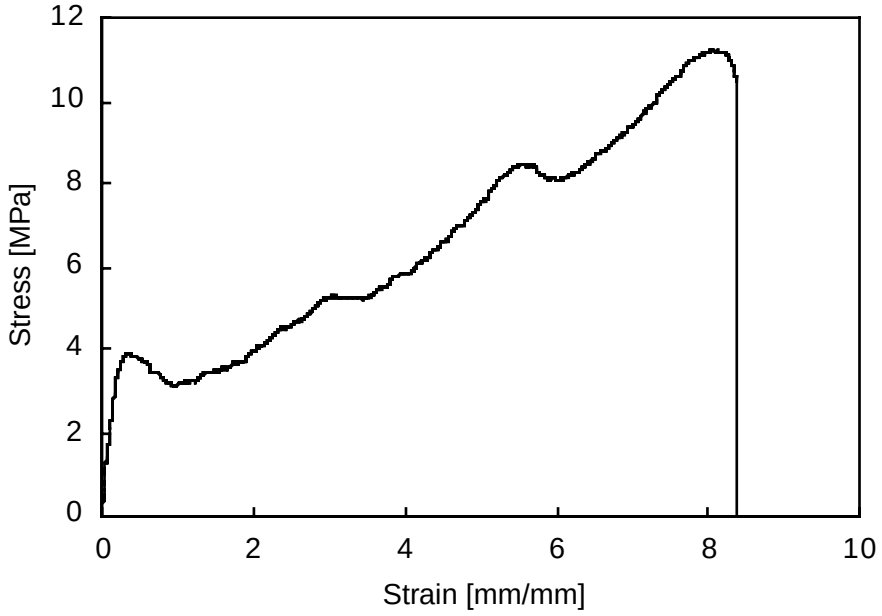

Figure 5.8: Stress-strain curve of the PA-6.34/sulfuric acid gel (procedure (B)) at 70 ˚C (two test bars at the same time, strain rate: 12.7 mm/min).

---

[1] This section is based on the publication: Structures of x 34-Nylons in Chain-Folded Lamellae and Gel-Spun Fibers: Ehrenstein, M.; Sikorski, P.; Atkins, E.; Smith, P. submitted to *J. Polym. Sci. Polym. Phys.* on May 2002.

5.2.4 X-ray Diffraction on the Gel-Processed Polyamide Fibers[1]

To obtain more information about the gel-processed polyamide fibers, X-ray experiments were conducted. Figure 5.9 a) shows the X-ray diffraction pattern of a gel-processed PA-6.34 fiber of a draw ratio of approximately $\lambda \approx$ 4-5 (drawn at room temperature) after extraction of the sulfuric acid with 5 M NaOH and water (preparing procedure see Experimental).

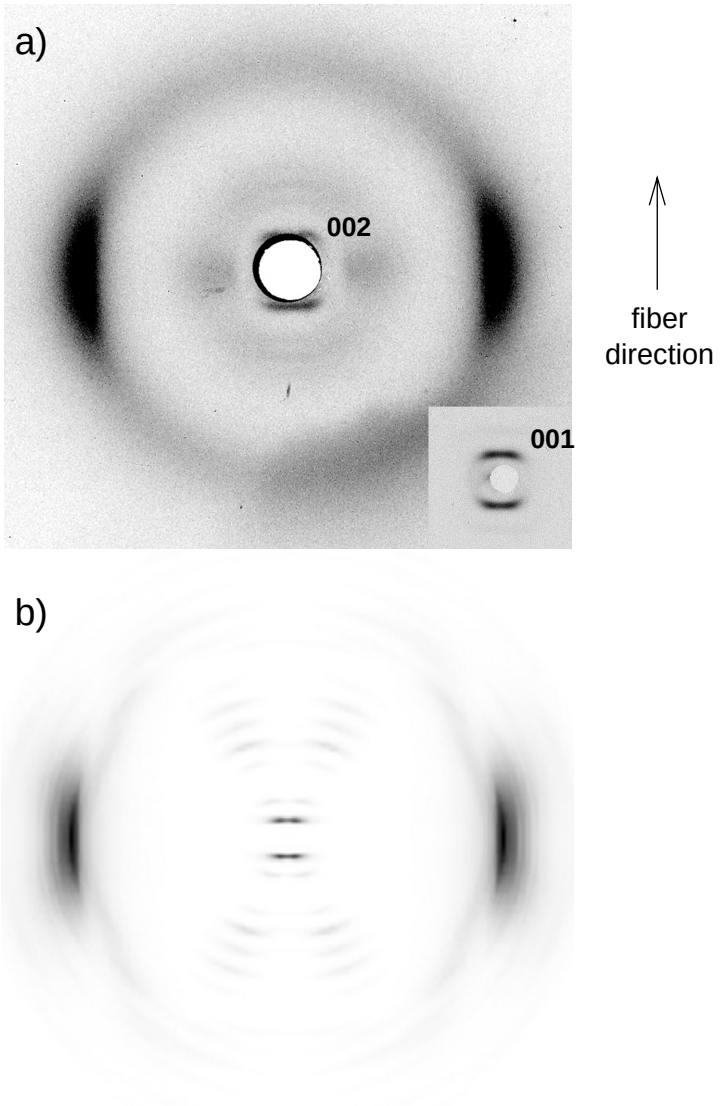

Figure 5.9: X-ray diffraction pattern from PA-6.34 gel-spun fiber; draw direction vertical. a) experimental composite; b) calculated. The chain axes are parallel to the draw direction and therefore the 00l diffraction signals lie at an angle (c^c) to the meridian. Note the single strong equatorial diffraction signal (100).*

This diffraction pattern is different from the pattern shown in Chapter 2 for a conventionally drawn PA-6.34 fiber (cf. Figure 2.7). The two characteristic interchain spacings at 0.44 nm (100) and 0.37 nm (010) expected on the equatorial line are merged together at the intermediate value of 0.42 nm (Table 5.1) [27]. The X-ray diffraction pattern shows two other important features. (1) The angular split of the 001 and 002 diffraction signals (c*-axis) off the meridian is a classical pattern of behavior for triclinic polyamide fiber structures, as shown and explained by Bunn and Garner in 1947 [27]. The chain direction (c-axis) is along the fiber axis (draw direction) and the angle of the 00*l* diffraction series relative to the meridian is 41.3° (c^c*) for PA-6.6 and 42.2° for the structure in the lamellar crystals of PA-6.34 (cf. Chapter 4) [27]. In the case of the PA-6.34 gel-spun fibers this tilt angle is reduced to 29.6° (see Table 5.1). (2) The length of the structural repeat (c-value) is reduced to 4.78 nm (layer line spacing) compared with 5.16 nm for the lamellar sample crystallized from DMF (cf. Chapter 4). There is a concomitant change in the d100-spacing (see Table 5.1). The basic features of the gel-spun fiber are similar to that of even-even polyamides heated to their Brill temperature. The shear angle reduces, the alkyl segments shorten and the arrangement of the chains in the crystal lattice, projected parallel to their axes, becomes hexagonal instead of triclinic (d100 = 0.42 nm).

Table 5.1: X-ray diffraction d-spacings and structural parameters. Key: [1]c-repeat measured from the layer line spacing.

d_{hkl}	**PA-6.34 (Gel-processed Fiber)**
100 (± 0.002)	0.420
001 (± 0.08)	4.78
002 (± 0.06)	2.39
c-repeat (± 0.04)	4.63[1]
c^c*	29.6°

The interpretation of the X-ray diffraction data is that the gel-spun fibers have a structure based on the PA-6.6 triclinic α-structure, but with reduced shear (≈ 30% in

terms of tilt angle) [27]. This interpretation was tested by generating, using the Cerius2 program, the fiber diffraction pattern. The calculated diffraction pattern for PA-6.34 is shown in Figure 5.9 b) and the comparison with the experimental pattern in Figure 5.9 a) is good. In experiments, it was found that the tilt angle and c-repeat are, to some extent, both a function of the fiber spinning and drawing procedure. The relative shear can vary with the length of chemical repeat unit for a particular PA-x.34 and also between different polyamides x.34 ($x \geq 4$). Further, more extensive, studies would need to be undertaken to establish the structural relationships.

It was judged that the interchain shear of 13° ($\beta = 77°$) inherent in even-even polyamide p-sheets remains constant and the change in the shear results from the intersheet shear (in ac-planes) controlled by van der Waals interactions. The alkyl segments are no longer in their all-trans conformation. Thus, the interaction with sulfuric acid has changed the interaction parameters resulting in room temperature structure that bears a resemblance to the high temperature phase of PA-6.6.

5.2.5 Possible Reasons for the Low-Modulus of Gel-Spun PA-6.34 Fibers

The just discussed results of X-ray investigation suggest that the sulfuric acid gel-process leads only to a change of the crystal modification in the PA-6.34 fiber similar to the change of crystal modification at the Brill transition of, e.g., PA-6.6. Therefore, the effect of the gel-process can described as a reduction of the Brill transition temperature under maintenance of the polyamide typical H-bond network between the amide groups. But, how is this consistent with the observed results, for example, the large draw ratios of around 20? An explanation could be that the orientation takes only place in the amorphous parts of the sulfuric acid/PA-6.34 fiber. The sulfuric acid breaks the H-bond between the amide groups in the amorphous parts and allows, therefore, an orientation of them at relative low temperatures. Due to this orientation the existing polyamide crystals get lined up, too. This explains then the good orientation shown in the X-ray diffraction pattern and the observed tensile modulus, which was similar to the one of a conventional draw PA-6.34 fiber. But, does this explain the draw ratio of 20, would not be a draw ratio of five more plausible and how does this match with the observed low melting temperature of the sulfuric acid/PA-6.34 gel and the possibility to spin fibers out of this gel at a temperature of 80 °C?

In the following, two possible reasons will be discussed in order to explain the observed results. Sulfuric acid is a bifunctional acid, and it is possible that all hydrogen bonds formed between the amide groups were indeed broken, but that new ones were established *via* the sulfuric acid molecules (see Figure 5.10). These new hydrogen bonds would behave like the hydrogen bonds in the polyamide crystal, and they were the reason that it was possible to produce orientation in the polymer fiber, even at temperatures above the melting temperature or dissolution temperature (T_d) of the aliphatic "crystallites". This assumption is supported by the observed tensile modulus of 4.0 GPa of the at 75 ˚C gel-processed PA-6.34 fiber (see Figure 5.6) which is similar to the tensile modulus of an untreated PA-6.34 fiber drawn five times at 150 °C(3.7 GPa; see Chapter 2) whose hydrogen bonds are formed by amide groups. Therefore, a certain network, which is different from the aliphatic "crystallites" network and stable at temperatures of at least 75 °C has to be presented in the PA-6.34/sulfuric acid gel fiber in order to allow this observed mechanical property.

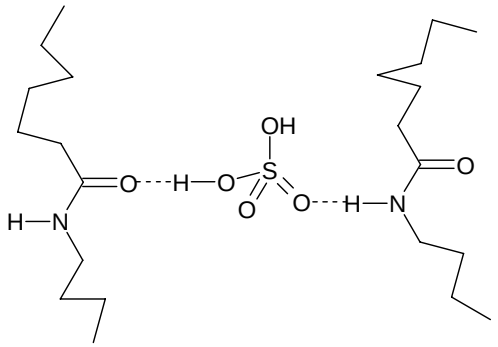

Figure 5.10: Schematic picture of polyamide chains linked via a sulfuric acid molecules.

The other explanation entails a consideration of certain crystal-transition behavior. In the literature, the phenomenon of chain movement in the crystalline phase is described as crystalline α_c-relaxation above the glass transition temperature (T_g) and below the melting temperature (T_m) [28,29]. At the so-called α_c-relaxation temperature ($T_{\alpha c}$), there is a significant rise in the coefficient of thermal expansion of the investigated polymer crystal and an attendant decrease in intra-crystalline forces within the crystalline fraction of the polymer. This decrease makes it possible to draw polymer chains out of the crystal to yield highly oriented polymer chains. It seems that those polymers which do not exhibit this transition cannot be oriented to a high degree by plastic deformation, e.g.

polyethylene terephthalate [28]. In contrast, polyethylene can be highly oriented by plastic deformation *via* a gel process at 130 °C [9]. The $T_{\alpha c}$ of polyethylene is about 88 °C. It was thus assumed that temperatures higher than 88 °C are needed for high draw ratios and consequently high orientation by means of plastic deformation in the case of polyethylene-like systems. From this assumption, it was concluded that the aliphatic segments of the PA-6.34 in sulfuric acid were too short to exhibit plastic deformation similar to that of polyethylene because their melting temperature of 50 - 60 °C was too low to exhibit the α_c-relaxation temperature of 88 °C required for polyethylene crystals. This view is supported by the deformation response and the draw ratios of 5-6 of PA-6.34/sulfuric acid gel samples observed at 28 °C and 45 °C which is similar to the one of PA-6.34 drawn at 150 °C (see Figure 2.7) and indicates that the sulfuric acid treatment of PA-6.34 increases of chain mobility in the amorphous phase at low temperatures but does not allow chain movement in the aliphatic “crystallites” or in the above described sulfuric acid network. At elevated temperatures, the aliphatic “crystallites” are molten and only the suggested sulfuric acid network transmitted the applied tensile force which leads to the observed orientation (see Figure 5.7).

A solution to confirm and overcome the above described situation is to use polyamide containing extended aliphatic segments with at least 60 methylene groups long. The PA-6.34/sulfuric acid gel exhibit a T_m of 54 °C, which is comparable to that of a C_{26} *n*-alkane. Consequently, a PA-6.60/sulfuric acid gel should melt at 90 °C, which is the T_m of a C_{52} *n*-alkane, and is above the α_c-relaxation temperature of polyethylene crystals (see Chapter 2) [30]. Thus, the gel might undergo polyethylene-like plastic deformation. In addition, the novel polyamide should be able to form a gel with a monofunctional acid, such as methanesulfonic acid (MSA). This is a realistic assumption because the PA-6.34 exhibit a certain degree of aggregation in MSA, as was demonstrated by light-scattering experiments (see Chapter 2). A second reason in favor of MSA is its monofunctionality as that would rule out the “new” hydrogen bonds discussed above.

5.2.6 Conclusions

The PA-6.34/sulfuric acid gel process does, unfortunately, not significantly improve the mechanical properties of the PA-6.34. The maximum draw ratio achieved is

of the order of $\lambda = 20$, i.e., about four times higher than observed for neat polyamides, but the observed tensile modulus is similar to that of a standard PA-6.34 fiber drawn five times. The X-ray experiments indicated a certain orientation of the polyamide after the gel process. But, unfortunately, this orientation is not enough and "weak" moieties were left in the fiber, which prevented the production of high-modulus PA-6.34 fibers.

5.3 Quenching

5.3.1 Manufacture and Properties of Quenched PA-6.34 Fibers

Another method of making high-modulus PA-6.34 fiber is to utilize the polymer's low crystallization rate. In Chapter 2, it was mentioned that a quenched sample of PA-6.34 exhibit significant recrystallization just before it started to melt. Figure 5.11 compares the differential scanning calorimetry (DSC) scan of a quenched PA-6.34 film with that of a quenched PA-6.6 film. Both were produced by quenching a melt-pressed film in liquid nitrogen, starting from a temperature 30 °C above the respective melting temperature.

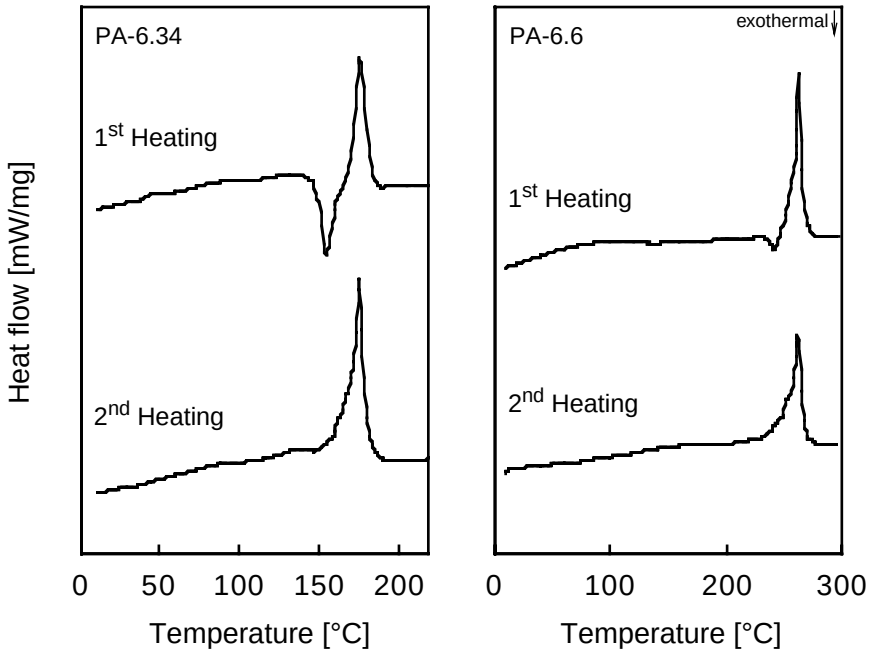

Figure 5.11: Differential scanning calorimetry scans of quenched PA-6.34 and PA-6.6 (Vydyne 21, Solutia) films (heating and cooling rate of 20 ˚C/min).

From these scans, it was evident that the PA-6.34 can be quenched much more easily than PA-6.6. The reason is the larger crystal unit cell of PA-6.34, the formation of which requires much more movement by the polymer chains; consequently, the crystallization rate is lower than the one of PA-6.6 and the fraction of amorphous polymer is higher after quenching. This was supported by the detection of the T_g at 40 °C in the first heating curve of the quenched sample but not after melting in the second (cf. Figure 5.11). Also, the enthalpy of recrystallization was 10 J/g lower than the enthalpy of fusion. In addition, the crystallinity of the quenched film was around 55 % of that for unquenched crystals, as shown by comparing the enthalpy of fusion of the corresponding crystals (cf. Table 5.2). Thus, the amorphous content of PA-6.34 was much higher after quenching than after relatively slow cooling and around 75 % of the crystals of the quenched sample were formed during the recrystallization process. Theoretically, it should have been possible to use this relatively small crystalline network for plastic deformation and produce higher draw ratios than the standard value of $\lambda = 5$. Because the number of hydrogen bonds restricting movement in the crystalline phase would now be so low that polymer chains could be drawn out of the crystal before they broke. The fact that the observed recrystallization temperature of the investigated polyamides was quite high had to be taken into account. Normally, recrystallization should take place at a temperature between T_g and T_m, as is, for example, the case for polyethylene terephthalate [31] – at this temperature, nucleation and movement of the polymer under consideration are conducive to crystallization. But this did not seem to be the case for polyamides, again the reason being the hydrogen bonds. They seemed to stay intact, thereby preventing any movement by the polymer chains until the polyamide started to melt as normal. Recrystallization therefore occurred just before the crystalline phase melted (cf. Figure 5.11).

The most promising temperature for the suggested drawing process was therefore just prior to that of recrystallization. However, the tensile tests at different temperatures (temperature of the oil bath: 125 °C, 132.5 °C, and 135 °C) failed to show an increase in draw ratio (the values do not exceed $\lambda = 6$). Another drawing temperature could be the point at which melting has just started after the recrystallization. For the quenched PA-6.34 sample, this was 170 °C; above this temperature the sample was molten and so no tensile force could be applied. For this tensile test, the temperature of 170 °C had to be reached as quickly as possible to prevent undesirable recrystallization in the temperature

range 135 °C to 168 °C. This temperature “jump” was attempted by putting the thin (0.05 mm), quenched PA-6.34 film in a pre-heated oil bath at 170 °C. The tensile test was performed in the same oil bath and yielded a maximum draw ratio of $\lambda = 6.5$ which is in the same range of a conventional treated PA-6.34 drawn at elevated temperatures (cf. Chapter 2).

Table 5.2: Thermal properties of PA-6.34 and PA-6.6 determined from the differential scanning calorimetry scans (cf. Figure 5.11). Key: [1] not acquired.

Property	**PA-6.34**		**PA-6.6**	
	1st Heating	**2nd Heating**	**1st Heating**	**2nd Heating**
Glass transition (point of inflection, ˚C)	40.3	n.a. [1]	61.9	n.a. [1]
Recrystallization temperature (peak, ˚C)	154.4	n.a. [1]	240.9	n.a. [1]
Recrystallization enthalpy (J/g)	- 30.1	n.a. [1]	- 3.8	n.a. [1]
Melting temperature (peak, ˚C)	176.1	175.9	262.7	261.9
Melting enthalpy (J/g)	39.5	72.5	64.3	74.0
1st Cooling:				
Crystallization temperature (peak, °C), enthalpy (J/g)	160.5 -75.6	n.a. [1]	229.6, - 60.4	n.a. [1]

5.3.2 Conclusions

The quenching method did not yield in higher draw ratios for polyamide 6.34 fibers. From the results, it was concluded that even after quenching enough hydrogen bonds between the amide groups were left in order to prevent the production of high-strength polyamide fibers. Consequently, only a process similar to the aforementioned gel process can lead to the successful production of a high-strength polyamide fiber.

5.4 Experimental Part

General Methods. The PA-6.34 was synthesized as described in Chapter 2. All reagents and solvents were purchased from Fluka and Aldrich, except PA-6.6, which was obtained from Solutia under the trade name Vydyne 21. The DSC measurements were performed under nitrogen on a Netzsch DSC 200 instrument at a heating rate of 20 °C/ min. T_m and T_g were determined by DSC; the peak value of the endothermic transition was taken as T_m and the point of inflection as T_g. X-ray measurements were performed on a Seifert ISO-Debyeflex 2002 with Ni-filtered Cu-Ka as radiation source (conditions: 30 mA, 35 kV) and on a Philips PW2213 sealed-beam X-ray generator with Ni-filtered Cu-Ka as radiation source (conditions: 35 kV, 40 mA). The software program Cerius2, Version 3.5, was run on a Silicon Graphics workstation. The mechanical measurements were made with the aid of an Instron tensile tester (models 4464 and 4411) equipped with a load cell of 100 N and a temperature chamber. All polyamide samples were dried under vacuum (10 mbar) at 75 °C for at least 14 h before being used for any experiment.

Gel Film Preparation *via* Mechanical Stirring (Procedure A). 567 mg of dry PA-6.34 was mixed with 2.5 mL of concentrated sulfuric acid (99.999 %) under nitrogen. After 10 minutes at RT, this mixture was stirred for 5 minutes at 95 °C. The PA-6.34/ sulfuric acid film samples were produced by melt-compression-force molding of the gel between two poly(tetrafluoroethylene) (PTFE) sheets 0.4 mm thick with two parallel stainless steel spacers 0.05 mm thick. This apparatus was heated in a Carver press to 90 °C. After 5 minutes, a force of 1 metric ton was applied for 1 min, and the apparatus was then cooled to ambient temperature in a cooling Carver press.

Gel Film Preparation *via* ESA-Solution (Procedure B). 0.214 g of dry PA-6.34 was carefully scattered over 2.137 g 99 % ESA under nitrogen. After 15 h at RT, a clear high-viscosity solution was observed. This solution was washed five times, each time with 45 to 47 g of 99.999 % sulfuric acid. Each mixture was allowed to stand for 12 h before the sulfuric acid was changed again. After the first addition of sulfuric acid, the top of the PA-6.34/ESA solution turned cloudy. The process is shown in Figure 5.12.

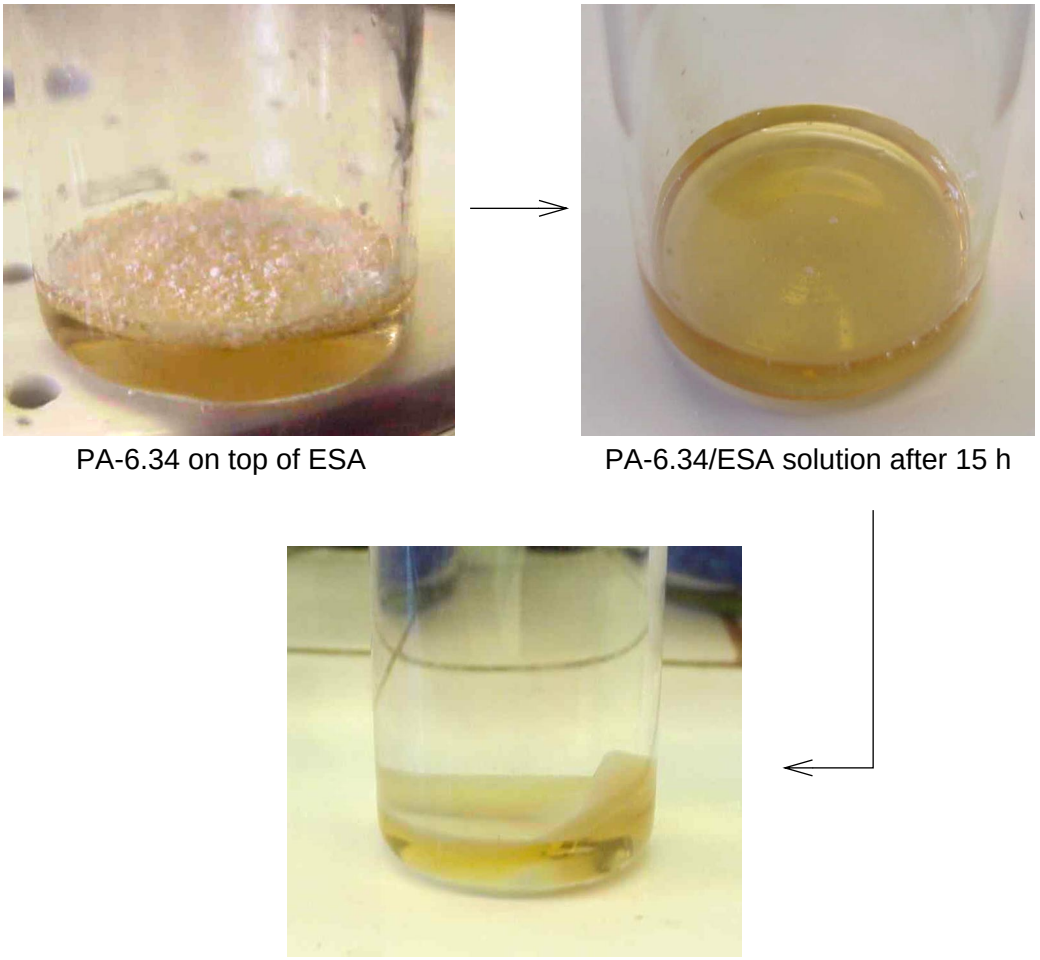

Figure 5.12: The beginning of the PA-6.34/sulfuric acid gel preparation via PA-6.34/ESA solution.

The PA-6.34/sulfuric acid film samples were produced on the same apparatus described above, but pressing was carried out at 65 °C instead of 90 °C. After 10 minutes, a force of 1 ton was applied for 1 min, followed by cooling to ambient temperature in a cooling press. A piece of this film was examined by means of DSC to determine the amount of polyamide in this gel. To this end, the sulfuric acid was extracted with 5 M NaOH, washed with distilled water for 24 h, and dried under vacuum (10 mbar) at 75 °C for 48 h. The amount of PA-6.34 was determined by weighing the sample before and after the extraction and drying procedures.

PA-6.34/Sulfuric Acid Gel Fiber for X-ray Diffraction (Figure 5.9). 2 wt % mixture of PA-6.34 and concentrated sulfuric acid (99.999%) was prepared at room

temperature in a nitrogen atmosphere to suppress absorption of water and stirred for 10 min. Subsequently, the mixture was heated to 80 °C and stirred for 5 min. Fibers were spun out of the high viscous solution at 80 °C and then allowed to cool to room temperature. The fibers were drawn to a draw ratio of 4-5, while necking occurred. The sulfuric acid was extracted using 5 M NaOH and washed thoroughly with distilled water for 16 h

Mechanical Characterization of the PA-6.34/Sulfuric Acid Film and the Corresponding Fibers. Tensile testing of the films (setup of film preparation see Chapter 2, p. 40) was performed over the temperature range 25 °C to 75 °C at a strain rate of 100 %/min on dog-bone-shaped tensile bars (test area approx. 12.7 mm x 2 mm x 0.05 mm). An Instron 4464 tensile tester equipped with a temperature chamber and nitrogen flushing was employed. To attain the optimum draw ratio, two tensile bars were tested at the same time. The unbroken sample was allowed to cool to RT under stress. At the start of sulfuric acid extraction with 5 M NaOH, the fiber was kept under stress for 3 min. The resultant PA-6.34 fiber was washed with distilled water for at least 16 h, and subsequently dried under stress and under vacuum (10 mbar) for 16 h at 75 °C.

X-ray Diffraction. X-ray diffraction patterns were taken on a Philips PW2213 sealed beam X-ray generator using a Ni-filtered Cu Kα (conditions: 35 kV, 40 mA, wavelength: 0.1542 nm). The diffraction photographs were recorded on a film using a flat-plate camera. The wide- and medium-angle X-ray diffraction patterns were obtained at room temperature and vacuum.

Model Building. The software package Cerius2, version 3.8 (MSI) was used in structural modeling.

Quenching. The PA-6.34 and 6.6 film samples were produced on the same setup as described in Chapter 2, p. 40. This apparatus was heated to 210 °C and 295 °C, respectively. After 10 minutes, a force of 1 ton was applied for 1 min. The whole setup was quenched in liquid nitrogen and the sheets were separated at the same time. The quenched films were immediately stored under vacuum in a desiccator over dry silica. To determine the water absorption of the quenched PA-6.34 and the resultant change in

glass transition temperature, part of the quenched film was immersed in water for 30 min. The DSC scan did not differ from that of samples stored under vacuum. Consequently, the absorption of water was neglected in this case.

Mechanical Characterization of the Quenching PA-6.34 Samples. To attain very rapid heating of the dog-bone tensile bars, the tensile tests were carried out in a pre-heated oil bath at the appropriate test temperature. The tensile test on PA-6.34 was carried out in the same oil bath with the aid of a custom-built manual tensile tester.

5.5 References

[1] Jaffe, M. *High Modulus Polymers*, in Kroschwitz, J. I. *Encyclopedia of Polymer Science and Engineering*; 2nd ed.; John Wiley: New York, 1988, Vol. 7, p. 699.

[2] Riggs, J. P. *Carbon Fibers*, in Kroschwitz, J. I. *Encyclopedia of Polymer Science and Engineering*; 2nd ed.; John Wiley: New York, 1985, Vol. 2, p. 640.

[3] Ward, I. M. *Structure and Properties of oriented Polymers*; 2nd ed.; Chapman & Hall: London, 1997.

[4] Ward, I. M.; Coates, P. D.; Dumoulin, M. M. *Solid Phase Processing of Polymers*, in Utracki, L. A. *Progress in Polymer Processing*; 1st ed.; Carl Hanser Verlag: München, 2000.

[5] From various company brochures, e.g.:
Aramid = Kevlar by DuPont, Polyarylte = Econol by Sumitomo Chemical, PIPD = M5 by Akzo-Nobel, PBT = Celazole by Celanese, UHMW polyethylene = SK 60 and SK71 by Dyneema

[6] Jaffe, M. *High Modulus Polymers*, in Kroschwitz, J. I. *Encyclopedia of Polymer Science and Engineering*; 2nd ed.; John Wiley: New York, 1988, Vol. 7, p. 699.

[7] Ward, I. M. *Progr. Coll. Polymer Sci.* **1993**, *110*, 103.

[8] Schaefgen, J. R. *Aramid Fibers: Structure, Properties, and Applocations* in Zachariades, A. E.; Porter; R. S. *The Strength and Stiffness of Polymers*; Marcel Dekker: New York, 1983, p. 327.

[9] Smith, P.; Lemstra, P. J. *J. Mater. Sci.* **1980**, *15*, 505.

[10] Smith, P.; Lemstra, P. J., Booij, H. C. *J. Polym. Sci. Polym. Phys. Ed.* **1981**, *19*, 877.

[11] Capaccio, G.; Crompton, T. A.; Ward, I. M. *J. Polym. Sci. Polym. Phys. Ed.* **1976**, *14*, 1641.

[12] Smith, P.; Matheson, R. R.; Irvine, P. A. *Polymer Commun.* **1984**, *25*, 294.

[13] Chuah, H. H.; Porter R. S. *Polymer* **1986**, *27*, 241.

[14] Postema, A. R.; Smith, P.; English, A. D. *Polymer Commun.* **1990**, *31*, 444.

[15] Weenink, W. D. *Nylon-Sulfonic Acid Systems*; Diss. ETH No. 13037, Zürich, 1999.

[16] Smith, P.; Lemstra, P. J.; Kalb, B.; Pennings, A. J. *Polym. Bull.* **1979**, *1*, 733.

[17] Smith, P.; Lemstra, P. J. *Makromol. Chem.* **1979**, *180*, 2983.

[18] Kanamoto, T.; Tsurata, A.; Takeda, M.; Porter, R. S. *Polym. J.* **1983**, *15*, 327.

[19] Savitsky, A. V.; Gorshkova, I.A.; Frolova, I. L.; Shmikk, G. N.; Ioffe, A. F. *Polym. Bull.* **1984**, *12*, 195.

[20] Fellers, J.; Kee, B. F. *J. Appl. Polymer Sci.* **1974**, *18*, 2355.

[21] Kramer, E. J.; Berger, L. L. *Adv. Polym. Sci.* **1990**, *91/92*, 1.

[22] Smith, P.; Lemstra, P. J. *Polymer* **1980**, *21*, 1341.

[23] Kausch, H. H.; Brecht, J. *The Role of Intra- and Intermolecular Cohesion in Fracture initiation of High Polymers*, in Kausch, H. H.; Hassell, J. A.; Jaffee, R. I. *Deformation and Fracture of Polymers*; Plenum Press: New York, 1972, p. 317.

[24] Weissenberg, C. *Nature* **1947**, *159*, 310.

[25] Kuhn, W.; Grün, F. *Kolloidzschr.* **1942**, *101*, 248.

[26] Ehrenstein, G. W. *Mit Kunststoffen konstruieren*; Carl Hanser Verlag: München, 1995, p. 11.

[27] Bunn, C. W.; Garner, E. V. *Proc. R. Soc. (Lond.)* **1947**, *189A*, 39.

[28] Aharoni, S. M.; Sibilia, J. P. *Polymer Engineering and Science* **1979**, *19*, 450.

[29] Hu, W.-G.; Schmidt-Rohr, K. *Acta Polym.* **1999**, *50*, 271.

[30] Lukes, C. *Collect. Czech. Chem. Commun.* **1958**, *23*, 497.

[31] Wegner, G.; Meyer, W. H. *Grundlagen und Überblick der Polymere*, in Schaumburg, H. *Polymere*; Teubner Verlag: Stuttgart, 1997, p. 33.

6. Attempt to Develop an Alternative Method for the Synthesis of Dicarboxylic Acids[1]

6.1 Introduction

In this chapter, the attempt to develop an alternative method for the synthesis of extended aliphatic dicarboxylic acids is described. This approach should enable the synthesis of diacids with a chain length of 60 methylene groups or more [1], which is desirable in the context of the present work, as described in Chapter 5. For this purpose, oligo- and polymerizations were investigated. The requirements for monomers prepared by this route are, of course, the same as those already mentioned in Chapter 1, and include, for example, high purity, well-defined chain length, and the absence of branches. One should bear in mind that polymerization reactions most often result in a certain polydispersity in chain length of the material produced. Consequently, only those polymerization reactions which lead to narrow[2] molecular weight distribution are of interest here. The most promising methods for this purpose are living or controlled polymerizations [2,3] such as living anionic polymerizations and atom transfer radical polymerizations [4].

Another requirement for the materials to be of use is the possibility to synthesize telechelic macromonomers[3], i.e., to be able to introduce well-defined functional end groups. In the literature a number of methods have been described that allow the synthesis of such telechelic oligomers/polymers [5,6].

A most interesting polymerization and potentially useful method for the synthesis of the present target monomers is the so-called polyhomologation of methylene, a living polymerization which was recently developed by Shea *et al.* [7-9]. The key step of this reaction is the attack of an ylide to an alkylborane (Scheme 6.1). The alkyl group of the borate complex thus formed undergoes a 1,2-migration to yield a linear extended alkylborane and dimethyl sulfoxide (DMSO) as a by-product. The 1,2-migration cycle is repeated until all of the ylide is consumed. Each ylide molecule consumed leads to a

---

[1] The experimental work of this chapter was conducted at the Exotic Materials Institute of Prof. F. Wudl at the Department of Chemistry and Biochemistry of the University of California, Los Angeles.

[2] Actually, the chain length of the produced polymers should be uniform or at least the amount of polymethylene segments smaller than 60 methylene groups should be negligible.

[3] The term “telechelic macromonomer” is used here for linear oligomers/polymers which possess two identical reactive groups at the chain ends.

growth of the oligomer/polymer chain by exactly one methylene group (see Scheme 6.1) [7]. Thus, it is possible to control the length of the alkyl chains through the molar ratio of the ylide and the organoborane initiator in the reaction mixture. Shea *et al.* observed an extremely low polydispersity (*PD*) for short chain length (e.g., $PD = \overline{M}_w / \overline{M}_n$ of 1.02 for a degree of polymerization of 25) and reported a slight increase at increased molecular weights (e.g., *PD* = 1.13 for a degree of polymerization of 120). Fortunately, functionalized or telechelic macromonomers could readily be synthesized by this method by carefully selecting the organic substituent of the borane and appropriate derivatitzation after the polyhomologation [8].

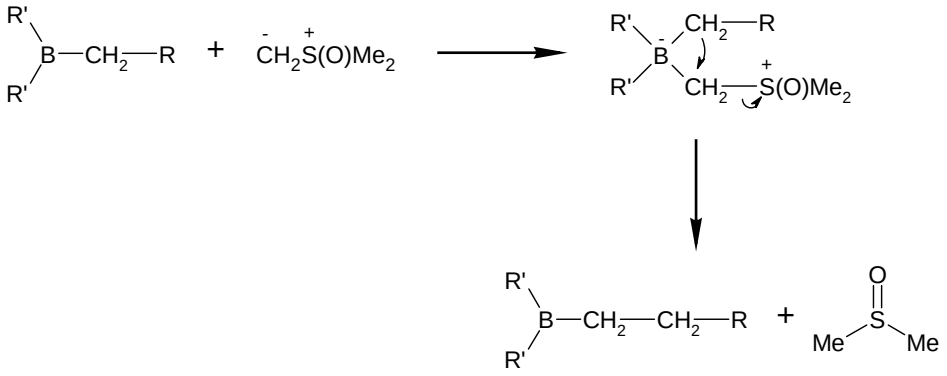

Scheme 6.1: Mechanism of the polyhomologation [7].

Thus, the polyhomologation of an organoborane seems to be a useful method for the synthesis of diacids with extended aliphatic segments. It may yield the required telechelic macromonomers and offers the possibility to predetermine the average alkyl chain length, particularly for chain lengths in the regime of between 30 and 250 methylene groups. As it is common practice [7], the employed organoborane compound is referred to as the initiator of the polyhomologation, because it is the starting segment of the growing oligomer chain and its addition to the ylide solution initiates the polyhomologation, as will be described in Section 6.3. This chapter summarizes the efforts to employ this method and to develop a useful synthetic framework which allows the introduction of the two necessary carboxylic functionalities to an extended alkyl chain. A schematic overview of the envisioned reaction sequence is shown in Scheme 6.2.

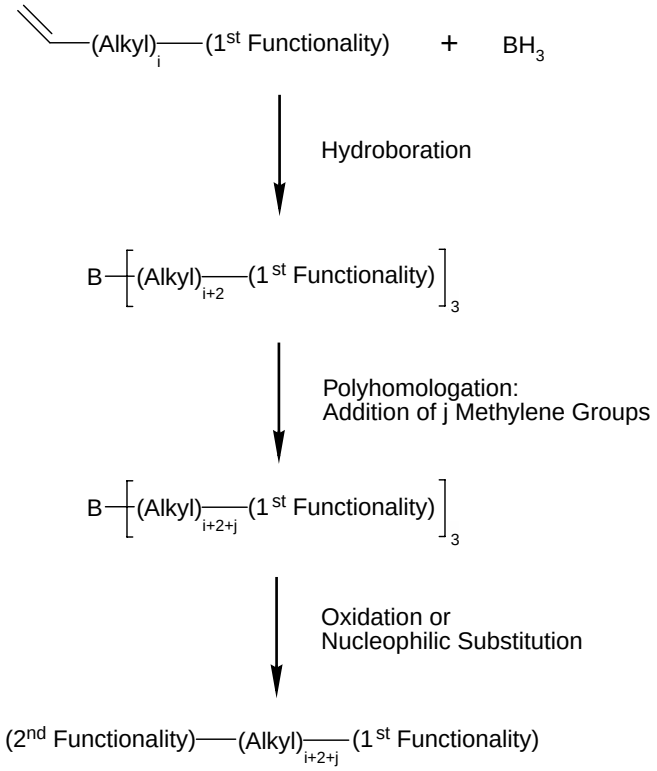

Scheme 6.2: Overview of the polyhomologation route to aliphatic dicarboxylic acids explored in the present chapter.

6.1.1 Nomenclature

1-dec-9-enyl-4-methyl-2,6,7-trioxabicyclo[2.2.2] octane (**1**)

tert-butyl undec-10-enoate (**2**)

1,2-dimethoxy-4-vinylbenzene (**3**)

(3-methyloxetan-3-yl) methyl undec-10-enoate (**4**)

1-(3,4-dimethoxy-phenyl) ethanol (**5**α)

2-(3,4-dimethoxy-phenyl) ethanol (**5**β)

tert-butyl 11-{1,1-di[11-(*tert*-butoxy)-11-oxoundecyl]boryl} undecanoate (**6**)

tri-(3,4-dimethoxyphenethyl) borane (**7**)

α-*tert*-butyl-ω-hydroxy-[polymethylene(8 + j)]-ate (**8**)

α-*tert*-butyl-ω-hydroxy-[methylene(44)]-ate (**8a**)

α-*tert*-butyl-ω-hydroxy-[methylene(180)]-ate (**8b**)

α-*tert*-butyl-ω-hydroxy-[methylene(53)]-ate (**8c**)

tri-{α-[methylene(28)]-ω-(3,4-dimethoxyphenyl)} borane (**9**)

α-ethyl-ω-(3,4-dimethoxyphenyl)-[methylene(18)]-ate (**10**)

1-(3,4-dimethoxyphenyl)-octacosane (**11**)

triacontanedioic acid (**12**)

α-carboxy-ω-*tert*-butyl-[methylene(52)]-ate (**13**)

6.2 First Functionality

6.2.1 Demands for the Olefinic Part of the Initiator

In the following section, the term functionality refers to a carboxylic acid or a precursor thereof, e.g. a protected acid or a chemical equivalent of the latter. The first functionality can readily be introduced into the alkyl chain through the borane initiator, which provides the first alkyl segment of the final macromonomer (Scheme 6.2). The principal aspect of concern here was the composition of the initiator itself. In general, the initiator is synthesized though hydroboration of a terminal olefine in a borane-THF solution [7,8]. The most simple approach would be to employ an aliphatic acid with a terminal olefinic functionality. However, the presence of an acid proton or a carboxylate group would prevent the formation of the initiator, because both would hydrolyze the borane. Therefore, only protected forms of carboxylic acids, such as esters of the corresponding acid, can be considered. An additional point which needs to be taken into account is the fact that the borane may act as a reducing reagent which might lead to a reduction of the carboxylic esters, for example, to the corresponding aldehydes (see Scheme 6.3). Fortunately, the reduction of an ester is much slower than the hydroboration [10]. However, a reduction of the ester should be avoided because this side reaction might inhibit the possibility to produce the pure diacid.

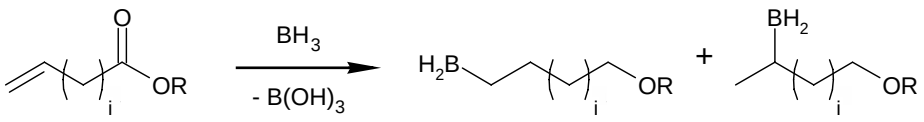

Scheme 6.3: Possible, undesired reduction of the carboxylic acid ester during the hydroboration.

In order to circumvent the above mentioned problem, another initiator for the polyhomologation reaction was considered. Instead of an olefinic ester, a 1,2-dimethoxy-4-vinylbenzene could be used as precursor for the first functionality. The desired acid functionality could be readily obtained by oxidative degradation of the electron-rich phenyl ring (Section 6.4). Another important aspect of this approach is the fact that it could provide the possibility of the simultaneous oxidation of the phenyl ring to the carboxylic group on one end of the alkyl chain, as well as oxidation of the second chain end which carries an alcohol as intermediate functionality. The latter moiety is formed in oxidative work-up after the polyhomologation, in order to eliminate the boron.

6.2.2 Regioselectivity of the Hydroboration

The regioselectivity of the hydroboration reaction is of a certain interest. Because the present work relies on the ability to direct the borane selectivity to the β-position: due to the fact that the insertion of the methylene group exclusively takes place between the borane-carbon bond, only a boron atom in the β-position would lead to strictly linear alkyl chains (see Scheme 6.4).

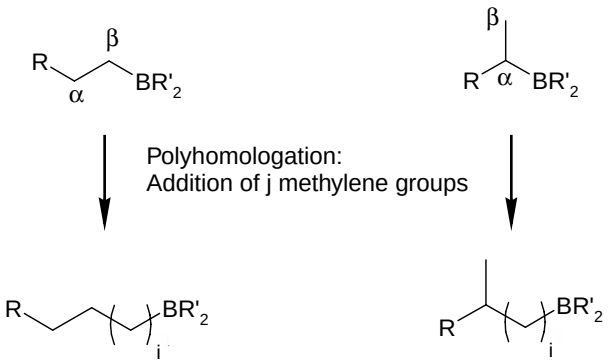

Scheme 6.4: Effect of the regioselectivity of hydroboration on the products of polyhomologation.

In general, the regioselectivity of the hydroboration is influenced by the substituent at the double bond. Steric as well as electronic factors govern the regioselectivity. An electron-donating substituent leads to boration predominantly in the α-position, whereas

an electron-withdrawing substituent directs the borane to the β-position (see Figure 6.1) [10].

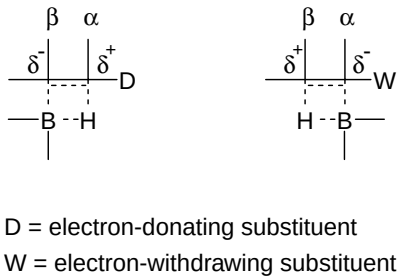

Figure 6.1. Selectivity of the hydroboration of an olefinic group [10].

Investigations of the reaction of unsaturated aliphatic esters with borane by Brown *et al.* have shown that the regioselectivity depends on two different effects: the procedure of the hydroboration itself and the chain length of the ester used [10]. Brown *et al.* showed that the selectivity improves significantly by increasing the chain length between the C=C double-bond and the electron-withdrawing ester functionality [10]. For example, for the hydroboration of an ethyl undec-10-enoate, a regioselectivity of 91 % β- and 9 % α-position was reported [10]. On the other hand, Brown *et al.* established that the regioselectivity of hydroboration is also influenced by an electron rich phenyl ring which is directly connected to a double bond. For 4-vinylanisole, they observed a selectivity of 93 % β- and 7 % α-position [10,11].

6.2.3 Synthesis and Properties of the Olefinic Part of the Initiator

Three olefinic compounds were investigated in order to identify the most promising initiator for the polyhomologation. Two different protecting groups for the carboxylic acid terminus were selected (see Figure 6.2), i.e. the ortho ester 1-dec-9-enyl-4-methyl-2,6,7-trioxabicyclo[2.2.2] octane (**1**) and the *tert*-butyl ester *tert*-butyl undec-10-enoate (**2**). In addition, the commercially available 1,2-dimethoxy-4-vinylbenzene (**3**) as a precursor of a carboxylic acid was employed.

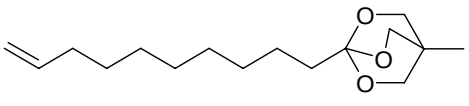

1

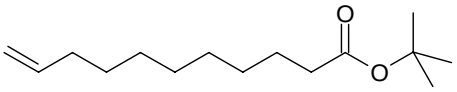

2

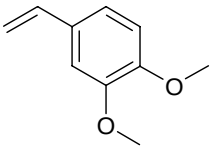

3

Figure 6.2: Three olefinic compounds investigated as possible initiators of the polyhomologation.

The ortho ester was chosen as it is inert against reduction by boranes and against attacks of nucleophiles, such as the ylide that is used in the polyhomologation [12]. The synthesis of the target ortho ester was based on the reaction of the carboxylic acid chloride with (3-methyloxetan-3-yl) methanol in a solution of pyridine and dichloromethane. The resulting (3-methyloxetan-3-yl) methyl undec-10-enoate (**4**) was readily converted to the bridged ortho ester by treatment with boron trifluoride etherate in dichloromethane (see Scheme 6.5), in analogy to the synthesis of a similar compound reported in the literature [13]. The achieved overall yield of the synthesis of 1-dec-9-enyl-4-methyl-2,6,7-trioxabicyclo[2.2.2] octane (**1**) was 90 %.

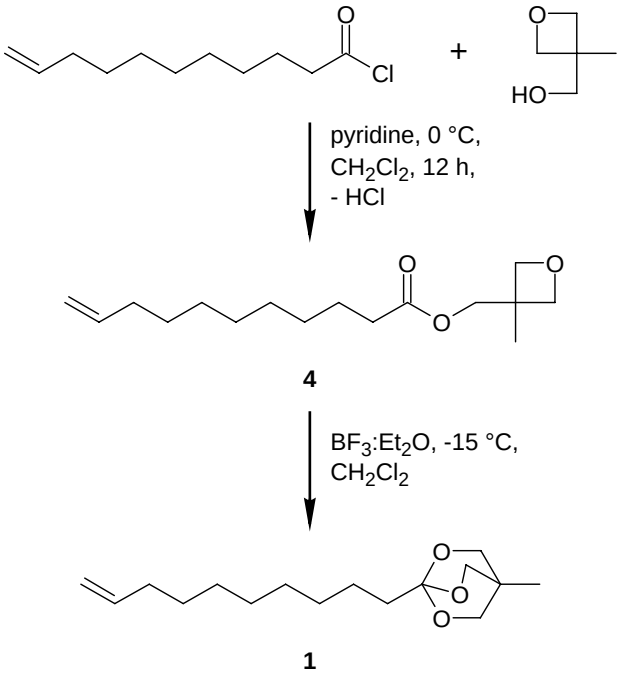

*Scheme 6.5: Synthesis of 1-dec-9-enyl-4-methyl-2,6,7-trioxabicyclo[2.2.2] octane (**1**).*

Tert-butyl undec-10-enoate (**2**) was prepared in 89 % yield from 10-undecenoyl chloride and *tert*-butyl alcohol [14]. No reduction of the *tert*-butyl group was observed during the hydroboration (see Scheme 6.6). This remarkable stability appears to be related to the steric hindrance by the *tert*-butyl group. Cleavage of the ester during the polyhomologation was also not observed. A possible reason could be the relatively fast consumption of the ylide during the polyhomologation (see Section 6.3).

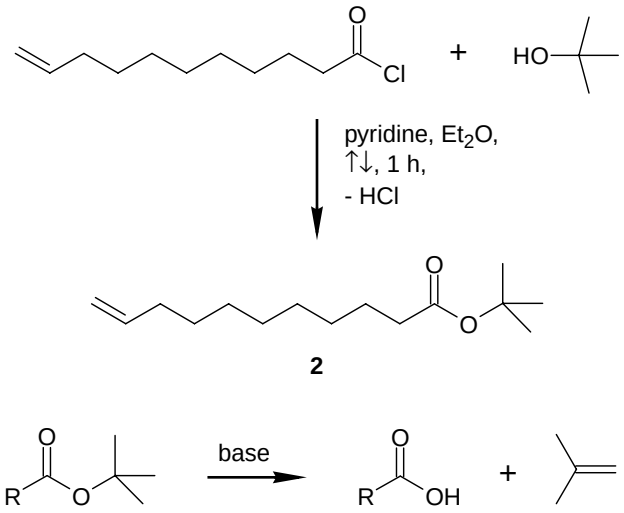

*Scheme 6.6: Synthesis of tert-butyl undec-10-enoate (**2**) and its cleavage.*

6.2.4 Investigation of the Regioselectivity

The regioselectivity of the hydroboration reaction was investigated at the example of 1,2-dimethoxy-4-vinylbenzene (**3**) by hydroborating the latter and subjecting the resulting intermediate to an oxidative work-up. The alcohol in β-position of the C=C double bond was produced with a regioselectivity of 94 % (see Scheme 6.7). This value was obtained by comparing the relative intensities of the ^{1}H-NMR signals of 1-(3,4-dimethoxy-phenyl) ethanol (**5**α) (C*H*-OH, s, 4.61 ppm) and 2-(3,4-dimethoxy-phenyl) ethanol (**5**β) (CH_2-OH, t, 2.81 ppm) [15]. Brown *et al.* found a regioselectivity of 91 % β– and 9 % α-position for the hydroboration in the case of ethyl undec-10-enoate [10]. Due to the relatively large distance between the alkoxy-group of the ester to the reacting C=C double bond, it can be assumed that the influence of different alkoxy-groups on the regioselectivity is small. Consequently, the regioselectivity of the hydroboration of 1-dec-9-enyl-4-methyl-2,6,7-trioxabicyclo[2.2.2]octane (**1**) and *tert*-butyl undec-10-enoate (**2**) was similar to that determined by Brown *et al.* for ethyl undec-10-enoate.

This regioselectivity influences the next step of the proposed synthesis route. The fact that two regioisomers of the initiators are formed during the hydroboration will yield two different polyhomologated products. The regioisomer with the B-C bond at the α-carbon will lead to a branching of the chain. The other regioisomer will give a strict linear chain due to the insertion mechanism of the polyhomologation (see Scheme 6.1).

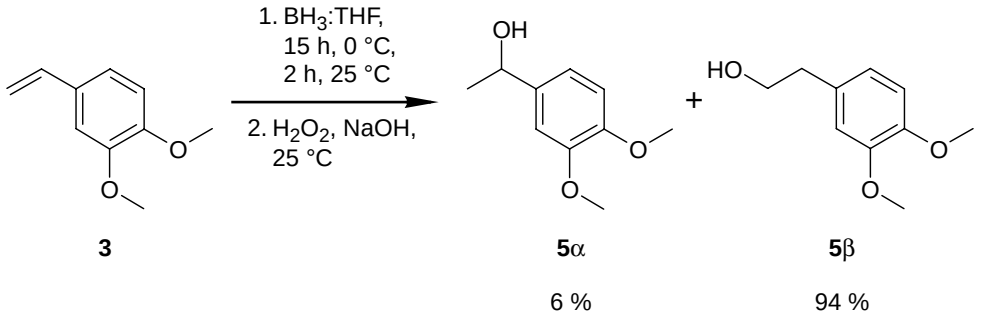

3 **5**α 6 % **5**β 94 %

*Scheme 6.7: Regioselectivity of the hydroboration of 1,2-dimethoxy-4-vinylbenzene (**3**).*

6.2.5 Selection of the Olefinic Part for the Initiator

On the basis of the obtained results, *tert*-butyl undec-10-enoate (**2**) and 1,2-dimethoxy-4-vinylbenzene (**3**) were considered to be the most useful initiators for the

polyhomologation. *tert*-Butyl undec-10-enoate (**2**) could be synthesized relatively easily. It was also found to be stable against reduction and against nucleophilic attack of the ylide during the polyhomologation, as will be shown in the next Section 6.3. The synthesis of 1-dec-9-enyl-4-methyl-2,6,7-trioxabicyclo[2.2.2]octane (**1**) required more effort with no additional advantages. 1,2-Dimethoxy-4-vinylbenzene (**3**) could even be used directly without additional chemical modifications. But, as will be shown in Section 6.4, the conversion of the phenyl ring of **3** into a carboxylic acid did not prove to be successful under the conditions used, and, therefore, it was used only as a model system.

6.3 Polyhomologation

6.3.1 Synthesis of the Dimethyloxosulfonium Methylide

The key reagent for the polyhomologation according to Shea *et al*. is dimethyloxosulfonium methylide [7,8]. The latter was synthesized by reaction of trimethylsulfoxonium chloride with sodium hydride in an anhydrous solvent (see Scheme 6.8).

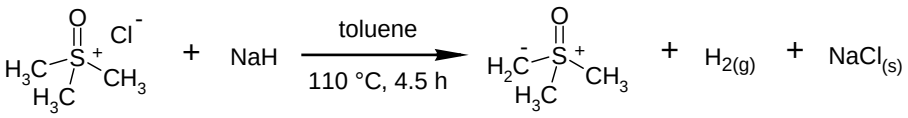

Scheme 6.8: Synthesis of dimethyloxosulfonium methylide.

In the literature three possible solvents for this reaction have been described, namely DMSO, THF, and toluene [7,16]. However, in the present work, only THF and toluene were employed. THF was the solvent which was used in the oxidative work-up after the polyhomologation; toluene has the ability to dissolve polyolefins at elevated temperatures. In order to ensure a good yield, all reagents were carefully dried, and the reaction was carried out under dry nitrogen atmosphere. During the reaction hydrogen was generated; it was, however, difficult to determine the end of the evolution of H_2 due to a slight over-pressure of the inert gas and because of some evaporation of the solvent

during the reaction. According to the literature, the typical reaction time is between 4 and 5 h [16], and hence, these reactions were terminated after 4.5 h. In order to produce a NaH-free ylide toluene solution, it was necessary to filter the reaction mixture through dry celite, which was best accomplished by using a vacuum-jacketed filter funnel under inert conditions. The concentration of ylide in THF or toluene was of the order of 0.5 - 0.9 μmol/mg, as determined by titration with hydrochloric acid. The actually measured concentrations corresponded reasonably well with theoretical values. Table 6.1 summarizes the relevant data.

Table 6.1: Overview of dimethylsulfonium methylide synthesis. Key: [1] Theoretical concentration of the ylide in the solvent as calculated from the starting materials. [2] Concentration of the ylide in the solvent determined by titration with HCl. [3] After storage at -10 ˚C for 2 months, deviation due to inaccuracy of the titration. [4] Shortly exposed to air.

No.	NaH	Trimethyloxosulfonium chloride	Solvent	Theo. Conc.[1] (μmol/mg)	Temp. (oil bath)	Time	Measured Conc.[2] (μmol/mg)
A	1.82 g (45.5 mmol)	4.96 g (38.6 mmol)	THF (55 mL)	0.79	80 ˚C	4.7 h	0.80
B	5.23 g (130.7 mmol)	14.12 g (109.8 mmol)	toluene (150 mL)	0.84	115 ˚C	20.0 h	0.63 (0.65)[3]
C	4.46 g (111.5 mmol)	10.98 g (85.4 mmol)	toluene (120 mL)	0.82	125 ˚C	4.5 h	0.88
D	4.83 g (120.8 mmol)	12.06 g (93.8 mmol)	toluene (120 mL)	0.90	125 ˚C	4.5 h	0.51[4]

6.3.2 Synthesis of the Organoborane (Initiator)

The initiator for the polyhomologation, *tert*-butyl 11-{1,1-di[11-(*tert*-butoxy)-11-oxoundecyl]boryl} undecanoate (**6**), was synthesized by hydroboration of *tert*-butyl undec-10-enoate (**2**) (see Scheme 6.9). For the following polyhomologation, it was critical to know the concentration of **6** in THF, as the length of the growing alkyl chain is determined by the ratio of dimethyloxosulfonium methylide to **6**. To avoid any consumption of BH_3 by water, which could be introduced through moisture in **2**, the ester was stored over activated molecular sieves. The effectiveness of the drying procedure was confirmed by the absence of any appreciable development of hydrogen during the addition of BH_3-THF to the *tert*-butyl undec-10-enoate (**2**) solution. The *tri*-(3,4-dimethoxyphenethyl) borane (**7**) was synthesized in analogy to **6**. The detailed procedures for the synthesis of the initiators **6** and **7** are described in the Experimental Section.

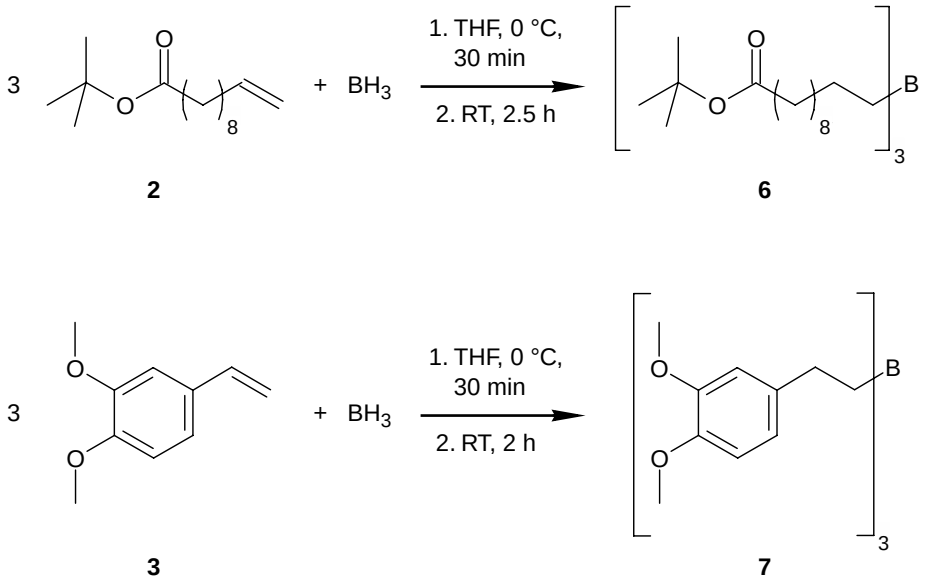

*Scheme 6.9: Synthesis of tert-butyl 11-{1,1-di[11-(tert-butoxy)-11-oxoundecyl]boryl} undecanoate (**6**) and tri-(3,4-dimethoxyphenethyl) borane (**7**).*

^{1}H-NMR spectroscopy was used to determine what fraction of **2** had actually reacted with the borane (olefinic proton signals at 5.8 and 5.0 ppm). A small excess of the unsaturated ester was used, in order to ensure that no excess borane would contaminate the polyhomologation reaction. This precaution was necessary, as the

initiator solution was used for the polyhomologation without further purification, and an excess of borane would consume the ylide and, consequently, lead to a shorter alkyl chain length.

6.3.3 Polyhomologation

In the general polyhomologation procedure, the initiator (**6** and **7**, respectively) was added as fast as possible to the ylide-toluene solution with constant stirring. The addition was of crucial importance as the polymerization started immediately and a simultaneous start of the growth of all alkyl chains is necessary in order to achieve a narrow molecular weight distribution of the material produced (see Scheme 6.10).

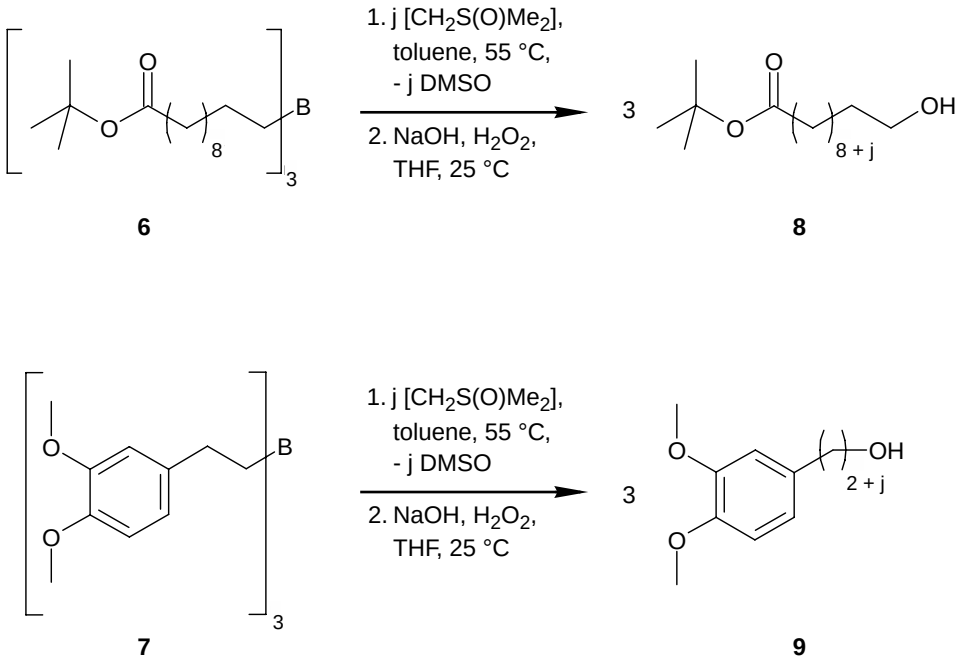

*Scheme 6.10: Polyhomologation of tert-butyl 11-{1,1-di[11-(tert-butoxy)-11-oxoundecyl]boryl} undecanoate (**6**) and tri-(3,4-dimethoxyphenethyl) borane (**7**).*

The polyhomologation is a fast reaction. After 10 min the reaction appeared to be complete, as detected by an effective test in which a small sample of the reaction mixture was added to a phenolphthalein-water solution. This test would result in a violet color if ylide was left due to the basic character of the ylide this showing that the reaction of the ylide and the organoborane was not complete. In this case, the test stayed colorless, all of

the ylide was consumed and the polyhomologation was successful. Table 6.2 provides an overview of selected polyhomologation experiments. The standard procedure of the polyhomologation is described in the Experimental Section. The nature of the initiators employed in this work (i.e. **6** and tris-(3,4-dimethoxyphenethyl) borane (**7**)) did not appear to influence the polyhomologation; both led to the expected oligomethylenes. One reason for the failure of certain attempts could be (undefined) decomposition products, which might have been formed during the storage of the ylide-toluene solution. These products could lead, for example, to an inhibition of the reaction or decomposition of the initiator. In order to ensure that the growing alkyl chains stayed dissolved until the polyhomologation was completed, the reaction temperature was kept at 55 ˚C. Higher temperatures were avoided, as this could decompose the organic borane compound.

Table 6.2: Overview of different polyhomologation reactions. Key: [1] A-D indicate origin of ylide of Table 6.1. [2] Total weight of the ylide solution. [3] Molar ratio between ylide and olefin. [4] Determined by ^{1}H-NMR. [5] n.d.: not determinable. [6] This batch was used directly for the next step, the oxidation of the phenyl ring (cf. Experimental Section). [7] Product was not successful synthesized.

No.	Olefin of Initiator	Initiator	Conc. of Olefin in THF	Ylide[1]: Conc. (mmol/mg)	Initiator (mmol)	Ylide[2] (g)	Ratio[3]	Solvent	Temp.	Chain Length[4]	Yield	Product
1.	**3**	**7**	1.16 mmol/g	A: 0.80 in THF	~ 0.78	28.68	28.7	THF / toluene	70 ˚C	insoluble at RT	n.d.[5]	**(9a)**[7]
2.	**3**	**7**	1.16 mmol/g (same batch as 1.)	B: 0.63 in toluene	~ 0.10	23.27	14.7	toluene	58 ˚C	insoluble	n.d.[5]	**(9b)**[7]
3.	**3**	**7**	1.16 mmol/g (same batch as 1.)	B: 0.63 in toluene	~ 1.13	28.69	16.0	toluene	58 ˚C	~ 27 CH_2	5 %[6]	**10**
4.	**2**	**6**	0.73 mmol/g	B: 0.65 in toluene	~ 0.54	19.08	23.0	toluene	RT	~ 44 CH_2	61 %	**8a**
5.	**2**	**6**	0.71 mmol/g (same batch as 5.)	C: 0.88 in toluene	~ 0.42	65.85	137.0	toluene	55 ˚C	~ 180 CH_2	40 %	**8b**
6.	**2**	**6**	0.71 mmol/g (same batch as 5.)	D: 0.51 in toluene	~ 2.20	66.47	30.2	toluene	55 ˚C	~ 53 CH_2	35 %	**8c**

6.3.4 Work-up of the Polyhomologation

The standard work-up of the polyhomologation was begun with evaporation of toluene and suspension of the obtained product in anhydrous THF. This change of solvent was necessary so that the product could react with the H_2O_2/NaOH/water solution for the final substitution of the boron atom at the end of the alkyl chain with an OH-group. While the data in Table 6.2 suggest that the synthesis of α-*tert*-butyl-ω-hydroxy-[methylene$_{(8 + j)}$]-ate (**8**) of different chain lengths was successful with the method applied, the resulting products did not always form homogeneous solutions in THF, especially for the extended **8**. This limited solubility prevented a quantitative conversion of the B-C bond to the C-O bond, as could be unequivocally detected by the different integrals of the ^{1}H-NMR signals of the α-CH_2 group of the ester (2.19 ppm) and of the alcohol (3.56 ppm). For batch No. 5 (i.e. product **8b**) this ester/alcohol ratio was determined as 1.68, while for batch No. 6 (i.e. product **8c**), it was 1.34 (see Table 6.2). In a most recent publication, Shea and co-workers have reported significantly improved conditions for the oxidation procedure [9]. The exchange of solvent and the oxidation with hydrogen peroxide can be avoided by the addition of trimethylamine-*N*-oxide dihydrate to the toluene reaction mixture which reacts directly with the polyhomologated organoborane and yields the corresponding alcohol [9].

The methylene chain length found was always determined to be higher than the calculated methylene chain length (see Table 6.2). This deviation can be explained by the overestimation of the real active concentration of the alkyl borane initiator. These concentrations were estimated from the used amount of 1 M borane-THF solution at the beginning of the initiator synthesis under the assumption of 100 % conversion.

6.3.5 Discussion of the Molecular Weight

The molecular weight and distribution of the molecular weight of the novel α-*tert*-butyl-ω-hydroxy-[methylene(8 + j)]-ates (**8**) will be discussed with the help of the obtained results of α-*tert*-butyl-ω-hydroxy-[methylene(180)]-ate (**8b**). The ratios of the intensities of the ^{1}H-NMR signals of the CH_2-group next to the ester group (2.19 ppm) and the signals of the CH_2-groups of the aliphatic chain (1.10-1.55 ppm) were calculated in order to determine the length of the aliphatic chain. By the use of this procedure, a

formula of $C_{185}H_{371}O_3$ was obtained for **8b**, which would correspond to a number-average molecular weight of 2638.

In addition, a matrix-assisted laser desorption/ionization (MALDI) time-of-flight (TOF) mass spectrometry (MS) of compound **8b** was also conducted (see Figure 6.3). An important requirement for mass spectroscopy is the ionizabilility of the investigated compound. **8b** is very similar to an extended *n*-alkane and the latter is known to be difficult to ionize due to the absence of polar and easy polarizable groups [17,18]. The sodium ions used in the present analysis do not form detectable positive complexes with methylene groups. Certainly, the polar ester group of **8b** enhanced the situation, but the sensitivity of the MALDI-TOF-MS was still limited due the above mentioned reason. Therefore, the spectrum of **8b** needs to be interpreted with exceptional care. For example, the spectrum showed one fragmentation of a molecular weight of m/z around 16 as outlined in Figure 6.3. This result can be interpreted as an indication that the alkyl chain was indeed built up by single methylene groups (14 g/mol) during the synthesis. However, the MALDI-TOF-MS analysis pointed out that the biggest detected molecule fragment of **8b** had an m/z value of 2664 (2687 (biggest M^+) - 23 (Na^+) = 2664) which is comparable to the molecular weight of 2638 ($C_{185}H_{371}O_3$) which was determined by ^{1}H-NMR. A high temperature gel permeation chromatography (GPC) at 100 °C in toluene supported these values, where $\overline{M}_n$ was found to be 2140. The relatively small value from GPC compared to the observed values from ^{1}H-NMR and MALDI-TOF-MS can be explained by the fact that toluene is not the most appropriate solvent for **8b** even at higher temperatures and that polystyrene was used as standard. Consequently, higher molecular weight material might have precipitated from the solution during the measurement. Nevertheless, it needs to be pointed out that the relatively high polydispersity ($PD = \overline{M}_w / \overline{M}_n$) determined by GPC of 1.69 of α-*tert*-butyl-ω-hydroxy-[methylene(180)]-ate (**8b**) is in contradiction to the reported small polydispersities by Shea *et al.* for polymethylenes of 1.04 to 1.17 [7-9]. This divergence can be attributed to the not rapid enough addition of the initiator to the ylide/toluene solution at the beginning of the polyhomologation. Consequently, the polymer chains did not start growing at a time, which leads to a broader molecular weight distribution.

6.3.6 Branching in the Macromonomer Backbone

Unfortunately, the ^{1}H-NMR spectra of the produced macromonomers indicated the existence of a methyl-group (0.9 ppm). A number of reasons can be responsible for this result: the incomplete conversion of the B-C bond to the corresponding C-O or the above mentioned branching (see Section 6.2.4). On the basis of the ^{1}H-NMR spectra, it was not possible to distinguish between these two possibilities. But the relative intensity of 5 : 1 of the signal at 0.90 ppm compared to the signal at 2.19 ppm (methylene group next to carboxylic ester group) indicated that at least branching existed. Since the relative intensities of the methylene-groups next to the ester-group and the OH-group were nearly equal, the NMR signal at 0.9 ppm could only be explained by the existence of methyl branching (see Experimental Section). Latest literature by Shea *et al.*, which was not available at the time of the experiments reported here, reports the existence of such a methyl group in their ^{1}H-NMR spectra [7,9]. They attribute the origin of this methyl branch to ethylidine incorporation that arises from a dimethylsulfoxonium ethylide impurity in dimethyloxosulfonium methylide. They found that the during synthesis of dimethyloxosulfonium methylide, small amounts of dimethyloxosulfonium ethylide (1.3 %) by-products are produced. This dimethyloxosulfonium ethylide is able to react with the organoborane and will incorporate a small number of ethylidine groups into the macromonomer chain [9]. Therefore, similarities are obvious between reported findings and the results described above.

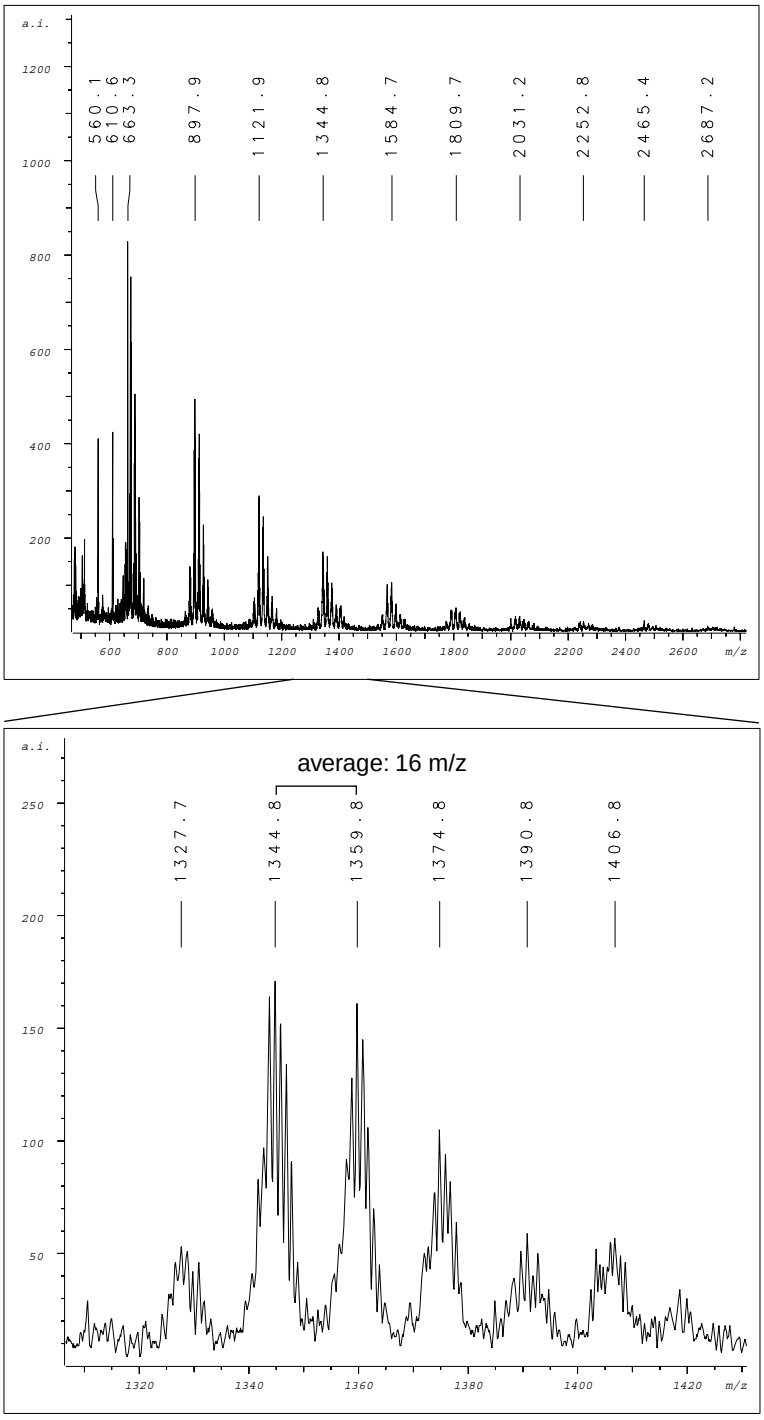

Figure 6.3: MALDI-TOF-MS of α*-tert-butyl-*ω*-hydroxy-[methylene(180)]-ate (**8b**) (the unit of the mass values are m/z).*

6.3.7 Conclusions

In summary, telechelic oligomethylenes with a chain length of between 28 to about 180 methylene groups were prepared. In these molecules, the first functionality was a *tert*-butyl ester and the second was an alcohol. Yields were in the range of 5 - 65 % (see Table 6.2). Thus, polyhomologation appeared to be a suitable method to obtain telechelic oligomethylenes with a chain length that was varied with the initiator/ylide ratio. The conversion of the alcohol to a carboxylic acid will be discussed in Section 6.4.

6.4 Second Functionality

In this section, different approaches will be discussed for the introduction of the second carboxylic acid into the above type of compounds. In a first approach to explore different oxidation protocols, triacontanol were used as a model compound for α-*tert*-butyl-ω-hydroxy-[methylene(8 + j)]-ate (**8**).

6.4.1 Attempt to Substitute the Borane Atoms

After the polyhomologation with dimethylsulfoxonium methylylide, a boron atom was still present at the end of the oligomethylene chain. As mentioned in the previous section, this boron atom was usually substituted with an OH-group during the work-up. The latter functionality, in principle, can be oxidized to the desired carboxylic acid if a suitable oxidation method can be found. As an alternative method, Brown *et al.* reported the possibility of directly converting the organoborane to an ester [19,20]. In this approach, the organoborane is reacted with ethyl bromoacetate in the presence of potassium *tert*-butoxide in *tert*-butanol to yield the corresponding ester (see Scheme 6.11).

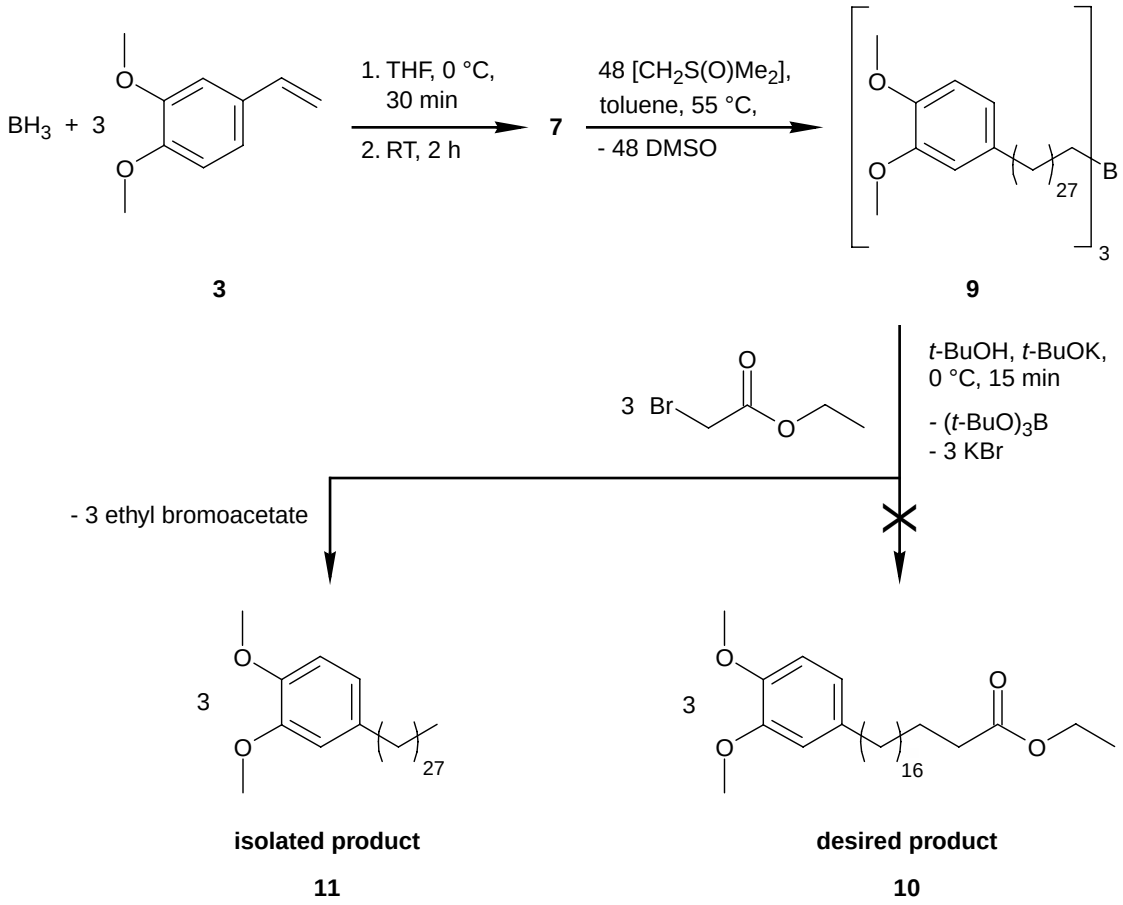

Scheme 6.11: Synthesis of 1-(3,4-dimethoxyphenyl)-octacosane (**11**).

Brown and co-workers reported that this reaction is “amazingly fast”, but provides only modest (~ 30 %) yields if linear aliphatic terminal olefins are used [19]. An experiment was conducted with the objective to explore the usefulness of this reaction, and, thus, *tri*-{α-[methylene(28)]-ω-(3,4-dimethoxyphenyl)} borane (**9**) was reacted with ethyl bromoacetate (see Scheme 6.11; Table 6.2, Entry No. 3). The solvent used in the polyhomologation (toluene) was substituted by THF in order to dissolve the reactants potassium *tert*-butoxide and *tert*-butylalcohol. Unfortunately, in this solvent and at the required low temperature of 0 °C, *tri*-{α-[methylene(28)]-ω-(3,4-dimethoxyphenyl)} borane (**9**) was insoluble. Also if the reaction temperature was increased to 20 ˚C, the reaction mixture was inhomogeneous. According to the literature [19], it is essential to conduct this reaction in a homogeneous solution; since this was not possible, this approach was not applicable for the systems discussed here. However, after the work-up 1-(3,4-dimethoxyphenyl)-octacosane (**11**) was isolated with a yield of 5 %.

6.4.2 Oxidation of the Alcohol

Because due to the absence of useful direct conversion reactions of an organoborane into a carboxylic group the attention was directed towards the conversion of the alcohol functionality into a carboxylic acid *via* conventional oxidation methods. In view of the extended aliphatic segments present in the molecules of interest, it was expected that the major problem for the conversion would be the limited solubility of α-*tert*-butyl-ω-hydroxy-[methylene(8 + j)]-ate (**8**). Clear mixtures of these compounds in toluene, 1,4-dioxane, or dichlorobenzene were only observed at temperatures above 100 °C which is in the region of the melting temperature of, for example, α-*tert*-butyl-ω-hydroxy-[methylene(180)]-ate (**8b**) (T_m = 99 °C, 109 °C). Therefore, the mixture could consist of a liquid-liquid mixture and may not be a homogenous solution. Two problems arise from this fact. First of all, the limited solubility or phase-separation excludes many of the well-known oxidation methods and secondly, purification of the product is likely to be cumbersome because of the limited physical differences between the educt and the product [21]. Hence, the present investigations are focused on reactions with a yield of 95 % or more.

For oxidation of the alcohol, efforts were concentrated on two methods, i.e. oxidation in concentrated nitric acid and oxidation with a potassium permanganate/ phase-transfer-catalyst system. In literature it is reported that concentrated nitric acid is able to oxidize aliphatic alcohols [21,22]. One interesting feature of this method is that it may provide oxidation and cleavage of the *tert*-butyl ester bond at the same time which would avoid an additional synthetic step. In order to simulate and vision systematic problems of conversion and at the same time solubility problems triacontanol was used as the model system. To enhance solubility of the starting materials, in contrast to procedures reported in the literature, the reaction was carried out at 100 ˚C, where the reaction mixtures appeared to be homogeneous, instead of 25 - 30 ˚C (Scheme 6.12) [23].

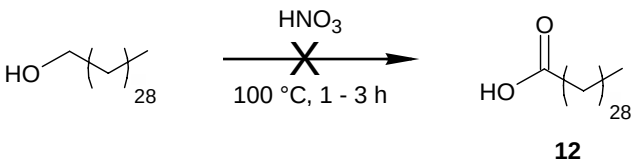

12

Scheme 6.12: Oxidation of triacontanol with concentrated nitric acid.

After about 4 min., brown vapors appeared, likely to be NO_x, which might be interpreted as a sign the oxidation reaction. The relative intensities of five characteristic NMR signals of the products of oxidation of triacontanol are shown in Table 6.3. For the ideal conversion, only one new NMR signal at 2.29 ppm of the methylene group next to the carboxylic group is expected, and the signal at 3.64 ppm of the methylene group in α-position of the alcohol should disappear. Thus, the NMR data clearly indicated that more than one compound was formed during the oxidation reaction. For example, the triplet observed at 4.44 ppm (not associated with the starting material) is not to be expected in the spectrum of the desired product: rather, it can be assigned to a methylene group in an α-position of a nitro group [15]. Thus, oxidation with concentrated nitric acid yielded considerable amounts of undesirable (by) -products and was found to be too unspecific.

Table 6.3: Relative intensities of ^{1}H-NMR signals of the products of two different 1-triacontanol oxidations with conc. nitric acid. [1] Expected chemical shift for the CH_2-group next to the generated carboxylic acid. [2] Chemical shift for the CH_2-group next to the alcohol group [15].

No.	**Time [min]**	**Relative intensities of ^{1}HMR-signals to the chemical shift for the CH_2-group next to the generated carboxylic acid**				
		2.29 ppm[1]	**2.36 ppm**	**3.64 ppm[2]**	**4.05 ppm**	**4.44 ppm**
A	60	1	(0.5)	1.3	0.7	13.2
B	180	1	-	0.2	0.9	3.0

Therefore, another oxidation method was investigated based on a potassium permanganate/phase-transfer-catalyst system. Potassium permanganate is soluble in organic solvents such as benzene if, for example, dicyclohexyl-18-crown-6 is added as a phase-transfer-catalyst (see Scheme 6.13) [21,24]. The color of the produced solution is purple due to the dissolved permanganate. The half-life time of the potassium permanganate crown ether complex in benzene is reported to be 48 h at 25 ˚C, but it rapidly degrades at elevated temperatures [24]. Therefore, a solvent for α-*tert*-butyl-ω-hydroxy-[methylene(8 + j)]-ate (**8**) at 25 ˚C had to be found. A 5 : 1 mixture of *o*-

dichlorobenzene and acetic acid was identified for this purpose. An advantage of the use of acetic acid is its ability to suppress the overoxidation in the presence of an organic solvent and a phase-transfer agent [25].

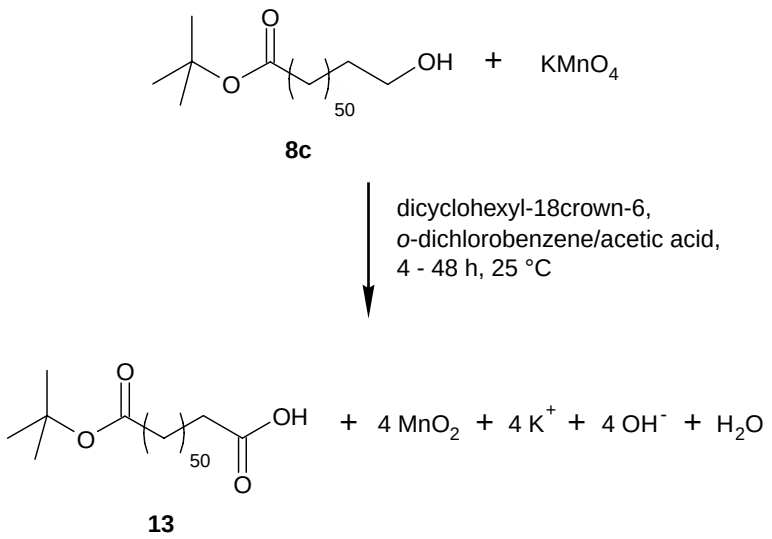

Scheme 6.13: Oxidation of α*-tert-butyl-*ω*-hydroxy-[methylene*(53)*]-ate (**8c**) with a potassium permanganate crown ether complex.*

As is evident from the ^{1}H-NMR spectra of α-*tert*-butyl-ω-hydroxy-[methylene(53)]-ate (**8c**) and the corresponding acid ω-*tert*-butyl-[methylene(52)]-oic acid (**13**) obtained through oxidation of the latter, shown in Figure 6.4, this reaction worked rather well. As can be seen from the spectrum of the reaction product, the ^{1}H-NMR signal of the CH_2-group next to the alcohol at 3.56 ppm vanished to a large extent. At the same time, a new signal appeared at 2.26 ppm, which is assigned to the methylene group next to the generated carboxylic group [15]. After a reaction time of 24 h, the ratio of the integrals of the two signals (CH_2-group next to the generated carboxylic acid group, 2.26 ppm/CH_2-group next to the carboxylic ester group, 2.18 ppm) was determined to be about 1.08; extending the reaction time to 48 h reduced this ratio to 1.05, suggesting a rather good (i.e. ~ 95 %) conversion of the hydroxy group into the carboxylic group. The product of this reaction was isolated in a yield of 55 %. It should be noted that, unfortunately, the signal of the methylene group next to the hydroxy group was still detectable by means of NMR, indicating some imperfection of the oxidation.

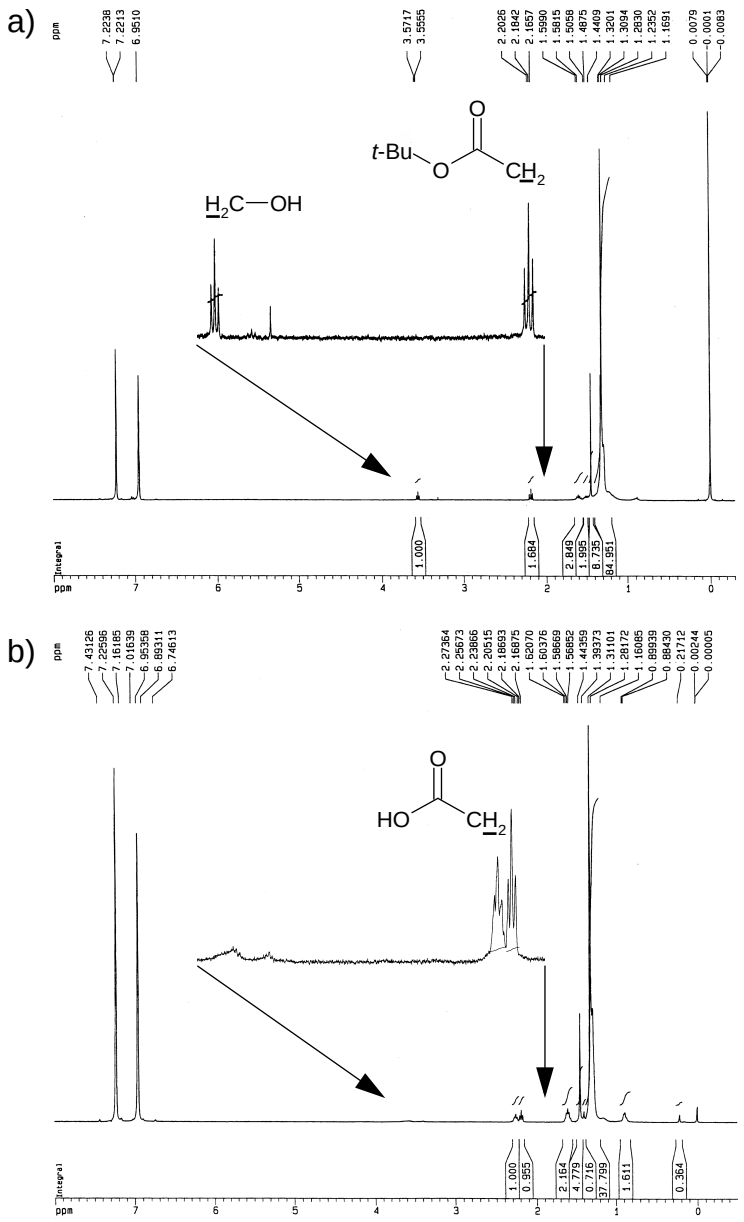

*Figure 6.4: a) ^{1}H-NMR of α-tert-butyl-ω-hydroxy-[methylene(53)]-ate (**8c**). b) ^{1}H-NMR of ω-tert-butyl-[methylene(52)]-oic acid (**13**) after a reaction time of 48 h (both in 1,2-dichlorobenzene-d_4 and at 373 K).*

6.4.3 Oxidative Degradation of the Dimethoxyphenyl

Finally, the synthesis of the first and second functionality of the 1,2-dimethoxy-4-vinylbenzene (**3**) initiator will be discussed. Oxidative degradation of the dimethoxyphenyl unit is catalyzed by ruthenium tetroxide, which can be prepared *in situ* through oxidation of $RuCl_3$ with sodium periodate. In the literature, a yield of 94 % is

reported for low-molecular weight systems containing a phenyl moiety [26]. However, the difficulty of this specific oxidative degradation reaction is the composition of the solvent mixture which is of significant importance for the success of this reaction [26]. Consequently, the latter could not be changed in order to match the solubility of the substrate to be oxidized. Unfortunately, 1-(3,4-dimethoxyphenyl)-octacosane (**11**) was insoluble in the required 2 : 2 : 3 mixture of acetonitrile, chloroform, and water [26]. Therefore this approach was not further investigated.

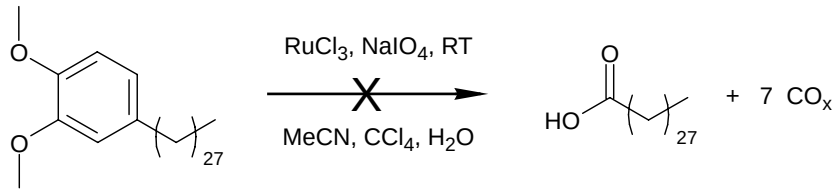

11

*Scheme 6.14: Attempted oxidation of 1-(3,4-dimethoxyphenyl)-octacosane (**11**).*

6.4.4 Conclusions

Efforts to develop a useful method to introduce the second carboxylic acid functionality were only partially successful. The main reason for this fact is the limited solubility of the polyethylene-like α-*tert*-butyl-ω-hydroxy-[methylene(8 + j)]-ates (**8**), which reduced the possible chemical reactions for the conversion; this applies to the C-C bond forming reaction as well as to the oxidation reactions.

6.5 General Conclusions

Polyhomologation is indeed a useful method to synthesize telechelic oligomethylenes with a controllable alkyl chain length. *tert*-Butyl undec-10-enoate (**2**) proved to be a suitable initiator for the synthesis of α-*tert*-butyl-ω-hydroxy-[methylene(8 + j)]-ates (**8**). The polyhomologation of this initiator yielded **8** with chain lengths between 27 and about 180 methylene groups. The incomplete conversion of the B-C bond into a hydroxy group after the polyhomologation caused by the limited solubility of

α-*tert*-butyl-ω-hydroxy-[methylene(8 + j)]-ates (**8**) in THF can be addressed, in the future, by use of trimethylamine-*N*-oxide dihydrate, which reacts directly with an organoborane in toluene in order to form the corresponding alcohol. However, the phase-catalyzed oxidation of α-*tert*-butyl-ω-hydroxy-[methylene(8 + j)]-ates (**8**) to the corresponding carboxylic acid with potassium permanganate proved to be successful. The conversion was in the desired region of 95 %. However, it remains to be demonstrated that the cleavage of the *tert*-butyl can be accomplished in quantitative manner, to yield the sought-after linear α-ω-oligomethylene-dioic acids.

The existence of methyl branching caused by the limited regioselectivity of the hydroboration and the incorporation of ethylidine groups instead of methylene groups due to impurities of ethylide in the ylide solution during the polyhomologation, and the observed polydispersity of 1.69 led to the decision to dismiss this approach. The branching and the irregularity of the molecular weight distribution of the possible dicarboxylic acid would most probably disturb or even suppress the crystallization of the corresponding polyamide. This situation would contradict the aim of this project. Consequently, polyhomologation is an interesting method from the chemical point of view but not for the here desired needs.

6.6 Experimental

General Methods. All reagents and solvents were purchased from Aldrich and Fisher. Only analytical grade quality chemicals were used. ^{1}H-NMR spectral ^{13}C-NMR data are expressed in ppm relative to internal standard (Tetramethylsilan (TMS) or $CDCl_3$) and were obtained on various Bruker NMR spectrometers. Mass spectroscopy (MALDI-TOF) and elemental analyses were carried out by the Mass Spectra and Microanalysis Laboratories of the Department of Chemistry of ETH Zürich. The T_m was determined with a Netzsch DSC 200 and taken as the peak value of endothermal in the scans. The GPC measurement was performed on a GPC consisting of a Waters pump, three columns connected in series loaded with a SDV-gel (pore size: 10^3, 10^5, 10^6 Å), and a Soma FOMA UV- and refraction detector (conditions: flow 1.0 mL/min, solvent

toluene, 100°C; calibration: polystyrene standard; at MPI Mainz). IR-spectra were taken with CsCl pellets on a Bruker IFS-66v Spectrometer.

(3-Methyloxetan-3-yl) methyl undec-10-enoate (4). A 50 mL three-necked reaction flask was charged with 1.104 g (10.8 mmol) of (3-methyloxetan-3-yl) methanol, 0.927 g (11.7 mmol) of anhydrous pyridine, and 8 mL of anhydrous dichloromethane at 0 ˚C. 10-Undecenoylchlorid (2.433 g, 12.0 mmol) was added over the course of 15 min to this stirred solution, causing an immediate precipitate. After the addition was completed, the reaction mixture was stirred for 5 h at 0 ˚C, and, subsequently, 20 mL of ether was added to the mixture. The dilute mixture was poured over 35 mL of ice water. The organic phase was separated and washed with 50 mL of saturated NaCl solution. The solvent was evaporated, and (3-methyloxetan-3-yl) methyl undec-10-enoate (**4**) was obtained as a clear, slightly yellow oil (2.858 g, 10.6 mmol, 98 %). ^{1}H-NMR (200 MHz, $CDCl_3$, 298 K) δ 5.82-6.02 (m, 1H), 5.01-5.16 (m, 2H), 4.52 (d, *J* = 5.91 Hz, 2H), 4.38 (d, *J* = 5.94 Hz, 2H), 4.28 (s, 2H), 2.35 (t, *J* = 7.44 Hz, 2H), 1.98-2.05 (m, 2H), 1.59-1.68 (m, 2H), 1.29-1.40 (m, 13H).

1-Dec-9-enyl-4-methyl-2,6,7-trioxabicyclo[2.2.2]octane (1). A 100 mL flask charged with 244 mg of $MgSO_4$ was heat-dried under vacuum. In this flask a solution of 1.055 g (3.9 mmol) of (3-methyloxetan-3-yl) methyl undec-10-enoate (**4**) and 5 mL of anhydrous dichloromethane was cooled to -15 ˚C, and 0.1556 g (1.1 mmol) of boron trifluoride etherate was added under stirring. After stirring for 23 h at - 15 ˚C, the starting material had been quantitatively consumed (as determined by TLC analysis) and the reaction was quenched with a solution of 0. 465 g (4.6 mmol) of triethylamine in 20 mL diethylether, and filtered to remove the $MgSO_4$ and the amine-BF_3 complex. The resulting solution was added to a solution of 0.747 g (13.3 mmol) KOH and ice water (29 mL). The organic layer was separated off and washed with 50 mL of brine. After drying over $MgSO_4$, evaporating the solvent, and drying of the product for 16 h under vacuum 0.961 g (3.6 mmol, 92 %) of 1-dec-9-enyl-4-methyl-2,6,7-trioxabicyclo[2.2.2]octane (**1**) were obtained as a colorless oil. ^{1}H-NMR (200 MHz, $CDCl_3$, 298 K) δ 5.70-5.91 (m, 1H), 4.88-5.03 (m, 2H), 3.89 (s, 6H), 1.97-2.04 (m, 2H), 1.61-1.70 (m, 2H), 1.15-1.45 (m, 12H), 0.76 (s, 3H).

***tert*-Butyl undec-10-enoate (2)**. A 50 mL three-necked flask was charged with 2.543 g (34.3 mmol) of *t*-butylalcohol, 3.028 g (38.3 mmol) of anhydrous pyridine, and 6 mL of anhydrous diethylether. 10-Undecenoylchlorid (7.724 g, 38.1 mmol) was slowly added to this stirred solution. After refluxing the solution for 1 h, 20 mL of water was added and the mixture was stirred until the precipitate was dissolved. The organic layer was washed with aqueous sulfuric acid (10 v/v % of concentrated sulfuric acid), and saturated sodium hydrogen carbonate solution, and subsequently dried ($MgSO_4$) and concentrated *in vacuo*. 7.324 g (89 %) *tert*-butyl undec-10-enoate (**2**) were obtained as a slightly yellowish oil. ^{1}H-NMR (200 MHz, $CDCl_3$, 298 K) δ 5.70-5.9 (m, 1H), 4.88-5.03 (m, 2H), 2.19 (t, *J* = 7.42 ppm, 2H), 1.98-2.07 (m, 2H), 1.54-1.64 (m, 2H), 1.48-1.20 (m, 19H).

1-(3,4-Dimethoxy-phenyl) ethanol (5α) and 2-(3,4-dimethoxy-phenyl) ethanol (5β). 2 mL of anhydrous tetrahydrofuran and 1.023 g (6.23 mmol) 1,2-dimethoxy-4-vinylbenzene (**3**) were added to a 50 mL three-necked flask under argon atmosphere. This solution was stirred and cooled to 0 ˚C. 2.246 mL (2.246 mmol) of borane tetrahydrofuran complex solution was slowly added over a period of 10 min. After 15 h the reaction mixture was allowed to warm to ambient temperature. The oxidative work-up of this solution which comprise *tri*-(3,4-dimethoxyphenethyl) borane (**7**), was started after 2 h. Simultaneously, a mixture of 1.1 mL of 30 wt % H_2O_2 and 2.5 mL of NaOH (3 N) was added. The two layers were separated, and the aqueous layer was extracted three times with ether. The combined organic layers were washed with brine and THF. The yield was not determined, because this reaction was only used to determine the regioselectivity. The regioselectivity was 92 % of β-position to 8 % of α-position determined by ^{1}H-NMR. ^{1}H-NMR (200 MHz, $CDCl_3$, 298 K) δ 6.74-6.88 (m, 3H), 3.80-3.89 (m, 8H), 2.81 (t, *J* = 6.48 Hz, 2H), (α-position of the OH-Group 4.61 ppm, s).

Dimethylsulfoxonium methylide in THF (see Table 6.1, Entry No. A). Sodium hydride (1.82 g, 75.8 mmol) as a 55 % - 65 % powder moistened with oil was placed in a 250 mL three-necked flask and was washed three times with 15 mL of anhydrous hexane in order to remove the mineral oil. 4.96 g (38.6 mmol) of dry trimethylsulfoxonium chloride was added to the reaction vessel under a stream of argon. 55 mL of THF (distilled from sodium) was added to this mixture. The reaction mixture was stirred and

heated to reflux (80 ˚C). Evolution of hydrogen gas was observed, and after 5 h the reaction mixture was allowed to cool to room temperature. The cloudy mixture was filtered through an oven-dried Schlenk filter, which contained a 2 cm thick layer of dry celite, directly into a storage flask. In order to determine the exact concentration of the ylide, 0.2 mL of the ylide solution were hydrolyzed in water and titrated with 0.1-N hydrochloric acid. The color change of phenolphthalein was used to determine the end point of the titration. The concentration was calculated to be 0.78 μmol/mg.

Dimethylsulfoxonium methylide in Toluene (see Table 6.1, No. C). Sodium hydride (4.46 g, 111.5 mmol) as a 55 % - 65 % powder moistened with oil was placed in a 500 mL three-necked flask and washed three times with 50 mL of anhydrous hexane in order to remove the mineral oil. 10.98 g (85.37 mmol) of dry trimethylsulfoxonium chloride was added to the reaction vessel under a stream of argon. 120 mL of toluene (distilled from sodium) was added to this mixture. The reaction mixture was stirred and heated to reflux (112 ˚C). Evolution of hydrogen gas was observed and after 4.5 h the reaction mixture was allowed to cool down to room temperature. At room temperature the cloudy mixture was filtered through an oven-dried Schlenk filter, which contained a 2 cm thick layer of dry celite, directly into a storage flask. In order to determine the exact concentration of the ylide, 0.2 mL of the ylide solution were hydrolyzed in water and titrated with 0.1-N hydrochloric acid. The color change of phenolphthalein was used to determine the end point of the titration. The concentration was calculated to be 0.878 μmol/mg.

***tert*-Butyl 11-{1,1-di[11-(tert-butoxy)-11-oxoundecyl]boryl} undecanoate (6)**. 26.4036 g of anhydrous tetrahydrofuran and 5.7085 g (23.7 mmol) of dry *tert*-butyl undec-10-enoate (**2**) were added in a 50 mL three-necked flask under argon atmosphere. This solution was stirred and cooled to 0 ˚C. 6.8554 g (7.634 mL, 7.634 mmol, 22.9 eq) of a 1 M borane tetrahydrofuran complex solution was slowly added over a period of 20 - 30 min and the reaction mixture was stirred at 0 ˚C for another 30 min. The reaction mixture was subsequently allowed to warm to ambient temperature, and stirred for 3 h. The calculated concentration (based on the starting materials and assuming 100 % conversion) was 0.6082 mmol of *tert*-butyl 11-{1,1-di[11-(tert-butoxy)-11-oxoundecyl]boryl} undecanoate (**6**) per 1 g of its THF solution. This solution was used

as a polyhomologation initiator without further treatment. ^{1}H-NMR (400 MHz, CDCl3, 298 K) δ 5.70-5.90 (m, 1H), 4.88-5.03 (m, 2H), 2.19 (t, *J* = 14.84 ppm, 2H), 1.98-2.07 (m, 2H), 1.54-1.64 (m, 2H), 1.48-1.20 (m, 19H).

α-*Tert*-butyl-ω-hydroxy-[methylene(44)]-ate (8a) (see Table 6.2, Entry **No. 4**). The following description is representative for the synthesis procedure of α-*tert*-butyl-ω-hydroxy-[$(CH_2)_{(8 + j)}$]-ate. Under argon atmosphere, 19.078 g of the toluene solution of dimethylsulfoxonium methylylide (12.36 mmol, 23 eq) was stirred at RT. 0.94 mL (0.54 mmol, 1 eq) of *tert*-butyl 11-{1,1-di[11-(*tert*-butoxy)-11-oxoundecyl]boryl} undecanoate (**6**)/THF solution (prepared by the same procedure as noted above; however, a different batch was used) were added as quickly as possible by means of a syringe. After stirring the mixture for 10 min, the ylide was quantitatively consumed as was evident from an aliquot of the reaction mixture in phenolphthalein-water (indicator solution stayed colorless). The toluene was removed by rotary evaporation, and under argon atmosphere, 10 mL of anhydrous tetrahydrofuran were added. Subsequently, a mixture of NaOH (6 N) and 30 wt % H_2O_2 (each around 0.3 mL) was added dropwise at a temperature of 20 ˚C, leading to the formation of a precipitate. After stirring for 16 h at room temperature, the reaction mixture was heated to 60 ˚C forming a homogeneous solution, which was poured into acetonitrile. The precipitated polymer was filtered off and dried under vacuum for 18 h. After filtration, 0.242 g (0.33 mmol, 61 %, $C_{49}H_{98}O_3$) of α-*tert*-butyl-ω-hydroxy-[methylene(44)]-ate (**8a**) was obtained. The length of the synthesized aliphatic segment was calculated from the ratios of the intensities of the ^{1}H-NMR signal‘s intensity (sI) of the CH_2-group next to the ester group (2.19 ppm, sI = 0.08/H) or the signal‘s intensity of the CH_2-group next to the alcohol group (3.57 ppm, sI = 0.08/H), respectively, and the signal‘s intensities of the CH_2-groups of the aliphatic chain (1.10-1.55 ppm, sI = 6.59/0.08/H ≈ 82 H). α-*tert*-butyl-ω-hydroxy-[methylene(44)]-ate was obtained as a white powder. ^{1}H-NMR (400 MHz, 1,2-dichlorobenzene-d_4, 373 K) δ 3.57 (m, 2H), 2.19 (t, *J* = 7.44 ppm, 2H), 1.55-1.60 (m, 2H), 1.45 (s, 9H), 1.00-1.44 (m, 82H), 0.82-0.90 (m, 2H, -CH(C*H*$_3$)-, -C*H*$_3$).

*Table 6.4: Synthesis of α-tert-butyl-ω-hydroxy-[methylene(8 + j)]-ate (**8**): Reagents and results. Key: [1] See also Table 6.2.*

Entry	**Entry No. 4[1]**	**Entry No. 5[1]**	**Entry No. 6[1]**
Product	**8a**	**8b**	**8c**
Toluene solution of $CH_2S(O)Me_2$	19.078 g (12.36 mmol, 23 eq.)	65.854 g (57.82 mmol, 137 eq.)	66.465 g (33.90 mmol, 30 eq.)
Alkyl Borane Initiator (**6**) in THF	0.94 mL (0.54 mmol, 1 eq.)	0.694 g (0.42 mmol, 1 eq.)	3.616 g (2.20 mmol, 1 eq.)
THF after the Removing of Toluene	10 mL	45 mL	45 mL
NaOH/30 wt % H_2O_2 Solution (1:1 mixture)	0.6 mL	1.2 mL	1.2 mL
Acetonitrile	200 mL	450 mL	400 mL
Calc. CHO-Formula (by ^{1}H-NMR)	$C_{49}H_{98}O_3$	$C_{185}H_{371}O_3$	$C_{58}H_{116}O_3$
Recrystallized from 1,4-Dioxane at RT	-	100 mL	100 mL
Yield	0.242 g (0.35 mmol, 65 %)	0.461 g (0.17 mmol, 40 %)	0.656 g (0.76 mmol, 35 %)

α-*Tert*-butyl-ω-hydroxy-[methylene(180)]-ate (8b) (see Table 6.2, Entry **No. 5**). ^{1}H-NMR (400 MHz, 1,2-dichlorobenzene-d_4, 373 K) δ 3.56 (t, *J* = 6.47 Hz, 1H), 2.19 (t, *J* = 7.36 ppm, 2H), 1.58-1.62 (m, 2H), 1.44 (s, 9H), 1.10-1.43 (m, 346H), 0.88-0.91 (m, 10H, -CH(C*H*$_3$)-, -C*H*$_3$). ^{13}C-NMR (125 Hz, 1,2-dichlorobenzene-d_4, 373 K) δ 172.33 (-*C*OO-), 79.35 (-*C*-$(CH_3)_3$), 62.97 (-*C*H_2-OH), 37.50, 35.85, 33.35, 33.19, 30.36, 30.10-29.73, 28.34, 27.42, 25.47, 19.93 (all aliphatic -*C*H_2-, -*C*H_3, or -*C*H-). IR: ν_{max}: O-H, 3431; C-H 2918, 2849; C=O, 1735; -CH_2-, -CH_3, 1473, 1463; C-O, 1153, 1063. T_m: 99.4 °C and 109.1 °C. Mass spectrum MALDI-TOF, polarization: Na^+-ion, reflector, *m/z*: 2687.2 (M^+ parent). GPC: $\overline{M}_n$ = 2120, $\overline{M}_w$ = 3590, *PD* = 1.69. Anal. Calcd for $C_{185}H_{370}O_3$: C, 84.07; H, 14.11; O, 1.82; Found: C, 83.97; H, 14.18; O, 2.05.

α-*Tert*-butyl-ω-hydroxy-[methylene(53)]-ate (8c) (see Table 6.2, Entry **No. 6**). ^{1}H-NMR (400 MHz, 1,2-dichlorobenzene-d_4, 373 K) δ 3.55 (t, *J* = 6.48, 2H), 2.18 (t, *J* =

7.38, 2H), 1.58-1.62 (m, 2H), 1.44 (s, 9H), 1.10-1.43 (m, 100H), 0.88-0.90 (m, 1.5H, -CH(C*H*$_3$)-, -C*H*$_3$).

1-(3,4-Dimethoxyphenyl)-octacosane (11) (see Table 6.2, Entry **No. 3**). The desired product of this synthesis was α-ethyl-ω-(3,4-dimethoxyphenyl)-[methylene(18)]-ate (**10**). The synthesis of *tri*-(3,4-dimethoxyphenethyl) borane (**7**) was conducted in analogy to the descriptions above. Under argon atmosphere, 28.69 g of the toluene solution of dimethylsulfoxonium methylylide (18.07 mmol, 16 eq) were stirred at RT. 1.1 mL (1.14 mmol) of *tris*-(3,4-dimethoxystryene) borane (**7**) were added as quickly as possible by means of a syringe. After stirring the mixture for 10 min the ylide was quantitatively consumed as was evident from an aliquot of the reaction mixture in phenolphthalein-water (indicator solution stayed colorless). The toluene was removed by rotary evaporation, and under argon atmosphere the synthesized solid was dissolved at 50 ˚C in 10 mL of THF. Then the solution was cooled to 0 ˚C and, unfortunately, the oligomer precipitated again. The temperature was increased to 20 ˚C and a solution of 0.24 mg (1.57 mmol) methyl bromoacetate in 5 mL of *tert*-butyl alcohol was added. The mixture thus obtained was not clear. The reaction mixture was poured over 200 mL of ice water and, subsequently, washed three times with chloroform. The two layers were separated, and the solvent of the organic layer was removed by distillation. 0.033 g (0.06 mmol, 5 %, $C_{36}H_{66}O_2$) of a white solid was isolated which was identified by its ^{1}H-NMR spectrum as 1-(3,4-dimethoxyphenyl)-octacosane (**11**). The length of the aliphatic segment was calculated from ^{1}H-NMR by ratio of the intensities of the Ph-O-CH_3 protons (3.86 ppm, relative intensity (rI) = 0.67/H) to the aliphatic protons (0.81-1.59 ppm, rI = 36.22/0.67/H ≈ 54 H). ^{1}H-NMR (200 MHz, $CDCl_3$, 298 K) δ 6.71-6.82 (m, 3H), 3.86 (d, *J* = 3.67, 9H), 2.55 (t, *J* = 7.64 Hz, 2H), 0.81-1.59 (m, 54H).

Attempted Oxidation of 1-(3,4-Dimethoxyphenyl)-octacosane (11) with Sodium Periodate. The synthesized 1-(3,4-dimethoxyphenyl)-octacosane (**11**) was not soluble at room temperature in a 2 : 2 : 3 mixture of CCl_4 : acetonitrile : water as required for the oxidation with sodium periodate and the *in situ* formed ruthenium tetraoxide catalyst.

Attempted Synthesis of Triacontanoic Acid (12) (batches **A** and **B**). 1-Triacontanol (**A**:19.4 mg (0.04 mmol); **B**: 20.2 mg (0.05 mmol)) were stirred in 65 v/v % nitric acid (**A**: 1.418 g; **B**: 1.402 g) over 19 hours at RT. The mixture was subsequently rapidly heated to 100 ˚C. After 1 minute at this temperature, the solution became homogeneous, and after another 4 minutes, brown vapors appeared. The reaction mixture was poured in 20 mL of ice water after stirring for a total of 60 min. batch **A** and 180 min. batch **B**, respectively, at 100 ˚C. The precipitated solid was filtered off, washed with water and recrystallized from 1,4-dioxane at RT. ^{1}H-NMR of the synthesized white solid of batch **A** (400 MHz, 1,2-dichlorobenzene-d_4, 373 K) δ 4.44 (t, *J* = 6.72, relative intensity[a] (rI): 0.51), 4.05 (t, *J* = 6.77, rI: 0.03), 3.64 (t, *J* = 6.60, rI: 0.05), 2.29 (t, *J* = 7.49, rI: -[b]), 2.24 (t, *J* = -[b], rI: -[b]), 1.00-1.8 (m, rI: 19.45), 0.88 (t, *J* = 6.69, rI: 1.00). ^{1}H-NMR of the synthesized white solid of batch **B** (400 MHz, 1,2-dichlorobenzene-d_4, 373 K) δ 4.44 (t, *J* = 6.71, rI[a]: 0.37), 4.05 (t, *J* = 6.71, rI: 0.12), 3.64 (t, *J* = -[b], rI: 0.03), 2.29 (t, *J* = 7.51, rI: 0.12), 1.00-1.8 (m, rI: 19.18), 0.88 (t, *J* = 6.65, rI: 1.00). Key: [a] Intensity relative to intensity of the signal of the methyl-group at the end of the chain (0.88 ppm). [b] NMR signals not clear.

ω-*Tert*-butyl-[methylene(52)]-oic acid (13). 94.4 mg (0.11 mmol, $C_{58}H_{116}O_3$) of α-*tert*-butyl-ω-hydroxy-[methylene(53)]-ate (**8c**) was dissolved in 10 mL of 1,2-dichlorobenzene and 2 mL of acetic acid. At room temperature, 55.9 mg (0.35 mmol) of potassium permanganate and 25.7 mg (0.07 mmol) of dicyclohexano-18-crown-6 were added. The violet solution turned slowly brownish, indicating the presence of MnO_2. After 48 h, the reaction was cooled with an ice bath, and a mixture of 107.3 mg (0.85 mmol) sodium sulfite in 1 mL water was added. After the subsequent addition of 2 mL of a 1 : 1 mixture of conc. HCl and water, the brown color disappeared. The two obtained layers were separated, and the solvent of the organic layer was removed by distillation. The resulting white solid was washed three times with 10 mL of a saturated aqueous KCl solution, in order to completely remove the crown ether, and finally with diethyl ether. 52.5 mg (0.06 mmol, $C_{58}H_{114}O_4$, 55 %) of a white solid were obtained. ^{1}H-NMR (400 MHz, 1,2-dichlorobenzene-d_4, 373 K) δ 3.50-3.70 (m, signal of the α-CH_2-group next to the alcohol), 2.26 (m, 2H), 2.19 (t, *J* = 7.28, 2H), 1.56-1.63 (m, 4H), 1.00-1.45 (m, 106H), 0.88-0.90 (m, 1.5H, -CH(C*H*$_3$)-, -C*H*$_3$).

6.7 References

[1] Peacock, A. J. *Handbook of Polyethylene*, Marcel Dekker: New York, 2000.

[2] Elias, H. G. *Makromoleküle*; Wiley-VCH: Weinheim, 1999.

[3] Szwarc, M.; Van Beylen, M. *Ionic Polymerization and Living Polymers*; Chapman & Hall: New York, 1993.

[4] Queffelec, J.; Scott, G. G.; Matyjaszewki, K. *Macromolecules* **2000**, *33*, 8629.

[5] Nuyken, O.; Pask, S. *Telechelic Polymers*, in Kroschwitz, J. I. *Encyclopedia of Polymer Science and Engineering*; 2nd ed.; John Wiley: New York, 1989, Vol. 16, p. 494.

[6] Salamone, J. C. *Polymeric Materials Encyclopeadia*; CRC Press: Boca Raton, 1996.

[7] Shea, K. J.; Walker J. W.; Zhu, H.; Paz, M.; Greaves, J. *J. Am. Chem. Soc.* **1997**, *119*, 9049.

[8] Shea, K. J.; Busch, B. B.; Paz, M. *Angew. Chem. Int. Ed.* **1998**, *37*, 1391.

[9] Busch, B. B.; Paz, M. M.; Shea, K. J.; Staiger, C. L.; Stoddard, J. M.; Walker, J. R.; Zhou, X.-Z.; Zhu, H. *J. Am. Chem. Soc.* **2002**, *124*, 3636.

[10] Brown, H. C.; Keblys, K. A. *J. Am. Chem. Soc.* **1964**, *86*, 1795.

[11] Brown, H. C.; Sharp, R. L. *J. Am. Chem. Soc.* **1966**, *88*, 5851.

[12] Greene, T. W.; Wuts, P. G. M. *Protective Groups in Organic Synthesis*; John Wiley: New York, 1991.

[13] Corey, E. J.; Raju, N. *Tetrahedron Lett.* **1983**, *24*, 5571.

[14] Vogel, A. I. *Textbook of Practical Organic Chemistry including Qualitative Organic Analysis*; Longman: London, 1978.

[15] Pretsch, E.; Seibl, J.; Simon, W. *Tabellen zur Strukturaufklärung Organischer Verbindungen mit Spektroskopischen Methoden*; Springer-Verlag: Berlin, 1990.

[16] Corey, E. J.; Chaykovsky, M. *J. Am. Chem. Soc.* **1965**, *87*, 1353.

[17] Bauer, B. J.; Wallace, W. E.; Fanconi, B. M.; Guttman, C. M. *Polymer* **2001**, *42*, 9949.

[18] Chen, R.; Liang, L. *J. Am. Soc. Mass Spectrom*. **2001**, *12*, 367.

[19] Brown, H. C.; Rogic, M. M.; Rathke, M. W.; Kabalka, G. W. *J. Am. Chem. Soc.* **1968**, *90*, 818.

[20] Brown, H. C.; Rogic, M. M.; Rathke, M. W.; Kabalka, G. W. *J. Am. Chem. Soc.* **1968**, *90*, 1911.

[21] Haines, A. H. *Methods for the Oxidation of Organic Compounds*; Academic Press: London, 1988.

[22] Heyns, K.; Vogelsang, G. *Chem. Ber.* **1954**, *87*, 13.

[23] Grakauskas, V. *J. Org. Chem.* **1970**, *435*, 3030.

[24] Sam, D. J.; Simmons, H. F. *J. Am. Chem. Soc.* **1972**, *94*, 4024.

[25] Krapcho, A. P.; Larson, J. R.; Eldridge, J. M. *J. Org. Chem.* **1977**, *42*, 3749.

[26] Carlsen, P. H. J.; Katsuki, T.; Martin, V. S.; Sharpless K. B. *J. Org. Chem.* **1981**, *46*, 3936.

7. General Conclusions and Outlook

7.1 Results and Conclusions

The key objective of this thesis was to synthesize and explore properties of novel polyamides whose backbone contains well-defined, extended aliphatic segments. The underlying inspiration was the envisioned possibility of using this structural motif to synergistically combine into one (amphiphilic) homopolymer the advantageous properties of polyamides and polyethylene.

As the aim was to produce polymers with relatively high melting temperatures compared to those of polyethylene and AB polyamides, only AABB polyamides were investigated. This meant limiting the monomer synthesis to homo-bifunctional compounds. As diamines are generally easy to synthesize *via* the corresponding dicarboxylic acids, e.g. in the *Schmidt* reaction [1], attention was directed exclusively at the preparation and use of dicarboxylic acids. An important objective of the monomer synthesis was to identify and develop a method leading to well-defined, linear molecules as that would guarantee optimal crystallization of these new segments in the target polymers. The Hünig dicarboxylic acid synthesis was employed as the method of choice [2], and yielded 1,34-tetratriacontanedioic acid in relatively large quantities (i.e., up to 20 g), in high purity and in an overall yield of 45 %. The resultant availability of diacids enabled sufficient amounts of the corresponding polyamides to be produced by melt-polycondensation for subsequent investigation. Thus, a new class of PA-x.34 compounds (x = 2, 4, 6, 8, 10, 12) with weight-average molecular weights as high as 30,000 were produced. Commercial 1,24-tetracosanedioic acid was also used to prepare PA-6.24, to act as a representative of polyamides with slightly shorter aliphatic segments. Interestingly, and in contrast to PA-6.34 (see below), the properties of PA-6.24, especially its phase behavior, followed expectations based on extrapolations of characteristics of standard polyamides. Therefore, the length of the aliphatic moiety of the PA-x.34 compounds appeared to exceed the critical length needed for yielding novel (amphiphilic) properties.

Although the present polyamides x.34 have much lower concentrations of amide groups relative to normal polyamides, their common thermal transitions are not located at significantly lower temperatures. Their melting temperatures ranged from 166 to 190 °C; this was quite remarkable given that PA-12.12, which has a much higher amide concentration, has a melting temperature in the same range (T_m = 184 °C) [3]. Also, the glass transition temperature of the PA-x.34 series, namely 37 - 57 °C, was not unlike those of standard polyamides.

X-ray diffraction patterns for PA-x.34 revealed the 100 and 010/110 reflections typical of, for example, PA-6.6. It is concluded from these patterns that the former polymers crystallized in the PA-6.6-like triclinic α–structure which was supported by computer generated X-ray diffraction pattern, using the Cerius2 program, for the PA-6.34 lamellar crystal structure. The structure of PA-2.34 is noticeably different and matches the pattern of behavior of the PA-2.y family.

Most importantly, the study revealed that the novel PA-x.34 compounds exhibited phase behavior rather different from that of more classic polyamides. Consider the solubility of PA-x.34 for a start. Conventional solvents for polyamides, such as formic acid and concentrated sulfuric acid, were unable to dissolve the new materials at room temperature, and neither could solvents for polyethylene, including toluene (at elevated temperatures). The phase behavior of conc. sulfuric acid and 1,2,3,4-tetrahydronaphthalene was especially interesting. The PA-x.34 compounds were able to form gels in both these solvents under certain conditions. For example, mixtures of 5 - 20 wt % PA-6.34 in conc. sulfuric acid formed a remarkably coherent gel at 40 - 60 °C; at higher temperatures, the gel became a viscous fluid and fibers could be spun from it. Interestingly, this temperature range approximated to the melting temperatures of C_{22} - C_{26} *n*-alkanes (44.4 - 56.4 °C) [4]. It was concluded that the sulfuric acid broke the hydrogen bonds between the amide moieties, and that the gel was most likely generated by physical crosslinks formed by crystallites of the extended aliphatic segments. The reverse appeared to be true for mixtures of 1,2,3,4-tetrahydronaphthalene and PA-6.34: a mixture of 37.5 wt % PA-6.34 in 1,2,3,4-tetrahydronaphthalene also produced a macroscopic gel which melted at 138 °C and was capable of being spun into fibers. Thus, it seems that 1,2,3,4-tetrahydronaphthalene was a solvent only for the aliphatic moieties and that the hydrogen bonds were still intact up to 138 °C. The same observation was made for the other representatives of the PA-x.34 series, this fact demonstrating the

amphiphilic character of the novel PA-x.34 compounds. Again, it should be noted that this interesting behavior was not observed in “conventional” polyamides or in the PA-6.24 investigated here. Another major indication of the amphiphilic character of this novel class of polymer was an ability to decrease the domain size of a 1 : 1 polyethylene/ PA-6 blend when used as a compatibilizer.

The aforementioned property of PA-6.34 to form a gel in conc. sulfuric acid was also investigated with a view to producing highly oriented, high-strength polyamide fibers. In general, movement in the crystalline phase is limited in polyamides by the strong hydrogen bonds between the amide groups. Therefore, polymer chains cannot be drawn through these crystals, which prevents achievement of high degree of extension and orientation of the polyamide macromolecules. It seemed then that the PA-6.34/ sulfuric acid gel could provide a solution to this problem, because the sulfuric acid would disrupt hydrogen bonds between the amide groups, while the remaining aliphatic “crystallite” network would exhibit plastic deformation of the kind encountered in, e.g., polyethylene. Gratifyingly, the observed maximum draw ratio of the PA-6.34/sulfuric acid gel was λ = 15 - 20 at 75 °C as opposed to about 5 for melt-processed common polyamides. Unfortunately, this unusual gel-processing method was unable to give better mechanical properties on PA-6.34. Two possible reasons are discussed in order to provide an explanation for this finding. The first is that the bifunctional sulfuric acid may form hydrogen bonds between the polymer chains, creating a situation similar to that which occurs when common polyamides are drawn. This reasoning is, however, not consistent with the observed very high draw ratios, but on the other hand the observed mechanical properties of the produced PA-6.34 suggested a certain network different from the aliphatic “crystallite” network. The second, more plausible cause, could be the low melting temperature of the aliphatic “crystals” in the PA-6.34/sulfuric acid gel, which was below the α_c-relaxation temperature (~ 88 °C) of polyethylene. High orientation of polyethylene by plastic deformation is primarily possible above this temperature [5]. This means that any gelling process for improving mechanical properties requires more extended aliphatic segments leading to a higher dissolution temperature of such polyamide gels.

An alternative way of synthesizing more highly extended aliphatic diacids was explored. Especially, it was attempted to synthesize monomers with a chain length above 60 methylene groups so that the dissolution temperature (T_d) of the corresponding gel

would be higher than the α_c-relaxation temperature of polyethylene. As the PA-6.34/ sulfuric acid gel exhibited a T_d of 54 °C, which is comparable to that of the C_{26} *n*-alkane, a PA-6.60/sulfuric acid gel should melt at 90 - 99 °C (the melting temperature of a C_{52} - C_{60} *n*-alkane [6,7]). But, unfortunately, only methyl branched α-tert-butyl-ω-hydroxy-[methylene (180)]-ate with a chain length of around 180 methylene groups and ω-tert-butyl-[methylene (53)]-oic acid, which was the precursor of the dicarboxylic acid target, were synthesized with the aid of the polyhomologation method developed by Shea *et al*. This method proved useful for synthesizing telechelic macromonomers but is, in fact, not applicable for the here discussed project due to the existence of a methyl branch and the here observed polydispersity.

Another method for making highly oriented fibers utilizes the slow crystallization rate of PA-6.34. Theoretically, quenched samples of PA-6.34 should have low crystallinity and likely few hydrogen bonds in the crystalline phase; this would offer the possibility of achieving high draw ratios *via* plastic deformation. While it proved possible to produce small PA-6.34 samples of low crystallinity, the maximum draw ratio for these samples was the same as those observed for samples prepared by standard methods. Thus, even a relatively small number of hydrogen bonds was still able to prevent movement in the polyamide crystalline phase. From these facts, it was concluded that only plastic deformation would most likely produce extensive orientation in those polyamides which no longer contain any hydrogen bonds during orientation.

7.2 Outlook

One candidate for further work relates to the aforementioned assumption that the α_c-relaxation temperature of 88 °C of polyethylene crystals is the factor limiting the maximum attainable draw ratio. With a view to proving or refuting this assumption, polyamides with aliphatic segments of chain length in excess of 52 methylene groups should be synthesized and used for gel orientation as already described. These extended dicarboxylic acid targets could be synthesized, for example, by the following three methods. The first, namely the Hünig method, has already been discussed and will

increase the chain length by 24 methylene groups for every repetition of the three constituent steps. The limiting factor on this and all the other methods is, of course, the low solubility of the intermediates and the resulting diacids. The second method would be oxidation of the top and bottom surfaces of individual polyethylene crystals [8]. This has the advantage of roughly predicting the chain length of the synthesized diacid, which varies with the method for growing the individual polyethylene crystals, and can therefore be gauged from the resultant crystal thickness. However, the most promising the method is the Wittig reaction based synthesis developed from Whiting and co-workers, mentioned in Chapter 1. They were already able to synthesize extended aliphatic dicarboxylic acids [9]. The properties of the corresponding novel PA-x.60 compounds will most likely be very similar to those of polyethylene. Besides possible amphiphilic character, these polymers might offer, e.g., better creep behavior than polyethylene due to the incorporated hydrogen bonds. It would also be very interesting to investigate the crystal structure of these new polymers to see whether the very low number of amide groups is still able to force the polymer chain into a polyamide-like crystal structure.

Further work would be to incorporate the 1,34-tetratriacontanedioic acid synthesized here into other polymer backbones, e.g., polyesters; this will probably also lead to amphiphilic polymers. However, aliphatic polyesters might have very low melting temperatures on account of the incorporated extended segments. These low melting temperatures might be avoided by incorporating the 1,34-tetratriacontanedioic acid into aromatic polyesters. These novel polyesters could be used to synthesize new polyurethanes to produce amphiphilic properties. This then opens up another possibility. *Via* the *Schmidt* reaction [1], it is possible to synthesize 1,32-dotriacontanediamine by reducing 1,34-tetratriacontanedioic acid or the corresponding dialcohol with lithium aluminum hydride. Both could be used directly for the synthesis of novel polyurethanes and polyureas. Clearly, these polymers should also show amphiphilic phase behavior similar to the aliphatic polyamides discussed in this thesis. A whole new polymer field and applications would thus be opened (Scheme 7.1).

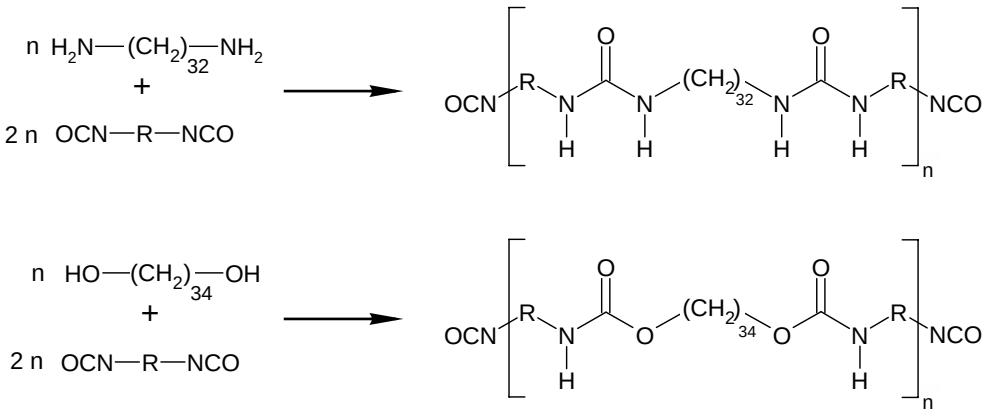

Scheme 7.1: Possible polyureas and polyurethanes with extended aliphatic segments.

A somewhat dissatisfying aspect of the method for making the PA-x.34 was the relatively low molecular weight of the resultant polymers. To be sure, a weight-average molecular weight in the region of 10,000 to 30,000 was a respectable result for small-scale melt polycondensation under laboratory conditions, and suffices for studies of most properties of interest. However, the value of 30,000 only represented a degree of polymerization of about 46. By comparison, the corresponding figure for PA-6.6 of the same molecular weight is about 114. In addition, three times as much polymerization is routinely achieved for PA-6.6 under similar reaction conditions. A few possible reasons why the molecular weight for PA-x.34 was not higher can be pointed out. One might be incompatibility between the relatively short diamine and the long 1,34-tetratriacontanedioic acid, leading to phase separation of these species and therefore to a reduced molecular weight. Another might be the relatively small concentration of reactive groups compared to the reaction volume. A solution to these two problems would be to effect better mixing during polymerization. The polymerization reaction was carried out in an autoclave without any mechanical stirring. Consequently, the chances of the reactive groups' meeting each other were diffusion-controlled and became slighter with increasing reaction time because the melt viscosity increased. This might be solved by an autoclave with a double-helix mixing screw; this would lead to good mixing and avoid the *Weissenberg* effect [10]. Such an autoclave should have an outlet for discharging the polymer with nitrogen pressure while it is still a melt as that would obviate the need for a glass liner when the polyamide has to be removed (Figure 7.1).

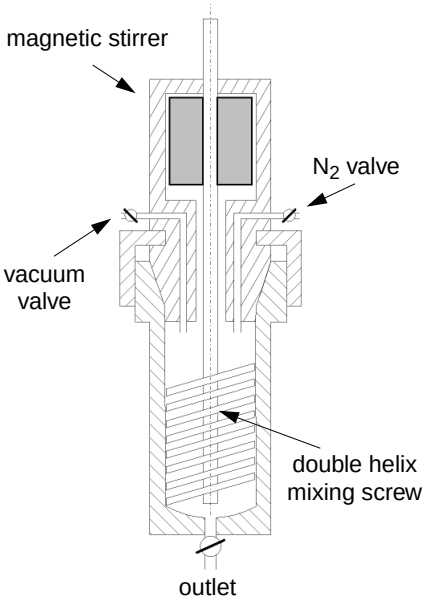

Figure 7.1: Suggestion for an autoclave.

7.3 References

[1] Schmidt, K. F. *Angew. Chem.* **1923**, *36*, 511.

[2] Hünig, S.; Buysch, H.-J. *Chem. Ber.* **1967**, *100*, 4017.

[3] Kohan, M. I. *Nylon Plastics Handbook*; Carl Hanser Verlag: Munich, 1995.

[4] Lide, D. R. *CRC Handbook of Chemistry and Physics*; CRC Press: Boca Raton, 1995-1996.

[5] Smith, P.; Lemstra, P. J. *J. Mater. Sci*. **1980**, *15*, 505.

[6] Lukes, C. *Collect. Czech. Chem. Commun.* **1958**, *23*, 497.

[7] Kim, Yesook; Strauss, H. L.; Snyder, R. G. *J. Phys. Chem.* **1989**, *93*, 7520.

[8] Clark, D. T.; Feast, W. J. *Polymer surfaces: symposium*; Wiley: Durham, 1978.

[9] Brooke, G. M.; Burnett, S.; Mohammed, S.; Proctor, D.; Whiting, M. C. *J. Chem. Soc., Perkin Trans*. **1996**, *1*, 1635.

[10] Weissenberg, C. *Nature* **1947**, *159*, 310.

Curriculum Vitae

The author of this thesis was born on October, 2nd 1972 in Ludwigshafen/Rhein, Germany. In 1992 he obtained his senior matriculation at the Jacob-Grimm-Schule Kassel. In the same year he started his chemistry studies at the Albert-Ludwigs-University of Freiburg and finished his studies with a focus on Technical and Macromolecular Chemistry at Eidgenössische Technische Hochschule Zurich (ETH, Swiss Federal Institute of Technology Zurich) in the spring 1997. He carried out his diploma thesis work in the Polymer Technology group of Prof. P. Smith at the Materials Department of the ETH Zurich. In this thesis he worked on poly(*p*-phenylene octylene)s, which he synthesized by acyclic diene metathesis (ADMET) polymerization. In May 1997, he started his Ph.D. research in the group of Prof. P. Smith. During this time he worked for six months (Summer 1999) as an exchange researcher in the Exotic Materials Institute of Prof. F. Wudl at the Department of Chemistry and Biochemistry of the University of California, Los Angeles. In November 2000 he worked together with Prof. E. D. T. Atkins for one month at the H. H. Wills Physics Laboratory, University of Bristol. Since August 1, 2001 he is employed at the Polymer Research at BASF AG.

Danksagung

Mein ganz persönlicher Dank gilt Frau Professor Dr. G. Schmidt für ihre Bereitschaft, die Betreuung meiner Promotion zu übernehmen. Ihrem Einsatz und wichtigen Hinweisen habe ich es zu verdanken, dass meine Promotion zu einem positiven Abschluss geführt werden konnte.

Den Korreferenten Herrn Professor Dr. H. Höcker und Herrn Professor Dr. G. Ziegmann möchte ich meinen besonderen Dank für ihr persönliches Engagement aussprechen. Ihre kritischen fachlichen Kommentare zu meiner Arbeit haben mir sehr geholfen, diese erfolgreich abzuschliessen.

Herrn Professor Dr. P. Smith möchte ich meinen Dank aussprechen, dass ich die Arbeiten zu meiner Promotion an seinem Institut durchführen konnte, ebenso für die wissenschaftlichen Diskussionen und die Möglichkeit zu Auslandsaufenthalten während dieser Zeit.

Für seine wissenschaftlichen Hinweise und die Unterstützung während meiner Doktorarbeit danke ich Herrn Professor Dr. Ch. Weder sehr.

Herrn Professor F. Wudl, Ph.D., möchte ich für die freundliche Aufnahme während meines Aufenthaltes in seiner Arbeitsgruppe an der UCLA in Los Angeles danken.

Mein besonderer Dank gilt auch Herrn Professor Dr. E. Atkins und Herrn Dr. Pawel Sikorski für die gute Zusammenarbeit und eine erfolgreiche Zeit an der University of Bristol.

Danken möchte ich Herrn Dr. Henry Chanzy, Frau Gaby Riedel und Herrn Professor Dr. P. Schurtenberger für ihre Beiträge zu dieser Arbeit.

Allen Mitgliedern der Polymertechnologie-Gruppe an der ETH Zürich danke ich für eine schöne und anregende gemeinsame Zeit. Besonders hervorheben möchte ich dabei Simon Dellsberger, Dr. Daniel Steiger, Dr. Theo Tervoort und Dr. Jeroen Visjager, die immer bereit waren mir mit Rat und Tat zur Seite zu stehen.

Meinen Eltern, Geschwistern und meiner Schwägerin danke ich dafür, dass sie immer für mich da waren und mich unterstützt haben.

Schliesslich möchte meiner Frau Inken Heusinger von Waldegge für ihr Verständnis und ihre stete Unterstützung danken in der für mich nicht immer einfachen Zeit der Promotion.

Oktober 2002

Moritz Ehrenstein